

# Smart Water Flooding and Production

Master Thesis in Enhanced Oil Recovery

Akam Petersen

7<sup>th</sup> June 2019

Supervisors:

Professor Erik Gydesen Søgaard

Associate Professor Jens Muff



**AALBORG UNIVERSITET**  
STUDENTERRAPPORT

Department of Chemistry and Bioscience

Aalborg University Esbjerg

# Title Page

**Project from:** Aalborg University Esbjerg (AAU)

**Address:** Niels Bohrs Vej 8, 6700 Esbjerg, Denmark

**Study:** Oil and Gas Technology, Master Degree

**Semester:** 9<sup>th</sup> and 10<sup>th</sup> Semesters

**Project title:** Smart Water Flooding and Production

**Author:** Akam Petersen

**Supervisors:** Professor Erik Gydesen Søgaard, Professor Jens Muff

**Project period:** September 2018 – June 2019

**Submission date:** 7<sup>th</sup> June 2019

By signing the author take the full responsibility for the contents of the master thesis

X

---

(Akam Petersen)

Author

# **Acknowledgements**

First of all, I would like to say special thanks to Erik Gydesen Søgaard and Jens Muff for their guidance and assistance and inspiring conversation on the topic of the project. I do appreciate all their efforts to guide me in the right direction of a perfect project.

I also would like to express my deep gratitude to Jacquelin E. C. Mora and Mahdi Nobakht for their great efforts to help and guide me during experimental work in laboratory.

I also want to thank our helpful laboratory technicians, Linda and Dorthe, who gave me a great assistance and contributed with me during all experiments.

Lastly, I would like to express my sincere gratitude to all of the persons who helped me during the project.

# Abstract

The main purposes of this thesis are to investigate wettability alteration of chalk upon injection of advanced water into reservoir, produce desirable advanced water using membrane technology and find an economical scenario of production of smart water. The current project consists of three major parts; In the first part of the project, wettability alteration in rock system of carbonate reservoir using modified flotation technique (MFT) are investigated. In order to test changes in wetting condition of rock (chalk) in reservoir, several sets of laboratory experiments using different brines (s.l.) were carried out at high temperature (100 °C) and data were used to calculate and analyze the results of the investigation. The brines were synthetically prepared based on synthetic seawater and Ekofisk formation water recipes and some of them were diluted up to 100 times. After analyzing the results of flotation experiments, it was observed that 20 times diluted synthetic seawater with a composition containing divalent ions (sulphate, magnesium and calcium) and low salinity had the greatest effect on the wettability alteration of chalk (ca. 60.67%) and consequently higher amount of oil recovery.

The second part of the project deals with production of smart water with favorable composition of seawater (with low salinity while retaining divalent ions) using a membrane process. Nanofiltration (NF) and reverse osmosis (RO) membrane processes were used in order to separate the ions in seawater and produce advanced water with desirable characteristic. For this purpose, the retentate flow from nanofiltration process (contains divalent ions and high salinity) was used as the main component of smart water and was combined with the permeate flow (contains low level of salinity) to reduce the salinity of the retentate of NF. The results from filtration experiments showed that NF membrane retained ca. 90% of  $SO_4^{2-}$ , 60%  $Mg^{2+}$ , 28%  $Ca^{2+}$ , 20%  $Cl^-$  and 23%  $Na^+$  in its retentate flow and RO membrane retained ca. 5% of  $SO_4^{2-}$ , 49%  $Mg^{2+}$ , 8%  $Ca^{2+}$ , 17%  $Cl^-$  and 26%  $Na^+$  in its permeate flow.

In the third part of the project, the wettability alteration in chalk using MFT and produced smart water from the membrane process are investigated. To this end, a set of flotation experiments using new produced smart water and original seawater were performed and

after calculating and comparing the results, it was observed that the new smart water increased ca. 25% of the wettability in chalk compared to the original seawater.

Finally, at the end of the project two proposed scenarios to produce the smart water using a membrane process are investigated. After simulating the process and performing an economic analysis, the optimal model of the smart water production using membrane technique with minimum energy consumption of ca. 4,63 kwh/m<sup>3</sup> was achieved.

# Abbreviations and Nomenclature

(s.l.): sensu latu/in a broad sense, 19

AN: Acid Number, 15

BN: Base Number, 15

CBR: Crude oil-Brine-Rock System, 8

DLVO: Derjaguin, Landau, Verwey and Overbeek, 20

EF: Electrostatic Force, 20

EFW: Ekofisk Formation Water, 41

EOR: Enhanced Oil Recovery, 2

FWI: Flotation Wettability Index, 77

gfd/psl: gallons/ft<sup>2</sup>/day)/psi, 58

IC: Ion Chromatography, 49

ICP-MS: Inductively Coupled Plasma-Mass Spectrometry, 51

IMSDesign: Integrated Membrane Solutions Design, 63, 96

IOR: Improved Oil Recovery, 2

MF: Microfiltration, 24

MFT: Modified flotation technique, 39

MIE: Multi-component Ion Exchange, 21

mS/cm: Millisiemens per Centimeter, 53

MWCO: Molecular Weight Cut-off, 24

NF: Nanofiltration, 12

PDI: Potential Determining Ion, 21

RO: Reverse Osmosis, 12

SF: Structural Force, 20

Syn. SW: Synthetic Seawater, 72

Syn. SW0S: Synthetic Seawater, Zero sulphate, 44

Syn. SW0S0Ca: Synthetic Seawater, Zero sulphate, Zero Calcium, 44

TAN: Total Acid Number, 15

TBN: Total Base Number, 15

TDS: Total Dissolved Solids, 45

TFC: Thin Film Composite Membrane, 26

UF: Ultrafiltration, 24

VDW: Van der Waals, 20

# Table of Contents

<b>1. CHAPTER 1 (Introduction)</b> .....	<b>1</b>
<b>1.1. Overview of Oil and Gas Production</b> .....	<b>2</b>
<b>1.2. Oil Recovery Process</b> .....	<b>3</b>
<b>1.3. Enhanced Oil Recovery (EOR)</b> .....	<b>6</b>
<b>1.4. Smart Water</b> .....	<b>8</b>
<b>1.5. Smart Water Advantages over other Methods of EOR</b> .....	<b>9</b>
<b>2. CHAPTER 2 (Problem Definition)</b> .....	<b>10</b>
<b>2.1. Problem Formulation and Delimitation</b> .....	<b>11</b>
<b>3. CHAPTER 3 (Background Knowledge)</b> .....	<b>13</b>
<b>3.1. Petroleum Systems and Reservoirs</b> .....	<b>14</b>
<b>3.2. Wettability and Concepts Related to Wettability</b> .....	<b>16</b>
<b>3.3. Wettability Alteration and Mechanism of Wettability Alteration</b> .....	<b>19</b>
<b>3.4. Factors Influencing Wettability</b> .....	<b>23</b>
<b>3.5. Membrane Separation</b> .....	<b>24</b>
<b>3.6. Structural Design of Membranes</b> .....	<b>26</b>
<b>3.7. Membrane Shapes and Configurations</b> .....	<b>28</b>
<b>3.8. Advantages of Membrane Separation Process over Traditional Separation Processes</b> ...	<b>29</b>
<b>3.9. Membrane Performance</b> .....	<b>30</b>
<b>3.10. Parameters Affecting the Performance of Nanofiltration Membrane</b> .....	<b>32</b>
<b>3.11. Membrane System Modes</b> .....	<b>34</b>
<b>4. CHAPTER 4 (Materials and Methods)</b> .....	<b>36</b>
<b>4.1. Flotation Experiment</b> .....	<b>37</b>
<b>4.2. Smart Water Production Experiment</b> .....	<b>49</b>
<b>5. CHAPTER 5 (Results and Discussion)</b> .....	<b>64</b>
<b>5.1. Flotation Technique and Wettability Alteration</b> .....	<b>65</b>
<b>5.2. Sea Water Filtration and Smart Water Production</b> .....	<b>81</b>
<b>5.3. Flotation Technique Using Smart Water</b> .....	<b>94</b>
<b>6. CHAPTER 6 (Scenarios and Recommendation)</b> .....	<b>95</b>
<b>6.1. Suggested Scenarios for Smart Water Production and Economic Analysis</b> .....	<b>96</b>
<b>7. CHAPTER 7 (Conclusions)</b> .....	<b>101</b>

7.1. <i>Future Work</i> .....	104
8. <b>Bibliography</b> .....	<b>106</b>
9. <b>Appendix</b> .....	<b>112</b>
9.1. <i>Data Entry Table for Flotation Experiment</i> .....	112
9.2. <i>Ions Analysis Results (IC and ICP Machines)</i> .....	113

# List of Tables

Table 4.1-1- Characteristics of crude oil from North Sea reservoir .....	38
Table 4.1-2- Composition of Dan Chalk.....	38
Table 4.1-3- Density of Dan Chalk .....	39
Table 4.1-4- Synthetic seawater recipe .....	42
Table 4.1-5- Ekofisk formation water recipe.....	43
Table 4.1-6- Types of brines and their dilutions.....	44
Table 4.1-7- Calculated molar concentrations, ionic strengths, TDS and densities of all brines .	46
Table 4.1-8- pH and measurement of brines at ambient temperature .....	47
Table 4.2-1- Characteristics of seawater.....	53
Table 4.2-2- Stokes Radius and hydration energy of different ions [13].....	57
Table 4.2-3- Filmtec Flat sheet NF270 Membrane Specifications .....	58
Table 4.2-4- Filmtec Flat sheet Reverse Osmosis (LPRO) Membrane Specifications.....	61
Table 5.2-1- Characteristics of smart water produced from membrane technology .....	93

# List of Figures

Figure 1.2-1- Displacement of oil through reservoir rocks by water-flooding in Five-spot pattern [5] .....	4
Figure 1.2-2- Oil Recovery Processes.....	5
Figure 1.2-3- Schematic of Waterflooding Process [7].....	5
Figure 1.3-1- Oil Recovery Mechanism [9].....	6
Figure 1.4-1- Effect of smart water on oil-wet rock [12].....	8
Figure 3.1-1- Carbonate ion chemical structure (left) rhombohedral structure of calcite and relative position of the Ca and CO <sub>3</sub> ions in the mineral lattice (right) [18].....	14
Figure 3.2-1- Plane view, cross-section view and fluid distribution in a hypothetical water-wet, oil-wet and fractional-wet pore [29] .....	16
Figure 3.2-2- Contact angle between the rock surface and droplets .....	17
Figure 3.3-1- Schematic model of the suggested mechanism for the wettability alteration induced by seawater. (A) proposed mechanism when Ca <sup>2+</sup> and SO <sub>4</sub> <sup>2-</sup> are active at lower and high temperature. (B) Proposed mechanism when Mg <sup>2+</sup> and SO <sub>4</sub> <sup>2-</sup> are active at higher temperatures [39].....	22
Figure 3.5-1- General comparison diagram of selected separation process based on size ranges of various materials found in raw water [48].....	25
Figure 3.5-2- Graphical representation of the membranes processes performance [49].....	26
Figure 3.6-1- Structure of cross-section of thin film composite membrane [51].....	27
Figure 3.11-1- A schematic of cross-flow filtration process [66].....	34
Figure 3.11-2- A schematic of dead-end filtration process [66].....	35
Figure 4.1-1- Titration Results for Acid Number (U is the potential (mV), V is the added volume of titrant and EP stands for equivalence point) .....	38
Figure 4.1-2- Modified Flotation Technique laboratory procedure at 100 °C of oven temperature. The drop shape represents the addition of brine (blue) and crude oil (brown) [17].....	41
Figure 4.2-1- Ion Chromatography (IC) machine.....	50
Figure 4.2-2- Inductively Coupled Plasma-Mass Spectrometry (ICP-MS) machine.....	52
Figure 4.2-3- Molecular Sieving occurring in membrane [76].....	56
Figure 4.2-4- Solution-Diffusion occurring in membrane [76] .....	57
Figure 4.2-5- Principle of Reverse Osmosis membrane .....	60
Figure 4.2-6- Dead-End Process, experimental setup for both nanofiltration and reverse osmosis membranes experiments .....	62
Figure 4.2-7-Schematic of IMSDesign software designed by Nitto Group Company.....	63
Figure 5.1-1- Effect of different dilutions of synthetic seawater on wettability at 100 °C. Error bars represent the standard deviation (in percent) of the data.....	66
Figure 5.1-2- Effect of different dilutions of syn. SW <sub>0</sub> SO <sub>0</sub> Ca on wettability at 100 °C. Error bars represent the standard deviation (in percent) of the data. ....	67
Figure 5.1-3- Effect of different dilutions of syn. SW <sub>0</sub> SO <sub>0</sub> Mg on wettability at 100 °C. Error bars represent the standard deviation (in percent) of the data. ....	68
Figure 5.1-4- Effect of different dilutions of syn. SW <sub>0</sub> Ca <sub>0</sub> Mg on wettability at 100 °C. Error bars represent the standard deviation (in percent) of the data. ....	69
Figure 5.1-5- Comparison of wettability alteration using different brine at 100 °C. Error bars represent the standard deviation (in percent) of the data. ....	70

Figure 5.1-6- Wettability alteration of Dan Chalk and variation of divalent ions concentration for non-diluted synthetic seawater and its dilutions at 100 °C.....	71
Figure 5.1-7- Dependency of rock wettability on pH for non-diluted seawater and its dilutions at 100 °C.....	73
Figure 5.1-8- Dependency of rock wettability on TDS for non-diluted seawater and its dilutions at 100 °C.....	73
Figure 5.1-9- Attached oil to water-wet grains for synthetic seawater and its dilutions at 100 °C .....	74
Figure 5.1-10- Attached oil to water-wet grains for syn. SW0S0Ca and its dilutions at 100°C ...	75
Figure 5.1-11- Attached oil to water-wet grains for syn. SW0S0Mg and its dilutions at 100°C ...	75
Figure 5.1-12- Attached oil to water-wet grains for syn. SW0Ca0Mg and its dilutions at 100°C.	76
Figure 5.1-13- Comparison of attached oil to water-wet grains for different brines at 100°C.....	76
Figure 5.1-14- Flotation wetting index for Dan Chalk using synthetic seawater and its dilutions at 100°C.....	78
Figure 5.1-15- Flotation wetting index for Dan Chalk using syn. SW0S0Ca and its dilutions at 100°C.....	78
Figure 5.1-16- Flotation wetting index for Dan Chalk using syn. SW0S0Mg and its dilutions at 100°C.....	79
Figure 5.1-17- Flotation wetting index for Dan Chalk using syn. SW0Ca0Mg and its dilutions at 100°C.....	79
Figure 5.1-18- Comparison of flotation wetting index for Dan Chalk using different brines at 100°C.....	80
Figure 5.2-1- Rejection of ions using Nanofiltration membrane (NF270) in different pressures..	82
Figure 5.2-2- Flux of nanofiltration process in different pressures .....	83
Figure 5.2-3- Total Dissolved Solids vs. pressure for nanofiltration process .....	84
Figure 5.2-4- Rejection of ions using Reverse Osmosis membrane (RO) in different pressures	85
Figure 5.2-5- Flux of reverse osmosis process in different pressures .....	86
Figure 5.2-6- Total Dissolved Solids vs. pressure for reverse osmosis process .....	87
Figure 5.2-7- Comparison of ion rejection between nanofiltration (NF) and reverse osmosis (RO) membranes .....	89
Figure 5.2-8- Comparison of flux between nanofiltration (NF) and reverse osmosis (RO) membranes .....	90
Figure 5.2-9- Comparison of TDS between nanofiltration (NF) and reverse osmosis (RO) membranes .....	91
Figure 5.2-10- A schematic of smart water production using nanofiltration (NF) and reverse osmosis (RO) membranes (at one to six ratio) .....	92
Figure 5.3-1- Wettability alteration of Dan Chalk using seawater and smart water at 100 °C.....	94
Figure 6.1-1- Combination of nanofiltration and reverse osmosis process to produce smart water at one to six ratio (Scenario 1).....	97
Figure 6.1-2- Proposed train for smart water production using NF and RO at one to six ratio (Scenario 2).....	98
Figure 6.1-3- Energy Consumption by different processes of smart water production in different ratio .....	99
Figure 7.1-1- A schematic of topside processes [87] .....	105
Figure 9.2-1- Anions present in permeate flow of nanofiltration under pressure of 12 bar .....	113

Figure 9.2-2- Anions present in retentate flow of nanofiltration under pressure of 12 bar ..... 114  
Figure 9.2-3- Cations present in retentate flow of nanofiltration under pressure of 10 bar ..... 115  
Figure 9.2-4- Cations present in permeate flow of nanofiltration under pressure of 10 bar..... 116

# ***1. CHAPTER 1*** ***(Introduction)***

## 1.1. Overview of Oil and Gas Production

Over the past few years most of the oil companies have survived tough years with weak demand and low prices of oil. The collapse of oil price triggered a wave of cost reduction among the oil exploitation and extraction processes cost. On the other hand, reducing the limited resources of oil and increased concern on environmental issues created conditions for oil companies to apply new strategies and methods to produce more oil. Although profitability in the oil and gas industry is always a key metric, the increase in oil production has often been more important.

Nevertheless, the development and implementation of the new technologies and methods that require low investment, while high profitability and revenue are of great importance. Enhanced oil recovery (EOR) and improved oil recovery (IOR) are two of the latest technologies that used to maximize the revenue of oil from existing fields. Waterflooding as a method of increasing the amount of oil for EOR can be implemented to displace the oil from the reservoir trapped in the rock and lead it to the producer. This effective method is implemented by injecting seawater into the reservoir and according to the recent studies and researches, the amount of oil recovery can be significantly increased by adjusting the ionic composition of the fluid (seawater) injected into the reservoir [1]. According to report of Godinho, "It is commonly known that globally average of field recovery from water-flooding currently is about 35% which leaves about 60-70% left in reservoir of which each additional percentage potentially be recovered is equivalent to significant amounts of hydrocarbons. Due to the potential in matured fields there is an increased focus on suitable EOR methods" [2] (2017, p. 3).

## 1.2. Oil Recovery Process

Oil recovery processes are subdivided into three major categories:

- Primary
- Secondary
- Tertiary

In the primary process or initial recovery, the oil is forced out of the reservoir by the existing natural pressure of fluids which are trapped in the reservoir. The amount of oil production in this stage depends mainly on existing natural pressure in the reservoir and this pressure originated from different forces such as gravitational force, expanding force of natural gas, buoyancy force of encroaching water and etc. but among these forces, the force which contributes mainly to produce oil is the expanding force of high-pressure natural gas. When the existing natural pressure of the reservoir is reduced to a point where it is no longer effective, the Secondary recovery process is employed to increase the pressure required to drive the oil to production wells [3], [4].

The general mechanism of the secondary oil recovery process is to augment and maintenance the reservoir pressure artificially in order to force oil to the production wells. In this stage more than one wellbore is involved (unlike the primary oil recovery process) and the decrease of the pressure in the depleted reservoir after Primary recovery can be restored by injecting a gas into the reservoir or water-flooding through injection wells to achieve a high pressure or driving oil through the reservoir rocks toward the producing wells respectively. Injection of air or aqueous solutions of polymer can be included as well in the secondary oil recovery process. In water-flooding process, the most common pattern of injection and production wells is five-spot configuration where water is injected into the central well and the oil is displaced to the four production wells which are located surround the central well [5]. The Five-spot pattern is shown in figure 1.2-1:

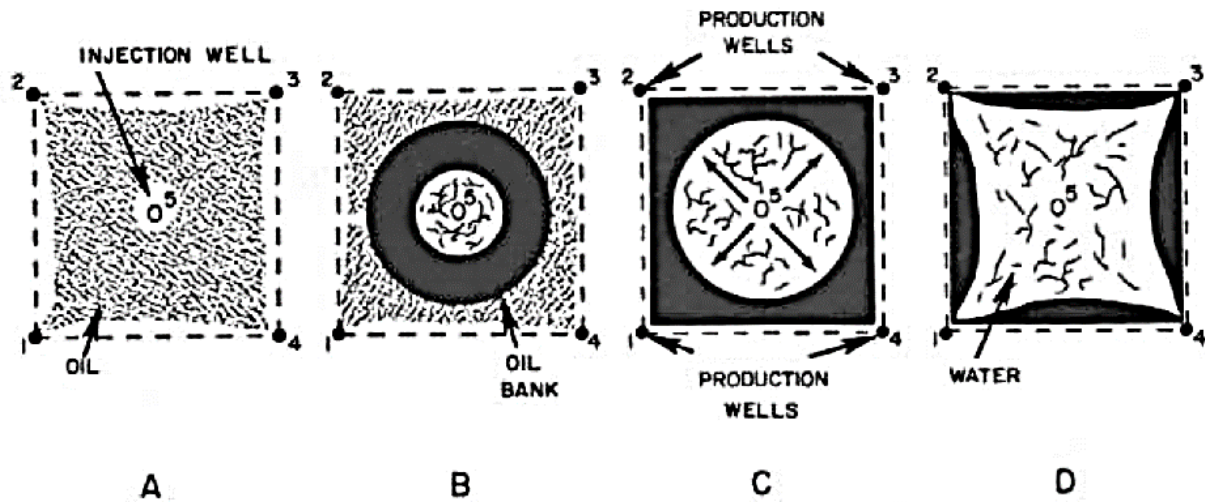


Figure 1.2-1- Displacement of oil through reservoir rocks by water-flooding in Five-spot pattern [5]

The amount of oil recovered by both the Primary and Secondary oil recovery processes ranges from 20% to 50% depending on reservoir and oil properties. In order to recover at least a part of the remaining oil-in-place, Tertiary oil recovery process takes place. This stage which is known as Enhanced Oil Recovery (EOR) can be divided into four major categories: Thermal Oil Recovery, Chemical Flooding, Miscible Displacement Methods and Water-Based Methods. The amount of oil recovered by Enhanced Oil Recovery is greater than 50% and up to 80% [6], [5].

Oil recovery process and a schematic of water flooding process are shown in figure 1.2-2 and 1.2-3, respectively:

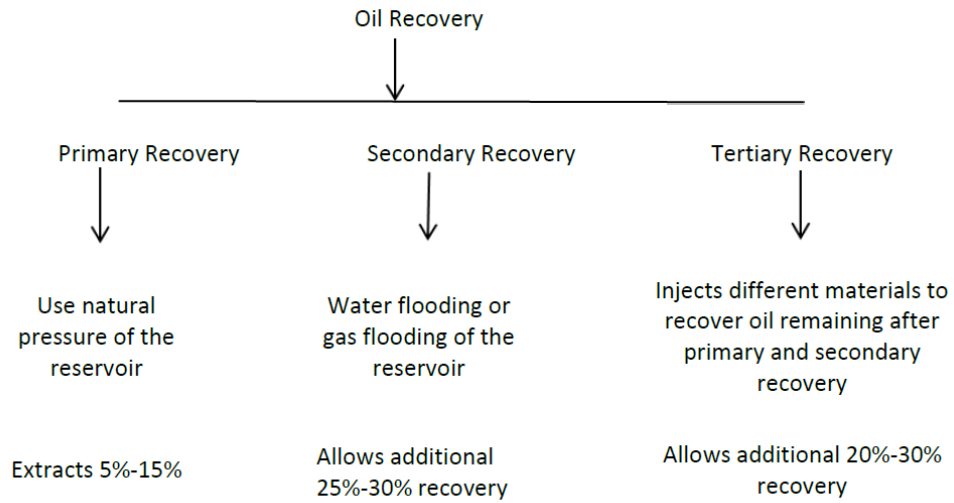


Figure 1.2-2- Oil Recovery Processes

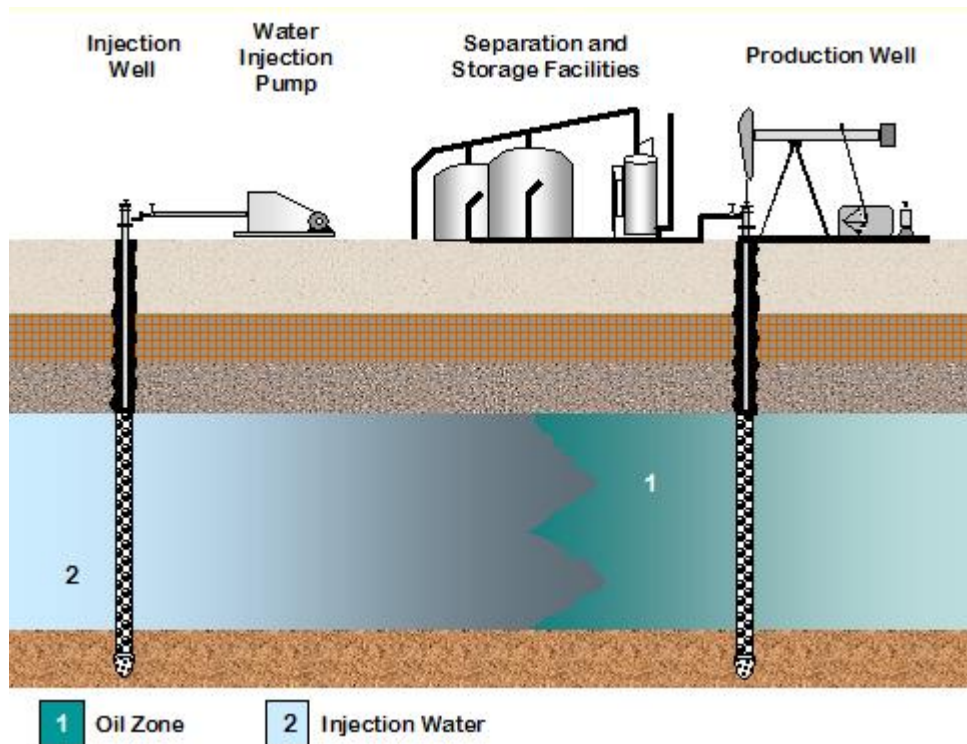


Figure 1.2-3- Schematic of Waterflooding Process [7]

### 1.3. Enhanced Oil Recovery (EOR)

The main purpose of the Enhanced Oil Recovery (EOR) processes is increasing of the oil recovery from reservoirs depleted by the Secondary recovery. The EOR method targets immobile oil which can not be easily recovered due to the viscous and capillary forces [5], [8]. As mentioned in the previous section, Enhanced Oil Recovery methods are classified into four categories which are summarized in the following figure 1.3-1:

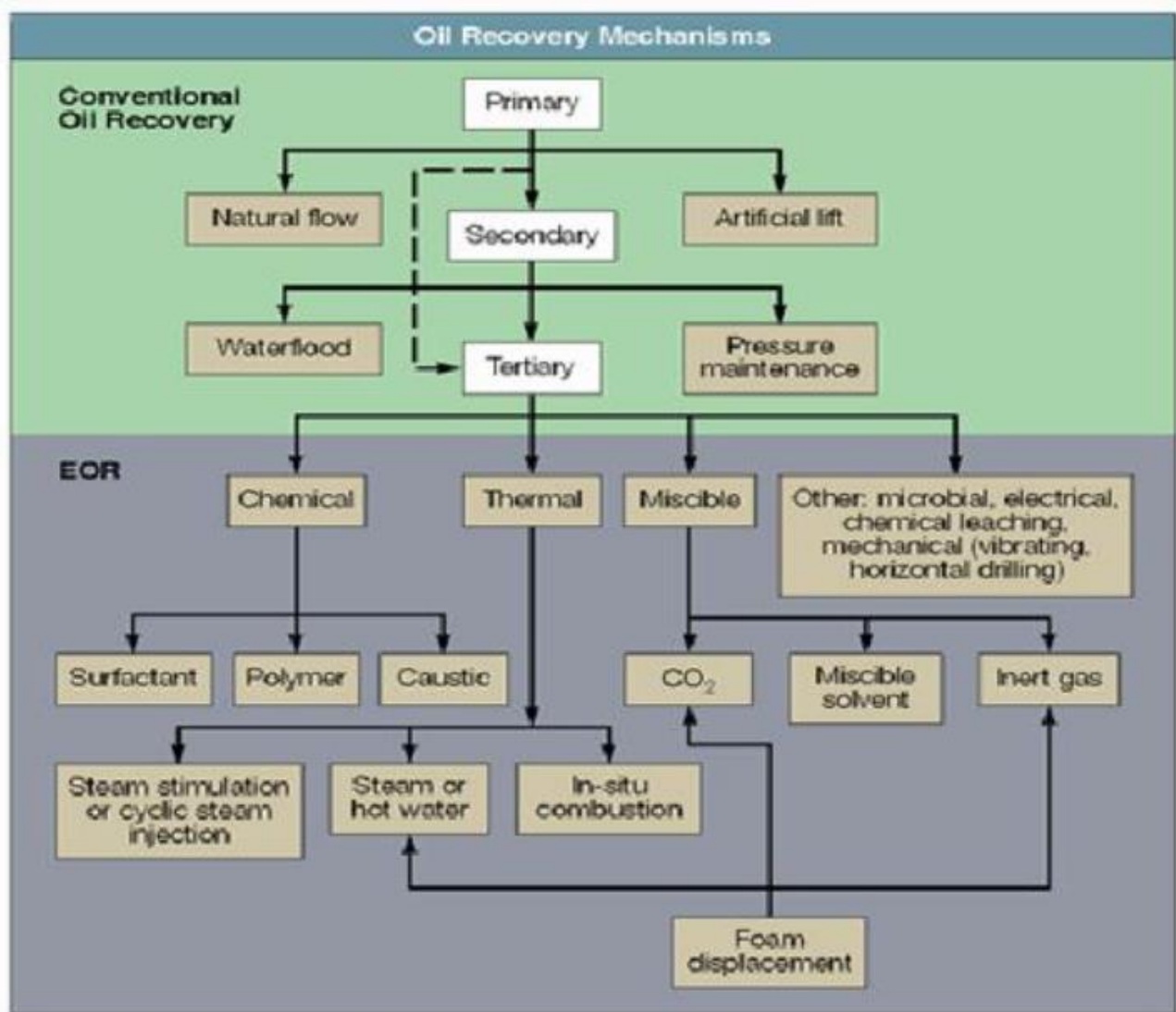


Figure 1.3-1- Oil Recovery Mechanism [9]

Since there are a large number of petrophysical, chemical, geologic and environmental properties must be considered in each method of EOR, selecting criteria for a specific EOR method is complex for all petroleum reservoirs as a general method for EOR and each case must be investigated individually. Nowadays, application of Water-Based EOR method is much considered among the other methods due to the advantages described below [10]:

- 1 The method doesn't need a high investment compared to other methods.
- 2 The Water-Based EOR method is environmentally friendly and no expensive chemical are used.
- 3 The method is cost-effective among the other methods even with small incremental oil recovery.
- 4 Water can be injected to the reservoir during the early life cycle of the reservoir.

The focus of this thesis is on the Water-Flooding for Enhanced Oil Recovery. It has been verified that injected water which is different in composition compared to the initial formation water, can change the amount of oil recovery. The question may come to mind is what is the difference between Water-Flooding in the Secondary and Tertiary stage of EOR, the answer is the injection of formation water into the reservoir is referred as Secondary oil recovery process and the injection of water with different compositions which so-called Smart Water is referred as Tertiary oil recovery process. Investigating of Smart water as EOR-fluid needs to chemical understanding of water and its most important properties which can affect the amount of oil recovery.

## 1.4. Smart Water

This section gives a brief introduction about what Smart Water is, how it works and what the main mechanism is for increase in the amount of oil recovery. Smart Water is a water which can be made by adjusting or optimizing the ion composition of it in such a way that is desirable as an injected fluid in the reservoir. This fluid changes the equilibrium of the initial CBR-system (Crude Oil-Brine-Rock System) and it will modify the initial wetting condition. Thus, the oil is more easily displaced from the porous network resulting in higher amount of oil recovery. Smart water alters the wetting properties of the CBR-system in the reservoir which has a positive effect on the capillary pressure and relative permeability of oil and water regarding oil recovery and this is the physical principle of smart water for enhanced oil recovery [1], [11]. Figure 1.4-1 shows the effect of smart water on the oil-wet reservoir.

By adjusting the ionic composition of injected seawater into reservoir, the seawater becomes smart water leading to increase the water wetness of chalk. The compaction of the rock caused by smart water when injected into reservoir is another important mechanism in addition to wettability alteration in oil production [1].

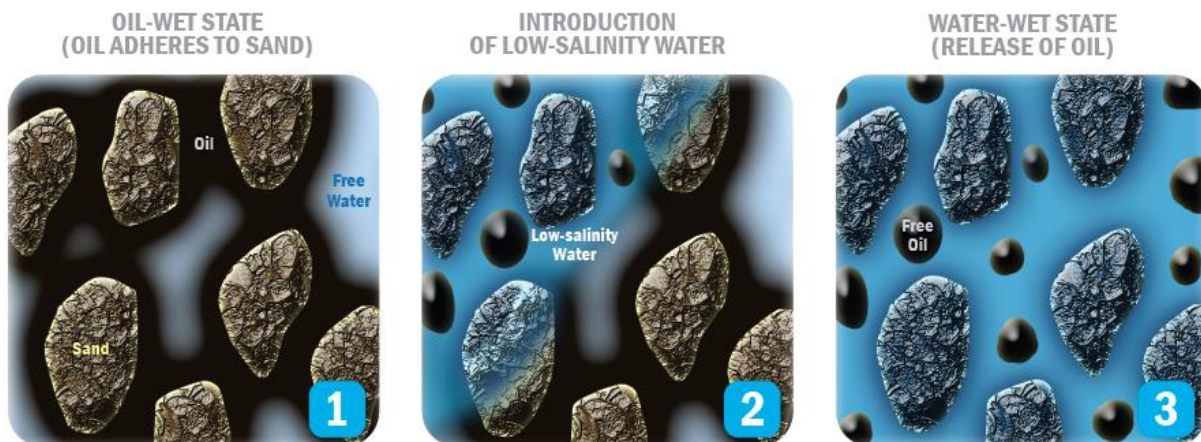


Figure 1.4-1- Effect of smart water on oil-wet rock [12]

## 1.5. Smart Water Advantages over other Methods of EOR

There are several advantages of smart water flooding compared to other methods of EOR as listed below [13]:

- In this method expensive chemical are not added.
- Achieving a higher level of oil recovery with lowest investment is a major advantage of smart water flooding.
- Smart water flooding is environmentally friendly and cheap.
- This technique can be done during the early life cycle of the reservoir.

Smart water contains high concentration of divalent ions and low concentration of monovalent ions with a salinity range between 6000 to 28000 ppm is the most suitable fluid in smart water flooding process [1], [14].

# **2. CHAPTER 2**

## ***(Problem Definition)***

## **2.1. Problem Formulation and Delimitation**

Based on what has been described so far, the water flooding process is known as an effective and economic technique for enhanced oil recovery. Easy access to main resource of the water flooding process (seawater), cost-effective investment, environmentally friendly and many other advantages of implementing the process have led oil companies to undertake extensive researches and studies to improve and develop the water flooding technique during the recent years. One of the most effective ways to improve the water flooding technique is to change and adjust the ionic composition of the seawater. By the way, it is possible to change the wetting condition of the rock that results in an increase in the amount of oil recovery.

The focus of the project is to investigate and study the potential of sea water with different composition to increase water wetness of the chalk using modified flotation technique as well as production of water with desirable composition (smart water) using membrane technology with the most optimal method.

### **2.1.1. Objectives**

During the past few decades, many hypotheses have been raised by researchers and authors to clarify the most important parameters that increase the production of oil in water-flooding process as an effective and environmentally friendly process. Change in wettability of the rock by changing the ionic structure of the injected fluid (seawater) into reservoir is known as effective mechanism to improve the production of oil. On the other hand, finding a method for converting seawater as the major resource and main input of the water-flooding process to water with favorable ionic composition (low salinity while retaining divalent ions) can be an effective step in reducing process costs and increasing the amount of oil production.

In current study, the main attention will be on wettability alteration of rock by altering the ionic composition of seawater to achieve the suitable fluid (smart water), followed by the production of the smart water using membrane technology. The more specific targets of the thesis that are based on laboratory experiments are summarized as following:

- Study and examine the effect of different ionic composition of seawater (synthetically-made) on the wettability properties of chalk using modified flotation technique.
- Production of smart water (favorable ionic composition of seawater) by membrane technology including nanofiltration (NF) and reverse osmosis (RO) membrane processes with an optimal and economic process.
- Examine the effect of the produced smart water from nanofiltration and reverse osmosis membranes on wetting condition of the chalk by modified flotation technique.

# **3. CHAPTER 3**

## ***(Background Knowledge)***

## 3.1. Petroleum Systems and Reservoirs

### 3.1.1. Reservoir Rock

Most of North Sea reservoir are estimated to be carbonate reservoirs which consists of chalk and sandstone as reservoir rock. The carbonate rock as a class of sedimentary rocks, can be formed by tiny particles of matter during the time either at the bottom of sea or on land. Chalk is a particular type of limestone which is pure, white and fragile. Ekofisk field is an example of chalk reservoir located in North Sea. Due to the high importance of petrophysical properties of the reservoir rock as well as variability within a single reservoir, it is necessary to be carefully evaluated. For example, the porosity of the reservoir rock varies between 30-48%, while in the tight zone of Ekofisk field this rage is between 10 and 20% [15], [16].

“In terms of mineralogy, chalks are dominantly composed by crystals of calcite, which is the more stable polymorph of  $\text{CaCO}_3$  for the most pressures and temperatures. Aragonite and vaterite are the two other polymorphs of  $\text{CaCO}_3$ , that occur at particular P-T conditions. Calcite is characterized by a rhombohedral structure, while aragonite and vaterite are defined by orthorombic and hexagonal systems, respectively” [17] (2017, p. 4).

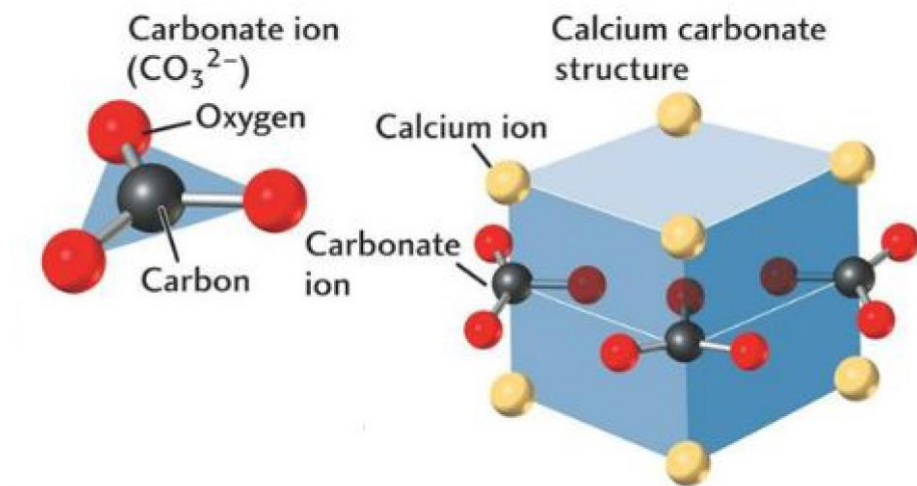


Figure 3.1-1- Carbonate ion chemical structure (left) rhombohedral structure of calcite and relative position of the Ca and  $\text{CO}_3$  ions in the mineral lattice [18]

The charge of calcite surface depends on the exposed sites of the surface (carbonate anions and metal divalent cations) which interact with the water surface. According their positions along the crystal lattice, coordination number of each is determined so that neutralization of the charge is dependent upon the position of each ion, either on face, corner or edge [19], [20].

### **3.1.2. Reservoir Fluid**

Crude oil as the major fluid of reservoir has not an unique elemental composition in different reservoirs and it can vary from formation to formation [21], [22]. Crude oil is generally composed of two major groups of compounds: Hydrocarbons and non-hydrocarbons. Alkanes (called paraffins as well), cycloalkanes (called cyclic paraffins or naphthenes as well) and aromatics. Approximately 95% of the crude oil compounds is hydrocarbons and the rest of the fluid is non-hydrocarbons including sulfur, metals, nitrogen and oxygens compounds [23], [24].

The quantity of acidic and basic components present in the crude oil is determined by total acid number (TAN or AN) and total base number (TBN or BN). Total acid number (TAN) is defined as the total amount of potassium hydroxide (KOH) in milligram required to neutralize one gram of crude oil, while total base number (TBN) can be defined as the total amount of potassium hydroxide in milligram per one gram of crude oil [25]. According to recent studies, base number is observed less relevant concerning the wettability alteration. However, it was observed that at a given acid number, increase in basic material, the wetting condition of the chalk can be improved [26], [16].

Asphaltenes are classified as the solubility fraction of crude oil that are generally classified based on the n-alkane used to precipitate them (commonly, n-pentane, n-hexane or n-heptane) [5]. "There are different variations for the standard procedures used to quantify the asphaltenes fraction present in the crude oil, for an example ASTM D3279-97 for n-heptane based precipitations" [17] (2017, p. 8).

### 3.2. Wettability and Concepts Related to Wettability

The tendency of a fluid to spread on or adhere to a solid surface in the presence of another immiscible fluid is named wettability. This property refers to the interaction between fluid and solid phases. The liquid (fluid) phase in the reservoir can be water, oil or gas and the solid phase can be the rock. The wettability of the reservoir rock is an important property of the rock which determines the success of the waterflooding process since it has a great influence on the flow, location and distribution of the fluid in the reservoir. A rock is defined as Water-wet system when water occupies the small pores and contacts the rock surface in the large pores and oil is located in the middle of the large pores. Vice versa, a rock is defined as Oil-wet system when the location of two fluids is partly reversed from the water wet case. In the Oil-wet system water continues to fill the very small pores since oil never enters the small pores due to capillary forces, but oil contacts the majority of the rock surface in the large pores [27], [28]. Wettability concepts and the location of connate water and oil in the layer pores are shown in the figure 3.2-1:

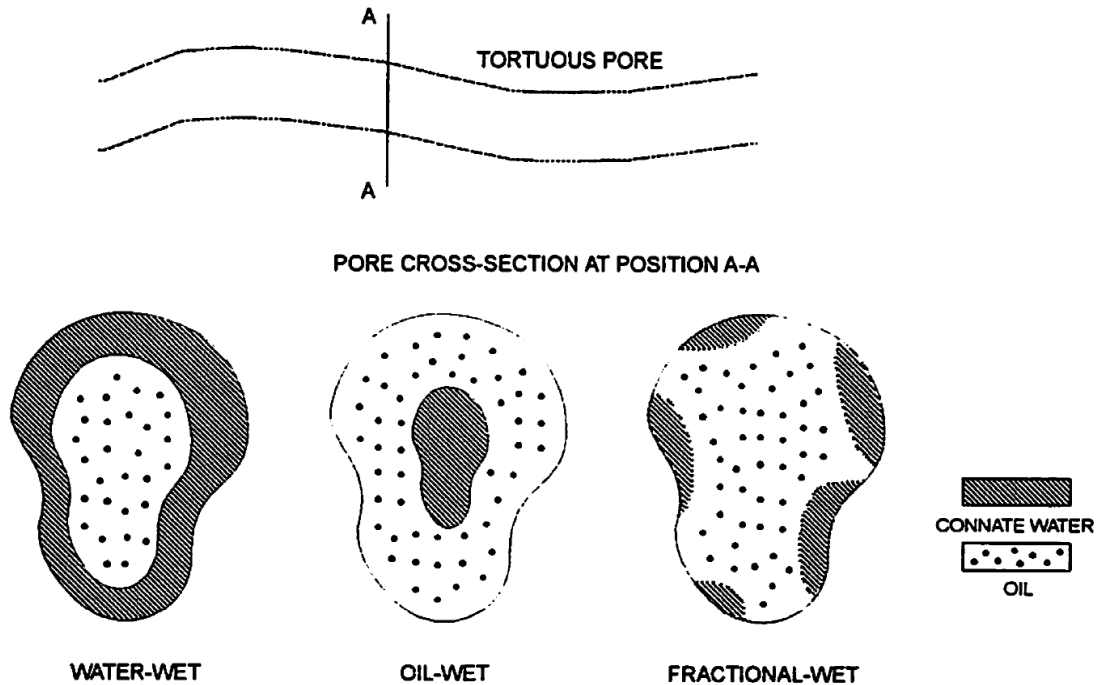


Figure 3.2-1- Plane view, cross-section view and fluid distribution in a hypothetical water-wet, oil-wet and fractional-wet pore [29]

Wettability as a parameter can have significant impact on relative permeability, residual oil saturation and capillary pressure which directly influence waterflooding performance but it is not a parameter which is used directly in the calculation of the waterflood performance [28], [30], [31].

Types of wettability are classified in three categories [32]:

- **Water-wet:** A system is defined as water-wet when its surface is wet by water more than 50%. In the reservoir condition, the contact angle between water and the rock surface is less than  $90^\circ$ .
- **Intermediate-wet:** A system is defined as Intermediate or neutral-wet when all current phases in the system have the same tendency to wet the rock surface. As it is shown in figure 3.2-2, the contact angle between the rock and water is  $90^\circ$ .
- **Oil-wet:** In an Oil-wet system, a thin film of the oil coats the rock surface and the contact angle between water and rock is greater than  $90^\circ$ .

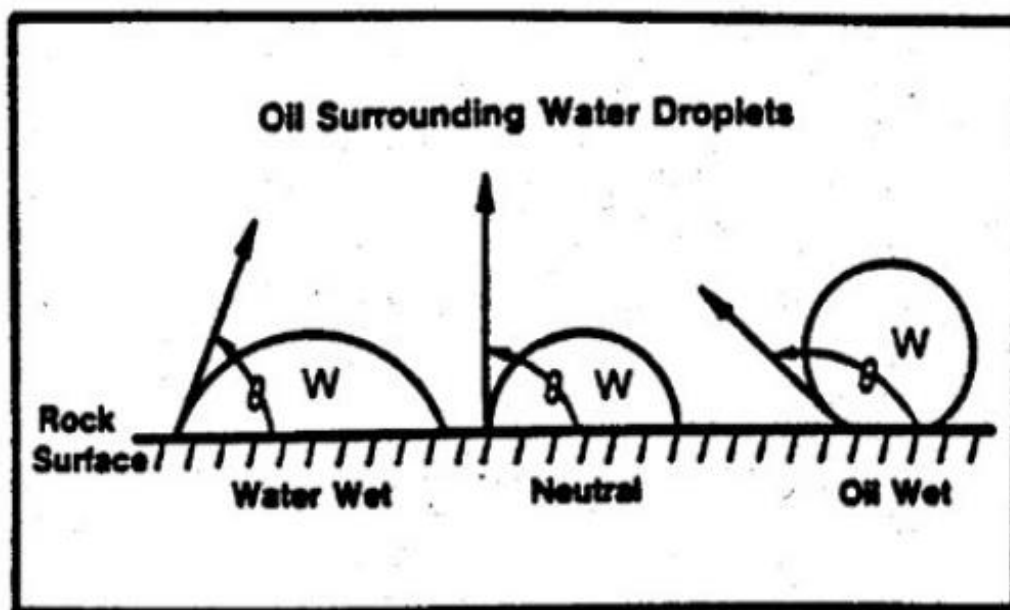


Figure 3.2-2- Contact angle between the rock surface and droplets

There are several different methods have been proposed to measure wettability of a system which can be classified in two main categories: quantitative methods and qualitative methods [33], [34].

- **Quantitative methods:** These methods are known as expensive and time-consuming methods and the most important of these as listed below:
  1. Contact Angles
  2. Imbibition and Forced Displacement (Amott)
  3. USBM Wettability Method
  
- **Qualitative methods:** The main qualitative methods which are generally used for measuring the wettability are the following list:
  1. Imbibition Rates
  2. Microscope Examination
  3. Flotation
  4. Glass Slide Method
  5. Relative Permeability Curves
  6. Permeability/Saturation Relationships
  7. Capillary Pressure Curves
  8. Capillary Metric Method
  9. Displacement Capillary Pressure
  10. Reservoir Logs
  11. Nuclear Magnetic Resonance
  12. Dye Adsorption

These methods are not described in detail in this thesis except for the flotation method since the focus of the thesis is on flotation experiments. The details of the above-mentioned methods can be found in the literature [33], [27].

### **3.2.1. Flotation Method**

Flotation method is a cheap and fast method unlike the other methods of measurement and the results can be obtained in short time instead of months but it works only for strongly wetted systems. In the easiest method of flotation, oil, water and grain are put in a bottle and the mixture is shaken. After a while, the result can be observed by taking a look at the amount of grain whether those that are suspended at the oil/water interface, or those that are settled to the bottom of the bottle. If the system is strongly water-wet, the grains will settle to the bottom of the bottle. The grains which are placed in the oil will form small clumps surrounded by a thin layer of water. Vice versa, if the system is strongly oil-wet, some of the grains will be suspended at the oil/water interface and oil-wet grains will form small oil globules in water [33], [35], [36]. In the oil industry, flotation method was developed by experiment conducted by Dubey and Doe several years ago in order to investigate the influence of oil and brine chemistry on wettability in reservoir.

### **3.3. Wettability Alteration and Mechanism of Wettability Alteration**

The wettability alteration mechanism (Oil-wet to Water-wet) as one of the most fundamental concepts, plays an essential role in enhanced oil recovery. Wettability alteration refers to methods which lead to make the reservoir rock more water-wet resulting higher amount of recovered oil in waterflooding process. Many studies were carried out during the last years in order to understand the mechanism underlying the wettability state in the reservoir and how to control it. Studies and findings show that some main factors generally control wettability as listed below [37]:

- Double Layer Expansion
- Multi-component Ion Exchange (MIE) and Potential Determining Ion (PDI)
- PH effects

### 3.3.1. Double Layer Expansion

The electrical double layer expansion which is described by DLVO theory, is extremely dependent on ionic strength (the concentration of species and present type of ions in a solution). The ionic strength is considered as one of the most important factors that strongly affects the surface charge of the rock by disturbing the pre-established equilibrium in the Oil-Brine-Rock system. Due to the DLVO theory, the intermolecular surface forces play an important role within wettability states. These surface forces which govern the equilibrium in the CBR system, whether attractive or repulsive, are as follow:

1. Van der Waals forces
2. Electrostatic forces
3. Structural or solvation forces

According to the theory of colloidal stability, total disjoining pressure (Total DP) is equal to the summation of the Van der Waals (VDW) and electrostatic forces (EF). The total disjoining pressure is defined as the interactive forces between the interface of water-rock and water-oil. The structural forces (SF) which was known later to dominate the limitation found in DLVO theory, has an intervening role on the system. The estimation of each force is detailed in the resource [38]. Due to the assumption of DLVO theory, the colloidal particles are very large compared to electrolyte ions which provides the description of the interaction between the surface and particle. The disjoining pressure describes the surface force per unit are and is given by equation as follow [17], [37]:

$$\Pi_{TotalDP} = \Pi_{VDW} + \Pi_{EF} + \Pi_{SF}$$

Equation 3.3-1

When two interfaces show a tendency to separate from each other, the total disjoining pressure is positive and vice versa, when two interfaces show a tendency to attract each other, the total DP is negative [19].

### 3.3.2. Multi-component Ion Exchange (MIE) and Potential Determining Ion (PDI)

As a definition for Potential Determining Ion (PDI), any ions which leaves the surface of a solid immersed in a liquid before equilibrium has been reached, while an electrical double layer building up and zeta-potential develops, such as  $Ca^{2+}$ ,  $Mg^{2+}$ ,  $SO_4^{2-}$  and  $PO_4^{3-}$ . These ions have a very effective role in the wettability alteration and changing the surface charge of carbonate rock reservoir, so that increasing the concentration of PDIs are associated with increased recovery [39]. In simple and clearer terms, in the waterflooding process, any changes in the ionic composition of injected water into the reservoir leads to disturb the pre-established equilibrium in the CBR system.

Carbonate rocks which are mainly calcite, are positively charged at relevant reservoir condition. On the other side, crude oil is negatively charged due to carboxyl group, -COOH, and it leads to a strong bond between the negatively charged carboxylic group, -COO-, and the positively charged sites on carbonate surface. Consequently, it can be stated that the oil-brine interface would be negatively charged while rock-brine interface is positively charged [1]. Multicomponent Ion Exchange (MIE) theory which is based on the water geochromatography (cation exchange), plays an important role in enhanced oil recovery process. This phenomenon occurs on the surface of the minerals due to the different affinities of various cations toward the rock surface [39].

Based on many studies and experiments that were carried out on the waterflooding process on carbonate reservoir, wettability alteration is proposed as a key reason for the improvement of the oil recovery. Due to these experiments, a chemical mechanism for the wettability modification in carbonate reservoir is suggested by Zhang et al. [39] as illustrated by 3.3-1.

It was suggested that sulfate in seawater, which is not present in the initial brine, will adsorb onto the positively charged rock surface resulting in lower the positive surface charge. As a result of reducing the positive charge of the rock surface and due to less electrostatic repulsion, more  $Ca^{2+}$  will adsorb onto the rock surface.  $Ca^{2+}$  will then be able to react with adsorbed carboxylic group bonded to the rock and release some organic carboxylic materials. As it is shown in the 3.1-4, it is further recognized that  $Ca^{2+}$  can be substituted by  $Mg^{2+}$  at the rock surface at high temperature. Since  $Mg^{2+}$  is able to

displace  $Ca^{2+}$  from the rock lattice close to the surface, it will consequently be able to displace  $Ca^{2+}$  bonded with two carboxylic group on the rock surface and it provides obtaining the access through the aqueous phase [39], [40].

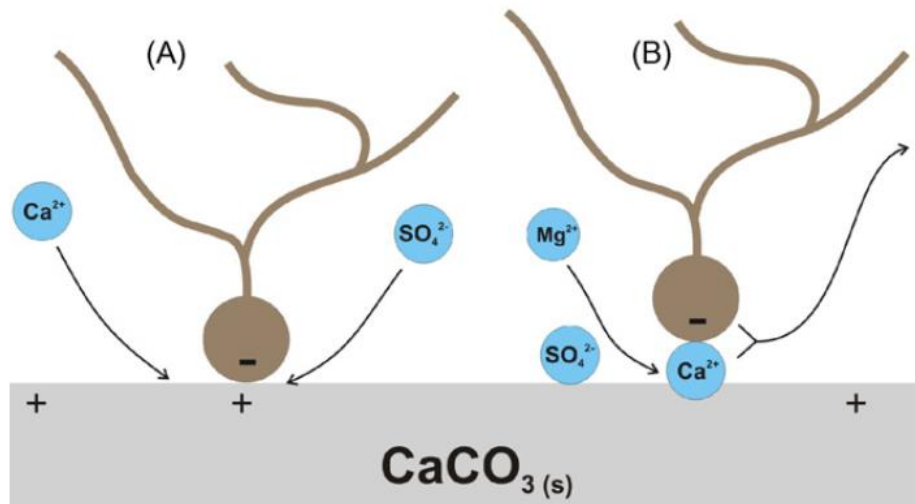


Figure 3.3-1- Schematic model of the suggested mechanism for the wettability alteration induced by seawater. (A) proposed mechanism when  $Ca^{2+}$  and  $SO_4^{2-}$  are active at lower and high temperature. (B) Proposed mechanism when  $Mg^{2+}$  and  $SO_4^{2-}$  are active at higher temperatures [39].

### 3.3.3. pH Effects

“Carbonates develop surface charge by these sites gaining or losing  $H^+$ s (surface acid-base reactions), and by subsequent adsorption of multi-valent cations or anions on the now-charged sites. For example, above pH 5 surface carbonate groups lose  $H^+$  and become negatively charged. This negative charge can be reversed if enough  $Ca^{2+}$  is adsorbed from solution onto the negatively charged carbonate groups. The net mineral surface charge is the sum of the individual surface species’ concentrations.” [41] (2017, p. 18).

Considering the fact that the pH value of smart water usually is greater than 7, the higher values of PH, the higher amount of oil recovered and it is because of changing the carbonate surface charge. According to zeta potential measurement, increasing the pH

values of smart water changes the surface charge of the both rock-brine and oil-brine interfaces [19], [42].

### 3.4. Factors Influencing Wettability

There are several main factors that affect the wettability of the rock in the reservoir. A list of these factors is briefly described as follow [1]:

- **Composition and characteristics of crude oil:** The wettability of the reservoir can be altered by deposition of organic component present in crude oil or by adsorption of polar components in crude oil. The polar end adsorbs on the surface of rock leading to expose the hydrocarbon ends and make the surface of rock more oil-wet.  
The basic components of the crude oil which are quantified by base number, have a minor affect on the wettability of rock.
- **Ionic composition of injected fluid:** The ionic composition of the injected fluid into reservoir can affect the wetting properties of the rock as well. According to many studies, presence of divalent ions such as sulphate, magnesium and calcium in the fluid will increase the wettability of the system [43].
- **Temperature:** High temperature condition makes carbonate reservoir more water-wet compared to low temperature condition [44]. As the temperature of the reservoir increases, the acid number (AN) of the crude oil decreases due to increased decarboxylation of the acidic material at high temperature [1].
- **Pressure:** As the pressure decreases toward bubble point of oil, the solubility of asphaltenes of the crude oil decreases resulting in precipitating and making the rock oil-wet by adsorbing on the rock [1].

### 3.5. Membrane Separation

Membrane separation technology which was developed in the 1950s, has been increasingly applied in large scale industrial plants in order to clarifying and concentrating dairy products, oily wastes and brine recovery and has been applied for water and wastewater treatment as well. Membrane separation (filtration) technology utilizes microporous materials to separate dissolved, colloidal and particulate constituents from a pressurized fluid. Membrane separation processes are generally classified in terms of pore size, applied pressure or molecular weight cut-off (MWCO) [45], [46]. Based on the size of the pores, membranes are categorized into 4 groups as listed below [47]:

- Microfiltration (MF)
- Ultrafiltration (UF)
- Nanofiltration (NF)
- Reverse Osmosis (RO)

Microfiltration (MF) is suitable for treatment of water with high turbidity and low organics content since it has the largest pore size of 0.1-10 microns. As it is shown in figure 3.1-5, it allows large particles to pass through, thus, it is commonly applied to separate large colloids, bacteria and suspended particulates.

Due to the pore size of Ultrafiltration (UF), 0.001-0.1 microns, shown in the figure 3.1-5, it can cut-off suspended solids, proteins, bacteria and dyes but it is not able to remove the dissolved organics.

Nanofiltration (NF) has smaller pore size compared to the MF and UF (0.0015 - 0.0030 microns) and it is suitable for water softening and removal of disinfection by-products. It allows only water and monovalent ions be able to pass through.

Reverse Osmosis (RO) with smallest pore size (0.0005 - 0.0015 microns) rejects almost all material from water and it is suitable for separation of ionic size particles in the range of the above-mentioned size.

MF and UF processes can also be applied as pre-treatment for NF and RO processes.

Figure 3.5-1 and figure 3.5-2 show a general comparison diagram of the four membrane separation processes and size ranges of each process.

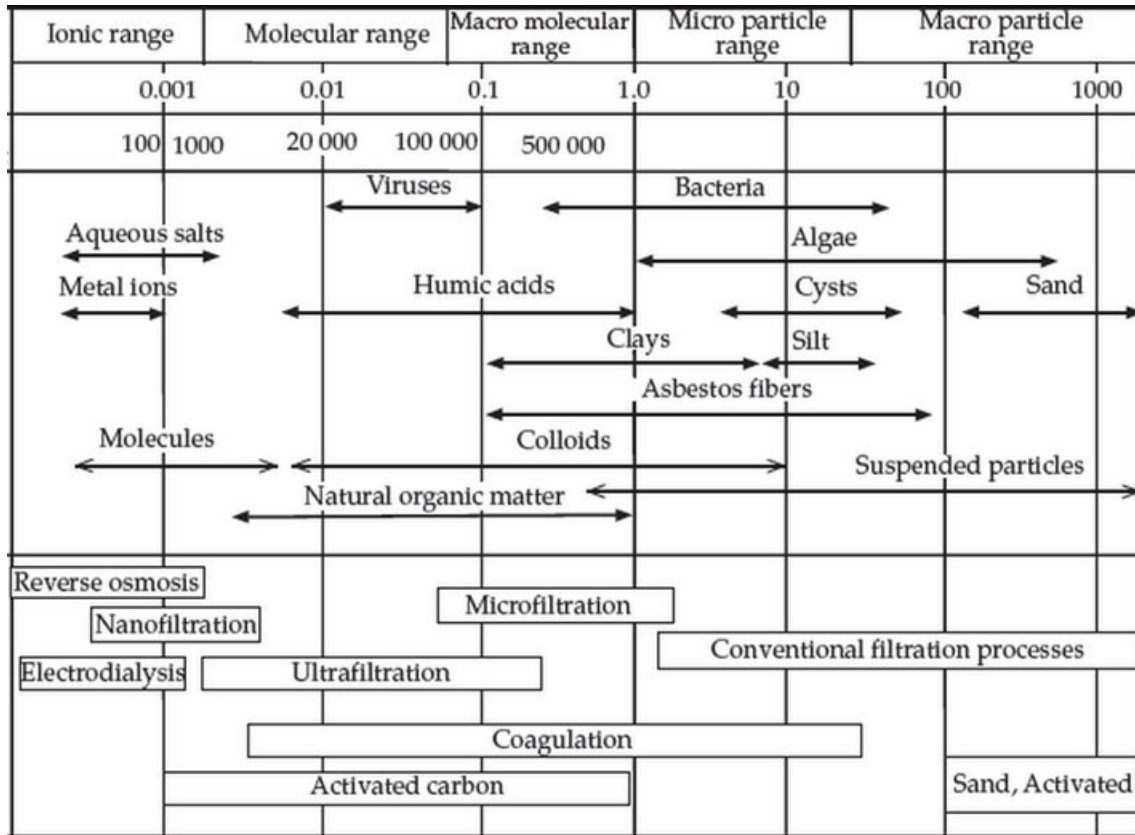


Figure 3.5-1- General comparison diagram of selected separation process based on size ranges of various materials found in raw water [48]

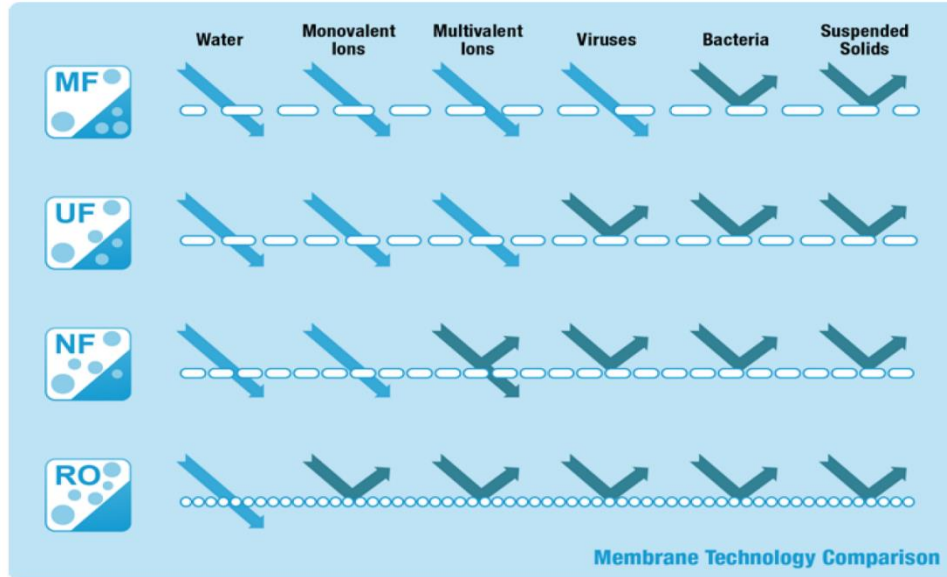


Figure 3.5-2- Graphical representation of the membranes processes performance [49]

### 3.6. Structural Design of Membranes

In order to choose a high-performance membrane and to optimize the process as well, the physical construction and chemical design can be considered as very important parameters [45], [50].

#### 3.6.1. Physical Construction of Separation Membranes

In the membrane permeation process, physical structure of the membrane can be considered as an important parameter. Due to uniformity of the pore structure along the membrane cross section, the membranes are categorized in three groups as listed below [45]:

- **Symmetric Membrane**
- **Asymmetric Membrane**
- **Thin Film Composite Membrane (TFC)**

Membranes which consist of at least two layers and are made from different polymer materials, are called "composite membranes". In thin film composite membrane, a thin dense skin layer (0,01 - 0,1  $\mu\text{m}$ ) is formed over a thick micro porous film of 100  $\mu\text{m}$ . In these membranes, the flexibility of the most design of the layers is significantly high compared to asymmetric membranes since the dense active layer and the porous support layer consist of different materials. Figure 3.6-1 shows the structure of cross-section of asymmetric and thin film composite membranes:

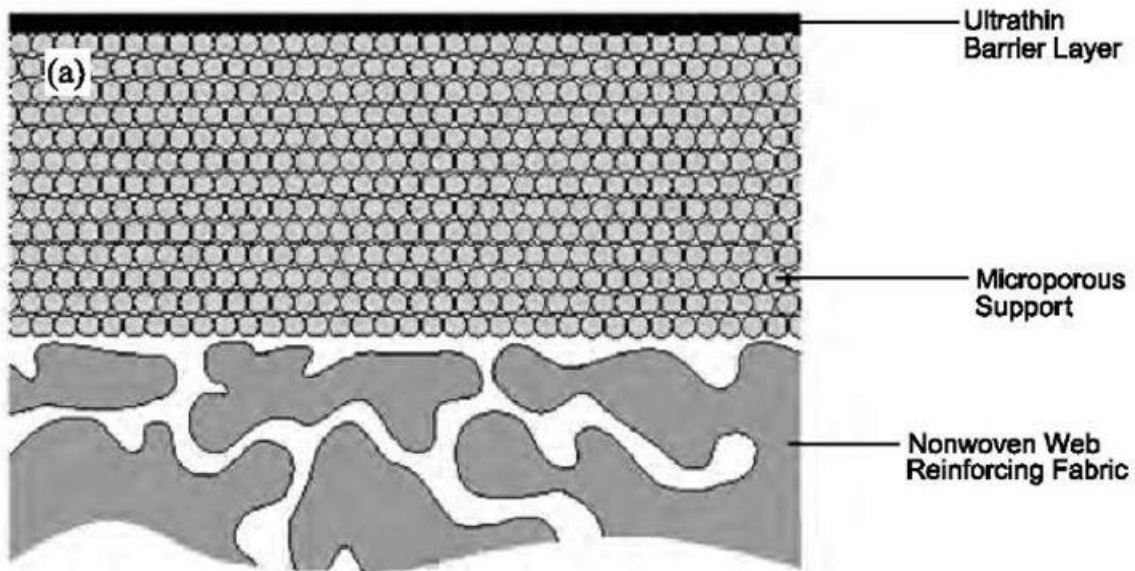


Figure 3.6-1- Structure of cross-section of thin film composite membrane [51]

In the thin film composite membranes, the different materials which are used for the dense skin layer and support layer, is adjusted for the well combination of low solute permeability and high water flux they are usually applied for Reverse Osmosis (RO) and Nanofiltration (NF) which requires high salt rejection rate and high flux [45].

### 3.6.2. Chemical Design of Membrane Materials

In terms of chemical structure, membranes are generally categorized into three groups as follow [45]:

- **Organic Membrane**
- **Inorganic Membrane**
- **Organic-Inorganic Membrane (Hybrid)**

Organic membranes which are usually made of polymer, have a particular importance in the industry. These membranes can be made of natural or synthetic polymers based on compatibility membrane fabrication technology or desired application use. Examples of natural and synthetic polymers include polysulfide, cellulose acetate, polyacrylonitrile, aromatic polyamides and etc. [52], [53], [54], [55], [56].

### 3.7. Membrane Shapes and Configurations

In terms of shape, there are several types of membranes available in material separation as listed and briefly described below [57], [45]:

- **Flat-Sheet Membranes**
- **Spiral Membranes**
- **Tubular Membranes**
- **Capillary Membranes**
- **Hollow-Fibre Membranes**

Flat-Sheet membrane is the simplest and most popular type of membrane which has been used since the beginning of the membrane study is Flat-Sheet membrane. They are manufactured of a sheet-like backing material with a membrane cast on the surface of the sheet and they are constructed with and without a support sheet. Spiral membranes are recognized as the most economical and inexpensive membranes which are basically

sheets arranged on top of each other to form several narrow slits for fluid flow. The spiral-wound membranes are constructed of one to more than 30 membranes leaves and each leaf is made of two membranes sheets attached together end-to-end by glue with a permeate spacer in between them. Tubular membranes are located on the inside or outside of a tube which is made of special kind of material and they have porous walls. Tubular membrane modules usually consist of a minimum of two tubes; inner tube which is called membrane tube and outer tube which is shell. Organic and inorganic membranes are used as materials of the tubular elements [58]. Capillary membranes work on the same basis of tubular membranes and the only difference is that the tubes used in the capillary membranes are smaller than the tubes used in the tubular membranes. Capillary membranes are recognized as a selective barrier since they are strong enough to resist filtration pressures. In capillary membrane chance of plugging is higher due to the smaller diameter but as a benefit the packing density is much greater [59]. Hollow-Fibre membranes work on the same principle as capillary and tubular shapes and the only difference is that the tubes used in the hollow-fiber membranes are smaller which allows for flexibility. Materials used for hollow-fiber membranes are almost all organic polymer such as polyethylene, polyacrylonitrile, cellulose acetate and etc. [60], [61].

### **3.8. Advantages of Membrane Separation Process over Traditional Separation Processes**

There are several advantages of membrane separation processes compared to the traditional separation processes that listed below [54], [55], [9]:

- Low energy consumption
- Highly selective separation
- Constant temperature operation with no phase change
- Relatively low capital investment and operating costs
- Continuous and automatic operation
- Simple modular construction

### 3.9. Membrane Performance

In order to evaluate the performance of a given membrane, there are three crucial parameters: flux (solvent permeability) through membrane, rejection of solutes and recovery or yield for the operation of a nanofiltration unite. These parameters which are known as permeation characteristics of nanofiltration membrane, are described below [62]:

- **Membrane Flux**

Membrane flux or permeation flux (J) is defined as the volume of fluid flowing through the membrane per unite membrane area per unit time. The parameter affecting the membrane flux mainly are pressure, fluid viscosity and pore size. The simplified form of the flux equation is:

$$\text{Membrane Flux (J)} = \left( \frac{F_p}{A} \right) * 100$$

Equation 3.9-1

Where,

$$J = \text{Membrane Flux } \left( \frac{L}{m^2hr} \right)$$

$$F_p = \text{Flowrate of Permeate } \left( \frac{L}{hr} \right)$$

$$A = \text{Nominal Membrane Area (m}^2\text{)}$$

- **Membrane Rejection**

Membrane rejection is defined as the amount of the solutes which have been rejected from fluid. Membrane rejection parameter is also known as desalting degree which shows the percent rejection of salts by the membrane and it can be calculated from the following equation:

$$\text{Membrane Rejection}(\%) = \left(1 - \frac{C_{pi}}{C_{ri}}\right) * 100$$

Equation 3.9-2

Where,

$C_{pi}$  = Concentration of salt (component i) in the permeate flow  
 $C_{ri}$  = Concentration of salt (component i) in the retentate flow

Membrane rejection is a dimensionless parameter and its value usually varies between 100% (complete rejection of solute) and 0% (solvent and solute pass freely through the membrane). The rejection of ions in NF membrane is predominantly dependent on the ion size, hydrophobicity, and charge.

- **Membrane Recovery**

Recovery of the membrane is usually defined as the amount of the water which is permeated from the membrane per unite time as the product of process. It can be calculated from the following equation:

$$\text{Membrane Recovery} = \left(\frac{F_p}{F_f}\right) * 100$$

Equation 3.9-3

Where,

$F_p = \text{Flowrate of Permeate } \left(\frac{L}{hr}\right)$

$F_f = \text{Flowrate of Feed } \left(\frac{L}{hr}\right)$

### 3.10. Parameters Affecting the Performance of Nanofiltration Membrane

During the designing a nanofiltration process, one should take into consideration several physical and chemical parameters which affect the permeation and rejection performance of the process. In the following section, the important operating parameters are briefly described [61], [45]:

- **Transmembrane Pressure**

This parameter is the driving force responsible for the transport in the NF process. The effective driving pressure is the exerted hydraulic pressure less than osmotic pressure which is exerted on the membrane by the solutes. The higher the transmembrane pressure, the greater driving force across the membrane resulting an increase in flux. But on the other hand, at higher pressure, deposition on the membrane occurs at faster rate leading to increasing in the osmotic pressure of the solution at the surface which leads to the reduction in the driving force of the solvent transport. Nanofiltration membrane provides fair separation at net pressure of 10 bar (150 psi) or higher [57].

- **Feed Concentration**

The osmotic pressure and the activity of the of the solution increase as the concentration of solute increases resulting to increase the membrane surface concentration and decrease driving force for the solvent flux. Thus, the increase in salt concentration leads to a decrease in the permeate flux. Since the effective pore radius of a charged pore increase as the ionic strength of the solution increases, the rejection of monovalent ions

decreases as their concentration in the feed increases. This phenomenon for divalent ions happens in a lower extent [61], [63].

- **Temperature**

The NF membrane flux increases with increase in the temperature of the process and it is due to reduction in the viscosity of the feed (reduction in the viscosity of the feed accelerate the higher diffusivity of solutes and polymer chain mobility) [9]. The rejection of NF membrane process doesn't change with the varying in the temperature of the process.

- **Cross flow Velocity**

This parameter is valid for cross-flow processes where with increase in the crossflow velocity in the NF membrane process the permeation flux increases due to efficient removal of fouling layer from the membrane surface [61].

- **Solution pH**

This parameter is a critical parameter since it affects the performance of the NF membrane process in more than one way. At neutral pH and higher, the NF membrane surface (charged side) is negatively charged but it loses its charged in the acidic solution (lower pH) which leads to increase in the rejection of NF membrane. According to the results of various studies, zeta potential becomes more and more negative for most of the membranes as the values of the pH are increased and it leads to increase the electrostatic repulsion between a co-ion and membrane surface. Vice versa, presence of counter-ions in the solution reduces the negative zeta potential of the NF membrane. Thus, different ranges of pH affect the performance of the NF membrane [13], [45].

### 3.11. Membrane System Modes

Filtration system modes using membrane technology can be categorized in two major types [64], [65]:

- Cross-flow filtration
- Dead-end filtration (throughflow)

When cross-flow filtration takes place, the concentrated feed solution is recycled and flows across the surface of membrane. Due to this process, only a small part of feed is permeated and the largest part of it leaves the system and it is recycled again. During the dead-end filtration process, all the solution that enters the membrane surface is passed through the membrane except some components and solids that stay behind the membrane. These collected solids and components on the surface of membrane grow in thickness and reduce the flow. The differences between two filtration system modes are illustrated in figures 3.11-1 and 3.11-2 below:

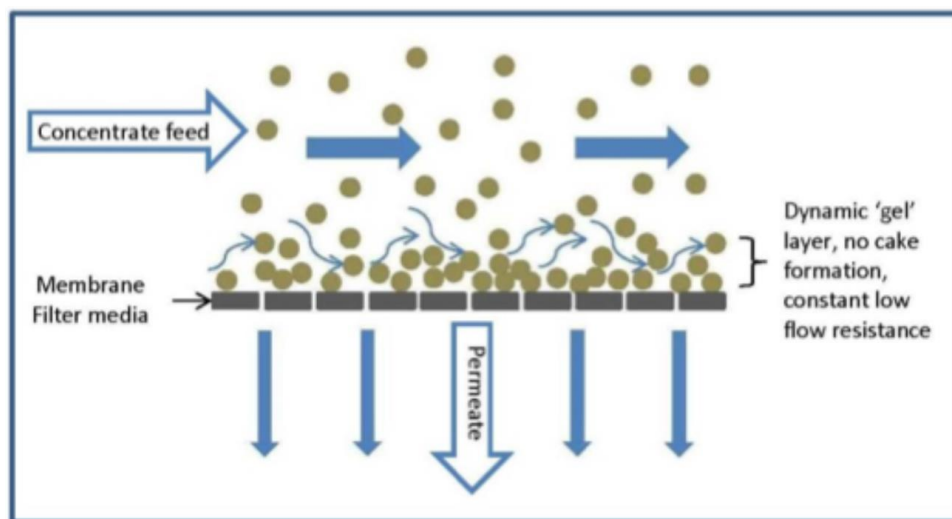


Figure 3.11-1- A schematic of cross-flow filtration process [66]

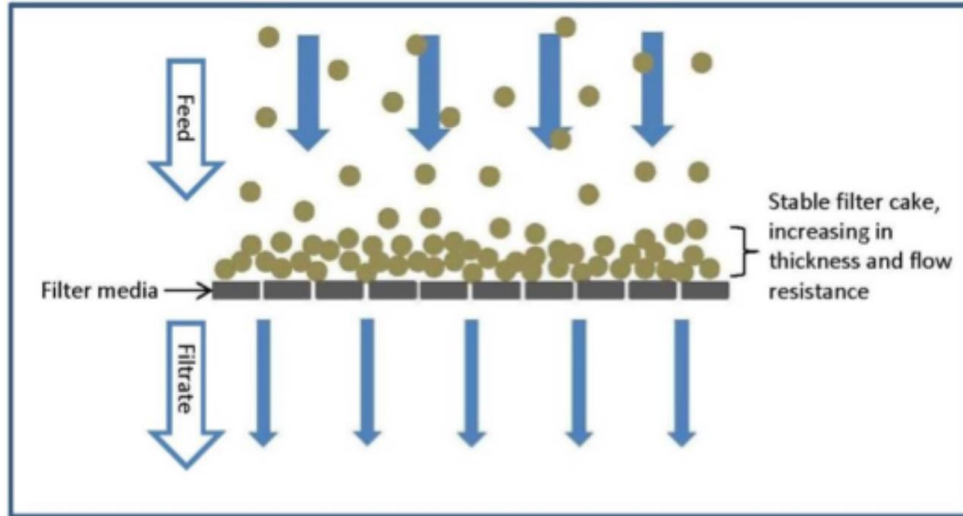


Figure 3.11-2- A schematic of dead-end filtration process [66]

In this thesis, dead-end process was used during filtration experiments using membrane.

# ***4. CHAPTER 4***

## ***(Materials and Methods)***

As stated in the problem delimitation, the purpose of the project in the first step is to investigate the wettability changes of rock system due to interaction between crude oil, rock and different brines using Modified Flotation Technique (MFT) and in the second step is to produce smart water with desired composition (Low salinity -low concentration of NaCl- while retaining divalent ions) to increase the wettability of rock system using membrane process technology. In the following sections, both the above-mentioned series of the experiments and materials are described in detail.

## **4.1. Flotation Experiment**

### **4.1.1. Experimental Materials and Methods**

The purpose of the project in this section is to investigate and measure the changes in the wettability of the rock system (Dan Chalk) in the reservoir using experiments which are called flotation technique. For this purpose, the experiments were carried out using crude oil provided by Maersk Oil company from Danish Nord Sea and chalk (reservoir rock) that was obtained from Dankalk A/S, Denmark. This method is a simulated procedure for waterflooding process in the reservoir which must be accurately done in the lab, taking into account all the parameters that affect the process and results. Therefore, it is important to consider the characteristics of crude oil, rock system and brines which govern the process and wettability properties. In the following sections the most important characteristics of CBR (Crude oil, Rock and Brine) system are described.

### **4.1.2. Crude Oil and Reservoir Rock Characteristics**

Crude oil characteristics such as density, acid number (AN) and base number (BN) are present in table 4.1-1. The density of the crude oil was determined by using Anton paar DMA35 portable density meter. Acid and base number of the crude oil were determined using Metrohm autotitrator tiemo 2.4, OIL PAK methods 4/5 for the acid number (AN) estimation and method 1/2 for the base number (BN) determination. In the figure 4.1-1 the plot obtained mentioned methodology is shown [41]:

Table 4.1-1- Characteristics of crude oil from North Sea reservoir

AN (mgKOH/g)	BN (mgKOH/g)	Density (at 25 °C)
0.2	0.2	0.834

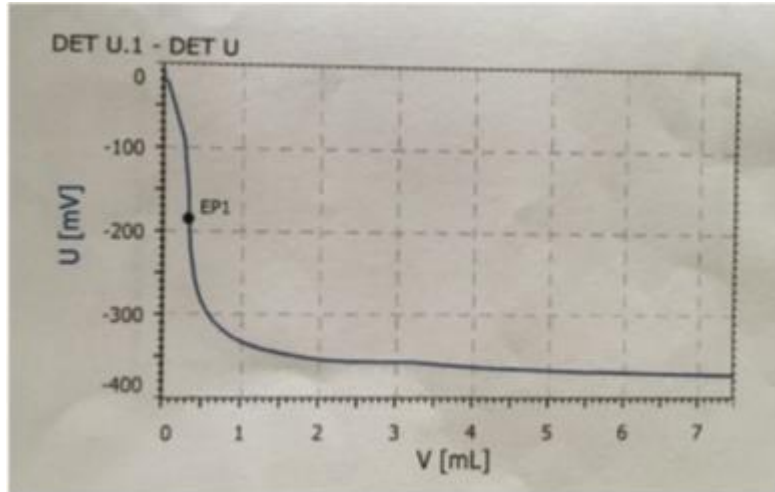


Figure 4.1-1- Titration Results for Acid Number (U is the potential (mV), V is the added volume of titrant and EP stands for equivalence point)

Table 4.1-2- Composition of Dan Chalk

Species	Percent (%)
$CaCO_3$	96.2
$Al_2O_3$	0.17
$MgCO_3$	0.54
$SiO_2$	1.25
Total $CO_3$	96.74

Chemical composition of the chalk as an important parameter which governs the wettability is present in table 4.1-2 and table 4.1-3. These characteristics were obtained from last studies done in the department. The chalk sample was dried to ensure no moist present in the sample and it was then pulverized and sieved to fraction smaller than 100 microns to ensure the smallest surface area for particles due to the flotation technique

idea. The chalk sample handled carefully during the preparation in order to avoid contamination.

*Table 4.1-3- Density of Dan Chalk*

Density (g/cm <sup>3</sup> )
0.709760

### **4.1.3. Modified Flotation Technique (MFT) Steps**

Modified flotation technique (MFT) is an effective and reliable technique to give an indication of wettability for a given type of chalk immersed in a crude oil and a formation brine [19]. Due to this technique in an aqueous solution, the particles (Chalk grain) with strong adhesion to water (water-wet or hydrophilic) sink in the bottom of test tube, while the particles (Chalk grain) with weak adhesion to water (oil-wet or hydrophobic) are suspended or float. The reason for this phenomenon is the difference in surface wettability of particles versus brine and crude oil [67]. Flotation technique allows valuable grains to float while unwanted grains sink. As the main advantage of the flotation technique, it is able to provide results in less time compared to the other methods of wettability measurement such as core flooding which take longer to complete. Furthermore, in the flotation technique it is easy to evaluate individual parameters. As an example, the influence of temperature or pH on wettability of grains.

The procedure of modified flotation technique consists of several stages as listed below [67]:

1. One gram of rock (Dan Chalk) with grain size less than 100  $\mu\text{m}$  is aged for a period of 24 hours in 10 ml of brine at temperature of interest (in this project 100 °C). The contents

of the test tube (chalk and brine) is shaken in a vortex shaker to ensure perfect contact of the rock surface and the brine;

2. The column of the brine above the saturated chalk grains is decanted into another test tube and sealed for pH measurement;
3. Brine-wet grains are then aged with a 5 ml of crude oil for 24 hours at the same temperature of interest (100 °C) and shaken with the vortex shaker twice a day;
4. After oil aging, the decanted brine from step 2 is poured back into the test tube and gently shaken;
5. Mixture of the crude oil, brine and rock is allowed to settle for a couple of hours;
6. The floating grains (oil-wet grains) are removed and the walls of test tube are rinsed with Deionized water and this step is repeated a couple of times to ensure the oil is completely removed;
7. The test tube containing the water-wet grains is dried at 100 °C and then the dried and cooled test tube is weighted;
8. After step 7, it is important to recognize that the water-wet grains in the test tube are partially coated with oil which couldn't be removed during the rising process. To remove the attached oil ca. 3-5 ml of a volatile organic solvent (in this project is pentane) is added to the tube and shaken and the dissolved oil is then decanted. This step is repeated until the attached oil is completely removed;
9. The test tube is dried at the temperature of approximately 38 °C;
10. The dried and cooled test tube is weighted.

In order to calculate the amount of oil-wet grains, the dried and cooled water-wet grains from step 10 are subtracted from original mass of chalk (one gram).

A general schema and step-by-step laboratory procedure of modified flotation technique is shown in the figure 4.1-2:

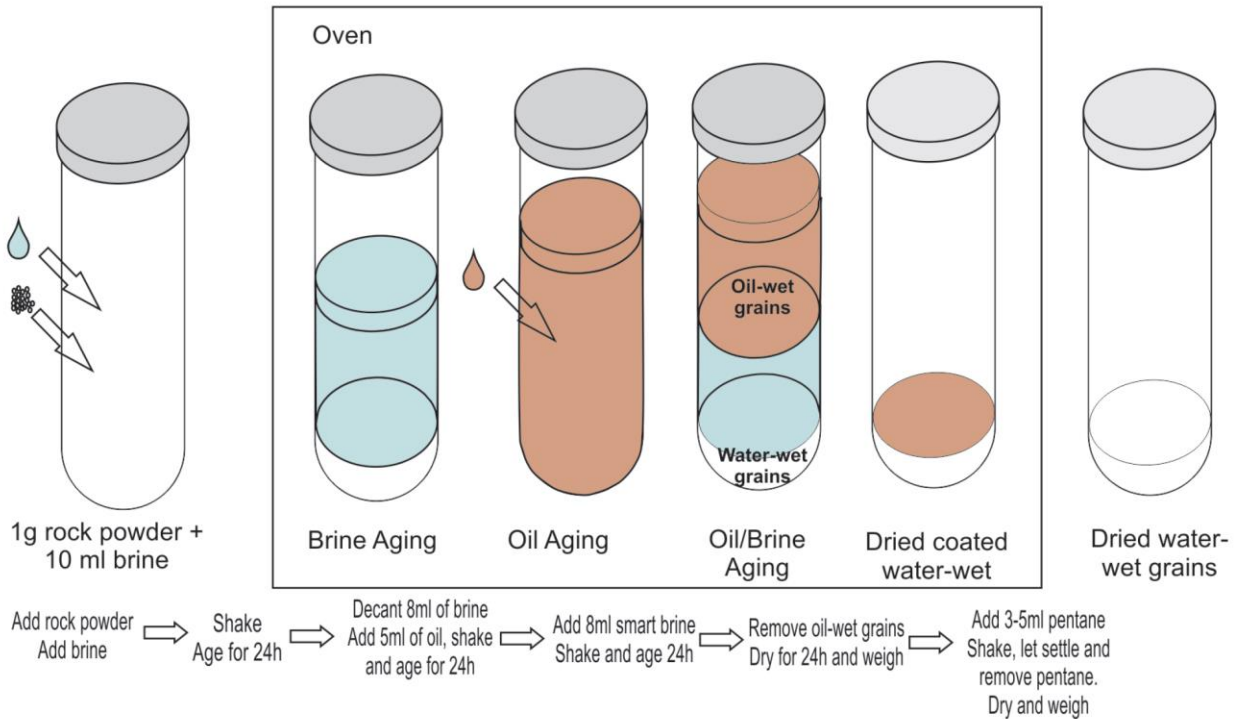


Figure 4.1-2- Modified Flotation Technique laboratory procedure at 100 °C of oven temperature. The drop shape represents the addition of brine (blue) and crude oil (brown) [17]

#### 4.1.4. Different Brines and Preparation

As mentioned in the previous section, at the first part of the experiments, the project is aimed to investigate the wettability alteration of the reservoir rock upon interaction with different brines which are differ in composition. The recipes that are shown in tables 4.1-4 and 4.1-5, were used to prepare synthetic seawater and its different composition and Ekofisk formation water (EFW) as well [2].

*Table 4.1-4- Synthetic seawater recipe*

<b>Salat</b>	<b>Concentration (g/l)</b>
NaCl	23.38
Na <sub>2</sub> SO <sub>4</sub>	3.41
NaHCO <sub>3</sub>	0.170
KCl	0.750
MgCl <sub>2</sub> * 6H <sub>2</sub> O	9.05
CaCl <sub>2</sub> * 2H <sub>2</sub> O	1.91
<b>TDS</b>	<b>38.67</b>

Table 4.1-5- Ekofisk formation water recipe

Salat	Concentration (g/l)
NaCl	67.3
KCl	0.549
NaHCO <sub>3</sub>	0.332
BaCl <sub>2</sub> * 2H <sub>2</sub> O	0.45
SrCl <sub>2</sub> * 6H <sub>2</sub> O	2.270
Na <sub>2</sub> SO <sub>4</sub>	0
MgCl <sub>2</sub> * 6H <sub>2</sub> O	4.45
CaCl <sub>2</sub> * 2H <sub>2</sub> O	14.69
TDS	90.041

The preparation of synthetic brine was based on published composition for a reference volume of 1 liter and room temperature [17]. The following steps were used to prepare the synthetic brines based on the recipes:

- a. Chloride salts are diluted in 400 ml of deionized water;
- b. Sulphate salts are diluted in 200 ml of deionized water;
- c. Carbonate salts are diluted in 200 ml of deionized water;
- d. The brines are mixed into a volumetric flaks and 200 ml of deionized water are added;
- e. The solution is stirred until all the salts are fully dissolved.

## 4.1.5. Ionic Concentration and Composition of Brines

Having use the instruction for preparing synthetic brines described in the last section, 7 sets of synthetic brines with their dilutions were prepared in the lab. Table 4.1-6 shows all types of brines with different composition used in the flotation experiments:

*Table 4.1-6- Types of brines and their dilutions*

Brines	Origin
Ekofisk FW	Synthetic
Syn. SW	Synthetic
Syn. SW 2D	Synthetic
Syn. SW 20D	Synthetic
Syn. SW 100D	Synthetic
Syn. SW0S	Synthetic
Syn. SW0S0Ca	Synthetic
Syn. SW0S0Ca 2D	Synthetic
Syn. SW0S0Ca 20D	Synthetic
Syn. SW0S0Ca 100D	Synthetic
Syn. SW0S0Mg	Synthetic
Syn. SW0S0Mg 2D	Synthetic
Syn. SW0S0Mg 20D	Synthetic
Syn. SW0S0Mg 100D	Synthetic
Syn. SW0Ca0Mg	Synthetic
Syn. SW0Ca0Mg 2D	Synthetic
Syn. SW0Ca0Mg 20D	Synthetic
Syn. SW0Ca0Mg 100D	Synthetic
Syn. SW0S0Ca0Mg	Synthetic
SEA WATER	North Sea

The composition of ions and ionic strength have an effective impact on the wettability alteration of rock system in reservoir. By dissolving an ionic solid in water, cations and anions are separated and it is then possible for them to move around in the solution leading to conduct the electrical current by the solution [19]. According to general dissociation

theory, when an ionic solid is dissolved in water, equilibrium is reached between anions and cations. General procedure of the calculation of the ionic concentration and ionic strength which is based on the dissociation theory, is described as following [68], [69]:

- A. Knowing the molecular weight of particular salt and the amount of mass added to the solution, one can calculate the molarity:
- B. Due to the general dissociation theory, the amount of moles of each dissociated anion and cation is calculated;
- C. The total amount of each cation and anion is summed;
- D. Total Dissolved Solids (TDS) is equal to the sum of total amount of salts added to the aqueous phase.

To estimate ionic strength which is used to express the ionic composition solution, the following equation 4.1-1 is used:

$$\mu = \frac{1}{2} \sum C_i Z_i^2$$

Equation 4.1-1

Where,

$$\mu = \text{Ionic Strength } \left(\frac{\text{mol}}{\text{l}}\right)$$

$$C_i = \text{Concentration of Ion } \left(\frac{\text{mol}}{\text{l}}\right)$$

$$Z_i = \text{Charge of Ion}$$

Table 4.1-7 shows the calculated molar concentrations, ionic strengths, TDS and densities of all brines:

Table 4.1-7- Calculated molar concentrations, ionic strengths, TDS and densities of all brines

Brine (s.l.)	Chloride (Cl <sup>-</sup> )	Sulphate (SO <sub>4</sub> <sup>2-</sup> )	Sodium (Na <sup>+</sup> )	Magnesium (Mg <sup>2+</sup> )	Calcium (Ca <sup>2+</sup> )	Potassium (K <sup>+</sup> )	Bicarbonate (HCO <sub>3</sub> <sup>-</sup> )	Strontium (Sr <sup>2+</sup> )	Barium (Ba <sup>2+</sup> )	Bromide (Br <sup>-</sup> )	Borate (BO <sub>3</sub> <sup>3-</sup> )	TDS	Ionic Strength	Density
	mmol/l	mmol/l	mmol/l	mmol/l	mmol/l	mmol/l	mmol/l	mmol/l	mmol/l	mmol/l	mmol/l	(g/l)	(mol/l)	(g/cm <sup>3</sup> )
Ekofisk FW	1423,306	0,000	1155,561	21,889	99,922	7,364	3,952	8,514	1,842	0,000	0,000	90,04	1,559	1,049
Syn. SW	525,142	24,007	450,107	44,515	12,992	10,060	2,024	0,000	0,000	0,000	0,000	38,67	0,657	1,021
Syn. SW 2D	262,571	12,004	225,054	22,258	6,496	5,030	1,012	0,000	0,000	0,000	0,000	19,335	0,328	1,011
Syn. SW 20D	26,257	1,200	22,505	2,226	0,650	0,503	0,101	0,000	0,000	0,000	0,000	1,9335	0,033	1,001
Syn. SW 100D	5,251	0,240	4,501	0,445	0,130	0,101	0,020	0,000	0,000	0,000	0,000	0,3867	0,007	0,998
Syn. SWOS	525,140	0,000	402,090	44,510	12,990	10,060	2,020	0,000	0,000	0,000	0,000	35,26	0,585	1,018
Syn. SWOSCa	499,160	0,000	402,090	44,510	0,000	10,060	2,020	0,000	0,000	0,000	0,000	33,35	0,546	1,017
Syn. SWOSCa 2D	249,580	0,000	201,045	22,255	0,000	5,030	1,010	0,000	0,000	0,000	0,000	16,675	0,273	1,011
Syn. SWOSCa 20D	24,958	0,000	20,105	2,226	0,000	0,503	0,101	0,000	0,000	0,000	0,000	1,6675	0,027	1,001
Syn. SWOSCa 100D	4,992	0,000	4,021	0,445	0,000	0,101	0,020	0,000	0,000	0,000	0,000	0,3335	0,005	0,996
Syn. SWOSOMg	436,110	0,000	402,090	0,000	12,990	10,060	2,020	0,000	0,000	0,000	0,000	26,21	0,451	1,017
Syn. SWOSOMg 2D	218,055	0,000	201,045	0,000	6,495	5,030	1,010	0,000	0,000	0,000	0,000	13,105	0,226	1,009
Syn. SWOSOMg 20D	21,806	0,000	20,105	0,000	0,650	0,503	0,101	0,000	0,000	0,000	0,000	1,3105	0,023	0,998
Syn. SWOSOMg 100D	4,361	0,000	4,021	0,000	0,130	0,101	0,020	0,000	0,000	0,000	0,000	0,2621	0,005	0,992
Syn. SWOCaOMg	410,132	24,007	402,090	0,000	0,000	10,060	2,020	0,000	0,000	0,000	0,000	27,71	0,460	1,019
Syn. SWOCaOMg 2D	205,066	12,004	201,045	0,000	0,000	5,030	1,010	0,000	0,000	0,000	0,000	13,855	0,230	1,012
Syn. SWOCaOMg 20D	20,507	1,200	20,105	0,000	0,000	0,503	0,101	0,000	0,000	0,000	0,000	1,3855	0,023	1,003
Syn. SWOCaOMg 100D	4,101	0,240	4,021	0,000	0,000	0,101	0,020	0,000	0,000	0,000	0,000	0,2771	0,005	0,994
Syn. SWOSCaOMg	410,132	0,000	402,090	0,000	0,000	10,060	2,020	0,000	0,000	0,000	0,000	24,3	0,412	1,011

#### 4.1.6. pH and Density of Brines and Measurement Method

pH/conductometer Metrohm 914 was used to measure the initial and final pH of synthetic brines. It was calibrated with two buffers (pH=4 and pH=7) at ambient temperature. The initial pH of the all brines were measured at ambient temperature and the final pH of all decanted brines were measured at 100 °C.

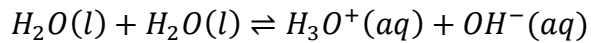
Anton Paar DMA 35 portable density meter (accuracy 0.001 g/cm<sup>3</sup>, reproducibility 0.0005 g/cm<sup>3</sup>) was used to measure the density of the all brines at the ambient temperature in the initial stage (before aging). The results are shown in table 4.1-8:

Table 4.1-8- pH and measurement of brines at ambient temperature

Brine (s.l.)	Density	pH
	(g/cm <sup>3</sup> )	
Ekofisk FW	1,049	6,99
Syn. SW	1,021	7,77
Syn. SW 2D	1,011	7,8
Syn. SW 20D	1,001	8,32
Syn. SW 100D	0,998	8,6
Syn. SW0S	1,018	7,6
Syn. SW0S0Ca	1,017	7,8
Syn. SW0S0Ca 2D	1,011	7,92
Syn. SW0S0Ca 20D	1,001	8,1
Syn. SW0S0Ca 100D	0,996	8,19
Syn. SW0S0Mg	1,017	7,72
Syn. SW0S0Mg 2D	1,009	7,9
Syn. SW0S0Mg 20D	0,998	8,17
Syn. SW0S0Mg 100D	0,992	8,29
Syn. SW0Ca0Mg	1,019	7,33
Syn. SW0Ca0Mg 2D	1,012	7,44
Syn. SW0Ca0Mg 20D	1,003	7,81
Syn. SW0Ca0Mg 100D	0,994	8,15
Syn. SW0S0Ca0Mg	1,011	7,42

According to Le Chatelier's principle (equilibrium law), "when any system at equilibrium is subjected to change in concentration, volume, temperature or pressure, the system

readjusts itself counteract (partially) the effect of the applied change and a new equilibrium is established”, if the temperature of water increases, it leads to change the equilibrium of the system and it will cool down the system by absorbing extra heat. As it can be seen from the balanced equation 4.1-2 (water autoprotolysis), the forward reaction is favored as the result of the increase in temperature of the system. Thus, more hydronium and hydroxide ions are formed and the value of autoionization constant ( $K_w$ ) increases resulting to decrease the value of pH. This behaviour can be denoted by comparing the values of pH in table 4.1-8.



Equation 4.1-2

### 4.1.7. Reservoir Rock Water-wet and Oil-wet Fractions and Calculations

After performing the MFT experiments and collecting data with high precision, two important parameters including water-wet and oil-wet fraction were calculated using the following equations:

$$\text{Water-wet Fraction (\%)} = \frac{\text{weight of water-wet particles (g)} * 100}{\text{Initial weight of rock particles (g)}}$$

Equation 4.1-3

$$\text{Oil-wet Fraction (\%)} = \frac{\text{weight of oil-wet particles (g)} * 100}{\text{Initial weight of rock particles (g)}}$$

Equation 4.1-4

## 4.2. Smart Water Production Experiment

### 4.2.1. Experimental Materials and Methods

In this step of experiment, the project is aimed to produce smart water with desired composition (low salinity while retaining divalent ions such as magnesium, sulphate and calcium) using nanofiltration and reverse osmosis technology. For this purpose, the experiments of membrane process were carried out using filtered seawater collected from Esbjerg harbor as feed. Since the characteristics of the feed passing through the membrane has a decisive role in the performance of the process, determination of the characteristics of the seawater including pH, density, conductivity and composition was performed as the first and most important stage of the work.

- **pH:** pH/Conductometer Metrohm 914 was used to measure the pH of the filtered seawater. It was calibrated with two buffers (pH=4 and pH=7) at ambient temperature.
- **Density:** Anton Paar DMA 35 portable density meter (accuracy 0.001 g/cm<sup>3</sup>, reproducibility 0.0005 g/cm<sup>3</sup>) was used to measure the density of the filtered seawater at the ambient temperature.
- **Conductivity:** 912/Conductometer Metrohm (accuracy  $\pm 0.005$  at 0.1  $\mu\text{S}$  – 500 mS) was used to measure the conductivity and salinity of the feed at the ambient temperature.
- **Composition:** In order to determine and measure the concentration of major ions in seawater, two machines were used: Ion Chromatography (IC) was used for major anions (chloride and sulphate) and Inductively Coupled Plasma-Mass Spectrometry (ICP-MS) was used for major cations (Calcium, Magnesium and Sodium). Both machines are described in detail in the following sections.

### 4.2.2. Analysis of Ions (Ion Chromatography (IC))

Ion chromatography Metrohm (833 IC Liquid Handling Unit, 818 IC Pump, 819 IC Detector, 771 IC Compact Interface, 820 IC Separation Center, 813 Compact Autosampler) was used to measure the concentration of anions of feed and samples from

different membrane processes. The samples were diluted to 100, 1000, 10000 and 2000 times of its concentration depending on the membrane process in order to get more accurate results. The samples were poured into labeled glass tube (10 ml capacity- minimum amount of sample for analysis was ca. 5 ml) and were processed in the machine. Each sample took ca. 12 minutes in the machine to be processed.

The output report from the IC machine is a graph showing several peaks. Each peak represents a separate ion from the sample solution. The elution time (the time it takes for ion to move through the column) varies for each ion species as they elute from the column separately as the pH or ionic strength of the eluent is increased. The concentration of ions moving through the column at a particular time is represented by the area under each peak and it can be correlated to the concentration of a specific species in the sample solutions [70], [9]. Ion Chromatography machines usually provide a software which calculates the area under each peak and eventually reports the concentration of each ion in mg/l, ppm (parts-per-million) and etc. The IC machine is shown in figure 4.2-1 and the machine output reports including the graph and the concentration of ions in the samples are provided in the appendix section.



Figure 4.2-1- Ion Chromatography (IC) machine

### **4.2.3. Analysis of Metals (Inductively Coupled Plasma-Mass Spectrometry (ICP-MS))**

Inductively Coupled Plasma-Mass Spectrometry (ICP-MS) is an ionization source which completely decomposes a sample into its constituent elements and transforms these elements into ions. It is usually composed of argon gas and energy is coupled to it using an induction coil to form plasma [71]. Optical Emission Spectrometer PerkinElmer (ICP-MS, Optima 8000) was used to measure the concentration of cations of feed and samples from different membrane processes. The samples were diluted to 100, 1000, 10000 and 2000 times of its concentration depending on the membrane process in order to get more accurate results. The samples were poured into labeled tube (10 ml capacity-minimum amount of sample for analysis was ca. 5 ml) and were processed in the machine. Each sample took ca. 5 minutes in the machine to be processed. The machine was calibrated with standard solutions and certified reference material before placing the samples in the machine each time.

When the sample solution introduced into the device using a peristaltic pump, atomic elements are led through a plasma source where the elements become ionized and the ions are separated on the basis of their mass-to-charge ratio. These ions are then sorted on account of their mass and a detector receives an ion signal proportional to the concentration [72]. The output report of the ICP-MS machines for all the samples from different membrane processes are provided in appendix section.

Figure 4.2-2 shows the Inductively Coupled Plasma-Mass Spectrometry (ICP-MS) machine:



Figure 4.2-2- Inductively Coupled Plasma-Mass Spectrometry (ICP-MS) machine

#### 4.2.4. Properties of Seawater

In order to thorough analysis of the results, the main characteristics of the feed (Normal filtered seawater) and all the samples extracted after filtration including ionic composition, pH, conductivity and TDS were measured and recorded in all steps of experiments. The ionic composition (major ions) and other important characteristic of the feed are shown in the following table:

Table 4.2-1- Characteristics of seawater

<b>Characteristics of Filtered Seawater</b>	
Ions	Concentration (mg/l)
Chloride ( $Cl^-$ )	17151,50
Sulphate ( $SO_4^{2-}$ )	2100,00
Sodium ( $Na^+$ )	8962,50
Magnesium ( $Mg^{2+}$ )	1062,00
Calcium ( $Ca^{2+}$ )	427,50
<b>Other Characteristics of Filtered Seawater</b>	
pH	7.46
TDS (mg/l)	38670
Conductivity (mS/cm)	39.6

#### 4.2.5. Membranes for Separation

Separation experiments were carried out in Nano-Filtration Laboratory (AAU) using dead-end filtration process and two types of membranes; nanofiltration membrane (NF) and reverse osmosis membrane (RO). As mentioned in the previous sections, thin-film composite membrane was used for nanofiltration and reverse osmosis experiments. The experimental setup was performed by passing deionized water through the membrane at pressure of 10 bar for five minutes. Nitrogen cylinder was used to apply the pressure. The membranes used for separation processes and their process principles and mechanisms are described in detail below:

### 4.2.5.1. Nanofiltration Membrane (NF)

Nanofiltration technology with a reasonable water flux at relatively low pressures developed as pressure-driven membrane process for liquid-phase separation when the first efforts of reverse osmosis development with low water flux at high pressures was started. Although the rejection of nanofiltration was not as good as reverse osmosis, it was considered as a great improvement for membrane technology with high water permeability. As explained in previous sections, nanofiltration technique with a pore size of approximately 1 nm is located between reverse osmosis technique where transport is governed by a solution-diffusion mechanism and ultrafiltration technique where separation mechanism is due to size exclusion and in some case, due to charge effects. Thus, the separation mechanism in nanofiltration is based on a combination of RO and UF mechanism with an addition effect of charge which is due to surface characteristics of nanofiltration membrane [73], [57].

#### 4.2.5.1.1. Process Principle and Mechanism

In any process the mechanism of the fluid dynamic occurring inside the respective equipment is the most important part of the process to understand and improve it. The mechanism of separation of solutes at the nanofiltration membrane surface is a very complex phenomenon since the separation mechanism can be achieved by several mechanism whether physical or chemical selectivity. It implies that the separation mechanism occurs due to different phenomena such as charge repulsion, size exclusion and steric hindrance [73], [74], [75].

- Donnan exclusion (Sorption-surface capillary flow)
- Steric hindrance (Sieving effect)
- Solution-diffusion theory

**Donnan exclusion (Sorption-surface capillary flow):** Ion separation resulting from electrostatic interactions between ions and the membrane surface charge (most nanofiltration membranes are slightly negatively charged at neutral pH) is originally based

on the Donnan exclusion mechanism. In this mechanism co-ions which have the same charge as the membrane surface are repulsed by the membrane surface and in order to compensate the electroneutrality condition of the surface, an equivalent number of counter-ions is retained resulting in salt retention. According to the Donnan exclusion principle, the efficiency of ion exclusion depends on the valences of the co-ions and counter-ions respectively, salt concentration and charge of the membrane surface. In other words, the efficiency of ion exclusion increases as the valence of co-ion increases and it decreases as the valence of the counter-ion increases. For example, rejection of salts with divalent anions such as  $Na_2SO_4$  in a negatively charged membrane is higher than monovalent salts such as NaCl.

**Stearic hindrance (Sieving effect):** Sieving effect rejection is based on size differences of species in the solution. It means that membrane rejects solutes which have larger molecular weight than molecular weight cut-off (MWCO) of the membrane and solutes which have a lower molecular weight, will pass through the membrane (Molecular weight cut-off is defined as the minimum molecular weight of a solute which is 90% retained by the membrane. In other words, it is a term that expresses the potential separating capabilities of a membrane). Nanofiltration membranes have a molecular weight cut-off of approximately 150-250 Dalton [73], [61]. Therefore, the solutes with different molecular weight or size will be separated based on sieving effect and the transportation of the non-charged solutes through the NF membrane is determined by steric exclusion mechanism which applies to microfiltration and ultrafiltration as well. The mechanism of molecular sieving is shown in figure 4.2-3:

### Molecular Sieving

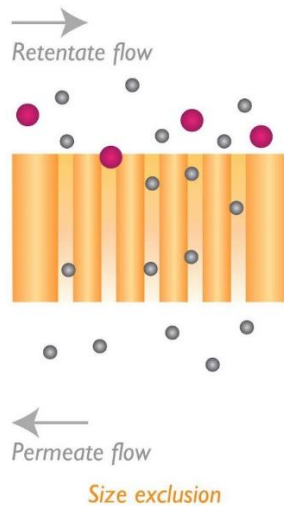


Figure 4.2-3- Molecular Sieving occurring in membrane [76]

According to the molecular sieving mechanism two important parameters must be considered related to ions and solutes rejection in water solution; Stokes radius and hydration energy of ions. Stokes radius or Stokes-Einstein radius of a solute is the radius of a hard sphere which diffuses at the same rate as that solute and it is related to the solute mobility, factoring in not only size but also solvent effects [61], [73]. Hydration energy is the energy required to extract the solute from the solvent to pass it through the membrane pores. The higher values of the hydration energy, the higher amount of energy needed to extract ions from the solvent.

Nevertheless, Stokes radius and hydration energy can be considered as two important parameters that can affect the retention of the ions in a solution as stated below:

- In a NF membrane rejection of a solute increases with increasing stokes radius.
- The ions which have higher hydration energy are more retained.

The stokes radius and hydration energy of different ions are shown in table 4.2-2:

Table 4.2-2- Stokes Radius and hydration energy of different ions [13]

Ions	Stokes Radius (nm)	Hydration Energy (KJ/mol)
$Na^+$	0.184	407
$Cl^-$	0.121	376
$F^-$	0.117	515
$NO_3^-$	0.128	329
$SO_4^{2-}$	0.231	1138
$Ca^{2+}$	0.310	1584
$Mg^{2+}$	0.341	2018

**Solution-diffusion theory:** Due to solution-diffusion theory, membrane is described as a porous film into which both water and solutes dissolve. The solutes moving in the membrane is mainly due to concentration gradient forces, while the water transport is dependent on the hydraulic pressure gradient. The solute transport through the membrane depends on hindered diffusion and convection [61], [50], [57]. The mechanism of solution-diffusion is shown in figure 4.2-4:

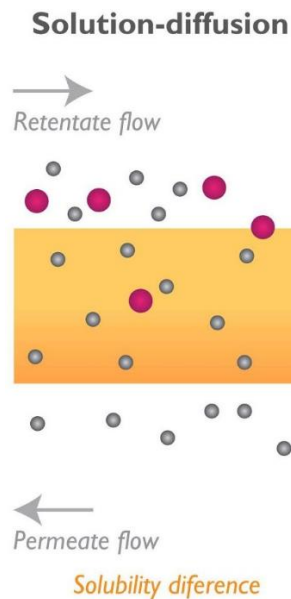


Figure 4.2-4- Solution-Diffusion occurring in membrane [76]

Filmtec Flat Sheet membrane, NF270, PA-TFC manufactured by Dow company was used for nanofiltration experiments. The specifications of the membrane are shown in table 4.2-3, [77], [78]:

Table 4.2-3- Filmtec Flat sheet NF270 Membrane Specifications

<b>Filmtec Flat sheet NF270 Membrane Specifications</b>	
Membrane Type	Polyamide Thin-Film Composite
pH range	2 - 11
Maximum Operating Pressure (bar)	41
Maximum Operating Temperature (°C)	45
Membrane Configuration	Flat Sheet
Nominal Membrane Area (cm <sup>2</sup> )	14.6
Rejection (%), MgSO <sub>4</sub>	99.2
Pore Size/ MWCO (Da)	~ 200 – 400
Flux (gfd/psl)	72.0-98.0/130
MWCO (Da)	200-400
Zeta potential (mV) at pH 5.3	-52
Zeta potential (mV) at pH 8	-74

The nanofiltration experiments were done using 100 ml filtered sea water as feed and the applied pressure was in the range of 4 to 12 bar (4 bar, 6 bar, 8 bar, 10 bar and 12 bar).

The recovery of permeate was fixed and assumed to be 60%. Samples from both permeate and retentate were collected and kept in order to measure pH, conductivity, salinity, TDS and ion chromatography. Flow rate for permeate stream was measured in different pressure as well to calculate flux and all data were recorded.

#### **4.2.5.2. Reverse Osmosis Membrane (RO)**

In 1953, Reverse osmosis (RO) was developed as a new method for the desalination of sea water and it could reject 96% of salts dissolved in the sea water [79]. Reverse osmosis technology uses a semi-permeable membrane in order to remove ions, molecules and even bacteria from fluid and the process needs to apply external pressure to overcome the osmotic pressure which is driven by the chemical potential differences of a solvent. Although, the permeation flux of the process was extremely low, it was introduced and developed as a successful innovation in the water purification technology [80].

##### **4.2.5.2.1. Process Principle and Mechanism**

As the name implies, the principle of reverse osmosis process is due to a natural phenomenon, spontaneous passage of water through a semipermeable membrane (membrane is permeable to some species but not to others). This phenomenon occurs when there are two aqueous solutions with different concentrations in two sides of the membrane and the aqueous solution with lower concentration flows through the membrane into the higher concentrated aqueous solution to equalize the concentration differences [79]. Osmotic pressure varies due to the concentration and temperature of the aqueous solution. As it is shown in figure 4.2-5, when pure water passes through the semi-permeable membrane, the levels of the two solutions become unequal and the difference in pressure finally stops the mitigation. This phenomenon is called osmotic equilibrium and the difference between the pressures of two aqueous solutions called osmotic pressure. In reverse osmosis process, an external pressure (higher than osmotic pressure) is applied in order to overcome the osmotic pressure and force the water from the higher concentration side through the membrane to the lower concentration side.

Thus, water flows in the reverse direction of natural tendency of the flow across the membrane and leaves the dissolved salts behind the membrane [45], [80], [81]. In reverse osmosis process, the driving force is the difference between the external pressure and osmotic pressure [82].

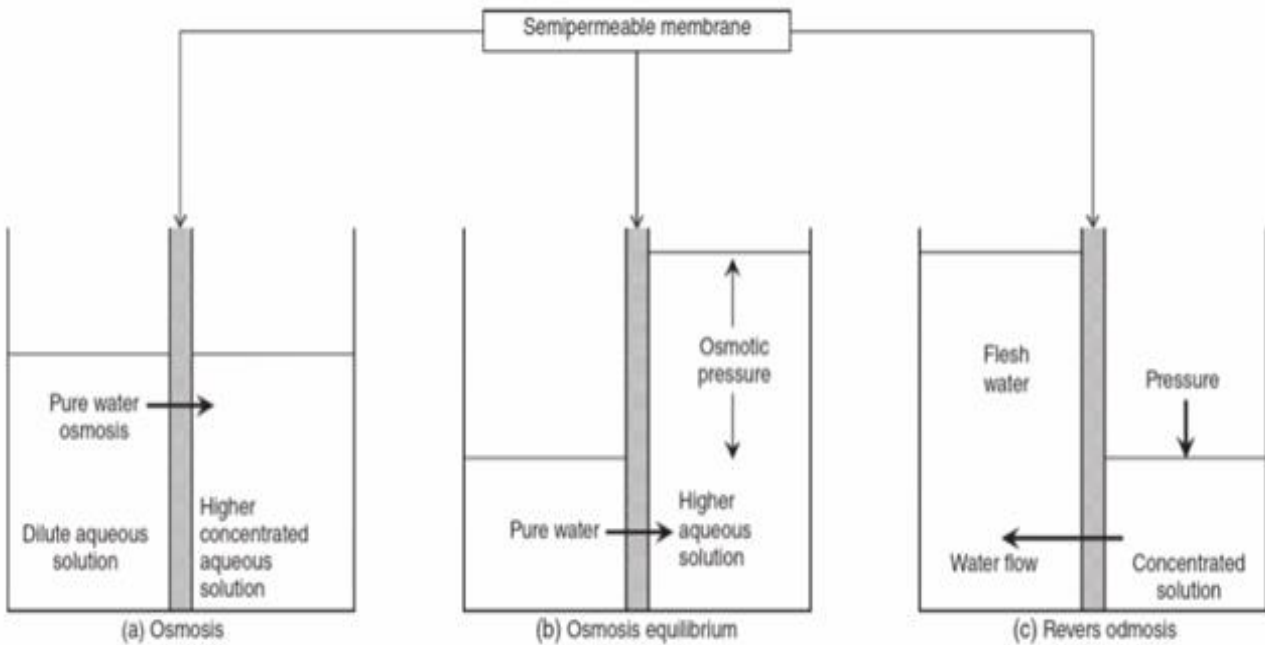


Figure 4.2-5- Principle of Reverse Osmosis membrane

Filmtec Flat Sheet membrane, Ro, XLE, PA-TFC manufactured by Dow company was used for reverse osmosis experiments. The specifications of the membrane are shown in table 4.2-4, [83], [78]:

Table 4.2-4- Filmtec Flat sheet Reverse Osmosis (LPRO) Membrane Specifications

<b>Filmtec Flat sheet RO (LPRO) Membrane Specifications</b>	
Membrane Type	Polyamide Thin-Film Composite, Extra-Low Energy
pH range (25°C)	2 - 11
Maximum Operating Pressure (bar)	69
Maximum Operating Temperature (°C)	45
Membrane Configuration	Flat Sheet
Nominal Membrane Area (cm <sup>2</sup> )	14.6
Stabilized Salt Rejection (%)	98.7
Pore Size/ MWCO (Da)	~ 100
Flux (gfd/psl)	33-41/125
MWCO (Da)	>100
Zeta potential (mV) at pH 5.3	-21
Zeta potential (mV) at pH 8	-38

The experiments were carried out using 100 ml filtered sea water as feed and varying the feed pressure from 10 to 30 bar (10 bar, 15 bar, 20 bar, 25 bar and 30 bar). The recovery of permeate was fixed and assumed to be 60%. Samples from both permeate and retentate were collected and kept in order to measure pH, conductivity, salinity, TDS and ion chromatography. Flow rate for permeate stream was measured in different pressure

as well to calculate flux and all data were recorded. Figure 4.2-6 shows the experimental setup for both nanofiltration and reverse osmosis membranes experiments:



Figure 4.2-6- Dead-End Process, experimental setup for both nanofiltration and reverse osmosis membranes experiments

## 4.2.6. Simulation Software

IMSDesign (Hydranautics, Integrated Membrane Solutions Design) designed by Nitto Group Company [84], was used to simulate, evaluate and estimate energy consumption of membranes process trains that are present in chapter 6. A schematic of the IMSDesign software is shown in figure 4.2-7:



Figure 4.2-7-Schematic of IMSDesign software designed by Nitto Group Company

# **5. CHAPTER 5**

## ***(Results and Discussion)***

## **5.1. Flotation Technique and Wettability Alteration**

### **5.1.1. General Principles**

As previously discussed, chemical composition of seawater has a significant effect on the wettability of the rock in the reservoir. This fact has been proven due to many researches and investigations on CBR system in the recent years that by changing the wetting properties of the rock it can be possible to improve oil production and led it in the desired direction.

According to the objectives of this thesis, several sets of experiments were carried out using modified flotation technique (MFT) in order to investigate the wettability alteration of rock system upon the interactions that occur in the CBR system. For this purpose, except for brines composition almost all the variables were assumed to be constant. Main focus of the experiments was on the effect of divalent ions ( $Mg^{2+}$ ,  $Ca^{2+}$  and  $SO_4^{2-}$ ) in the seawater, separately and paired together on the wetting properties of chalk in the carbonate reservoir. Using different brines with different compositions made it possible to evaluate the individual effect of each ion on the wettability alteration of the chalk. All experiments were done in temperature of 100 °C. Data obtained from the experiments were recorded, collected and analyzed as present in the following sections.

### **5.1.2. Influences of Synthetic Seawater and its Dilutions on Wettability of Rock**

The first series of MFT experiments was carried out using synthetic seawater and its dilutions in order to investigate how these brines affect the wettability of the chalk. Figure 5.1-1 shows the chalk wettability alteration upon interaction with synthetic seawater and two, twenty and hundred times of its dilutions at 100 °C. As it can be seen from the figure, the maximum amount of water-wet fraction of rock was achieved with 20 times diluted synthetic seawater, approximately 60.67% of wettability. Due to the 1.53% of standard deviation, it can be verified that the result is at high level of confidence. Non-diluted synthetic seawater has the maximum amount of water-wet fraction of chalk (59%) after the 20 times diluted syn. seawater and the both two and hundred times diluted syn.

seawater are placed in the third and fourth places of wettability, respectively. This tendency can be also confirmed by Sohal [19].

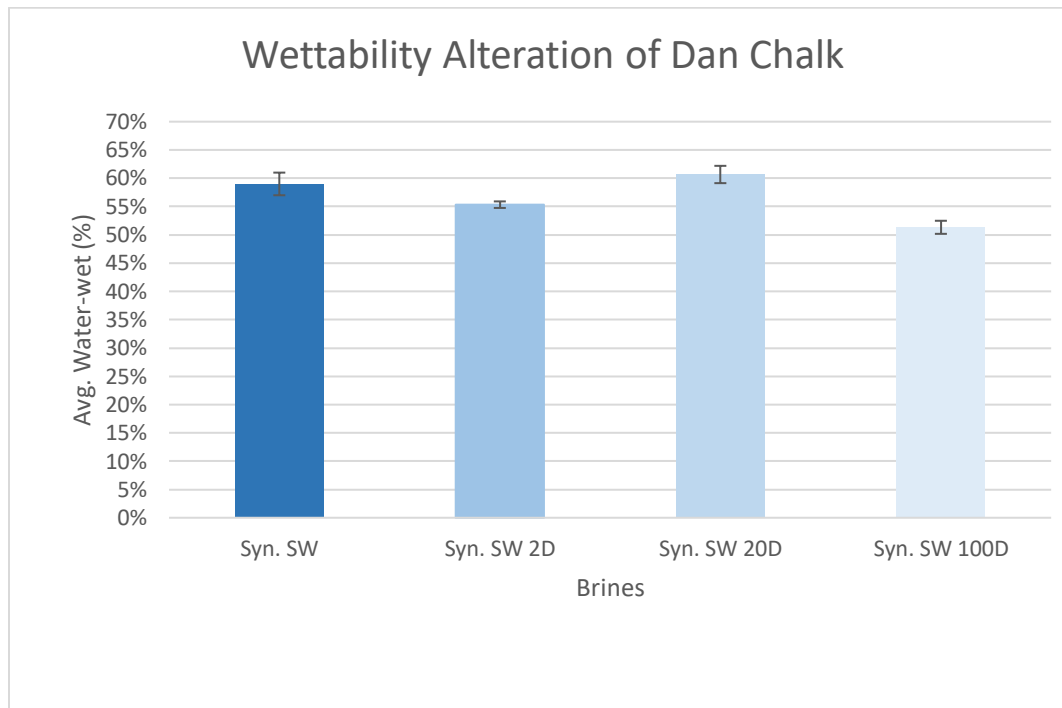


Figure 5.1-1- Effect of different dilutions of synthetic seawater on wettability at 100 °C. Error bars represent the standard deviation (in percent) of the data.

### 5.1.3. Influences of Divalent Ions on Wettability of Rock

As it was previously mentioned, one of the main objectives of the project is to investigate the influences of divalent ions in the seawater on wettability of rock in the reservoir. For this purpose, a set of brines with different compositions of divalent ions (Calcium, Magnesium and Sulphate) were synthetically prepared by removing two of the three mentioned ions in each step. By the way, it was possible to investigate the effect of each ion on the wettability of the chalk separately. The results of wettability alteration of Dan Chalk using non-diluted syn. seawater with only Magnesium (Calcium and Sulphate were removed) and its dilutions is shown in figure 5.1-2. According to the tendency in the figure, the increasing dilution improved the wettability of the grains up to 20x dilution where the

highest water-wet fraction was achieved (approximately 52.33%). Having compared to the original synthetic seawater recipe, it was revealed that wettability of the chalk decreased after removing calcium and sulphate from the seawater. The minimum amount of the water-wet fraction was obtained with non-diluted syn. seawater with only magnesium (approximately 49%).

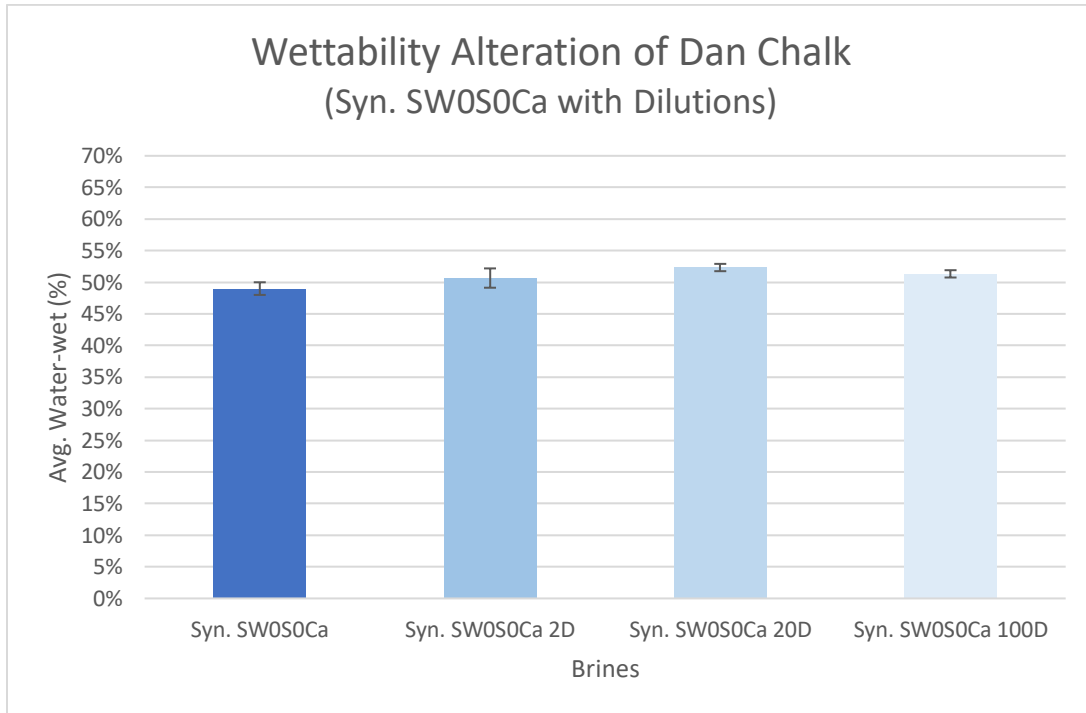


Figure 5.1-2- Effect of different dilutions of syn. SW0S0Ca on wettability at 100 °C. Error bars represent the standard deviation (in percent) of the data.

Figure 5.1-3 shows the results of wettability alteration of Dan Chalk using non-diluted syn. seawater with only calcium (Magnesium and Sulphate were removed) and its dilutions as brine in the flotation technique. It can be seen from the figure that the wettability of the grains was improved by reducing the concentration of the brine until 20x dilution (51.33%). The tendency of the graph shows that more than 20x dilution of the brine will cause the grains becoming more oil-wet as the lowest amount of water-wet fraction occurred with 100x dilution of the brine (Ca. 47.67%).

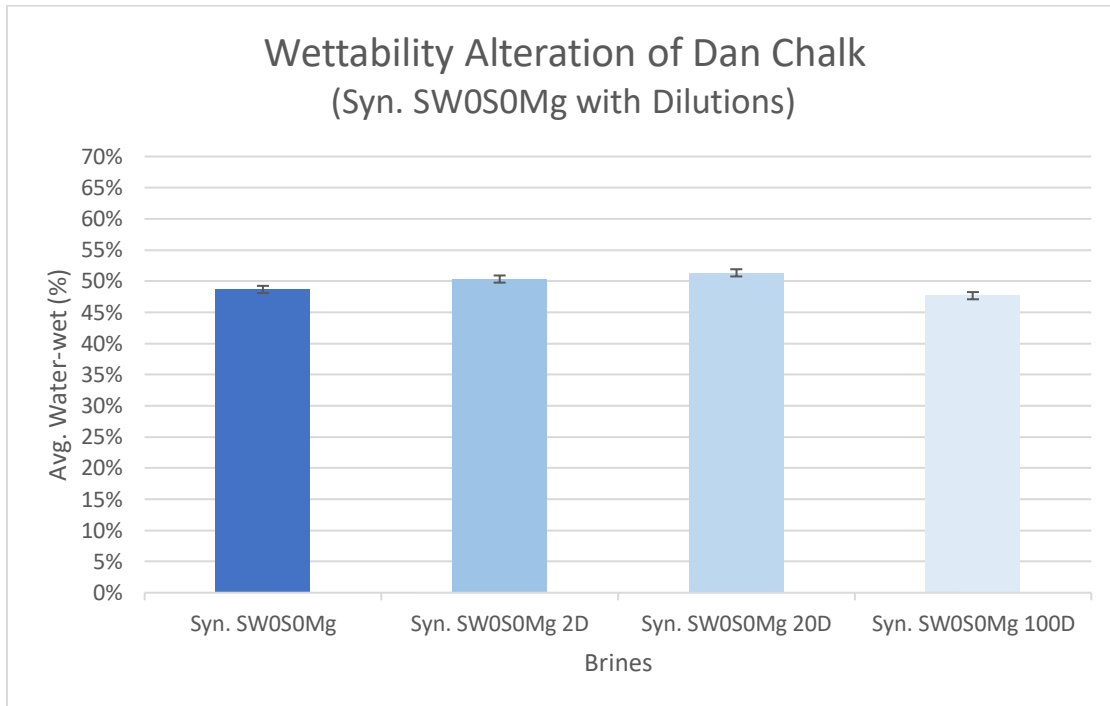


Figure 5.1-3- Effect of different dilutions of syn. SW0S0Mg on wettability at 100 °C. Error bars represent the standard deviation (in percent) of the data.

The results of wettability alteration of Dan Chalk using non-diluted syn. seawater, zero calcium and zero magnesium (only with sulphate) and its dilutions is shown in figure 5.1-4. Due to the trend of the graph, the decreasing in the brine concentration up to 20 times makes the system more water-wet while diluting the brine more than 20 times will move the system toward oil-wet. As the figure shows, the minimum amount of water-wet fraction occurred with the 100x diluted brine (approximately 48.33%).

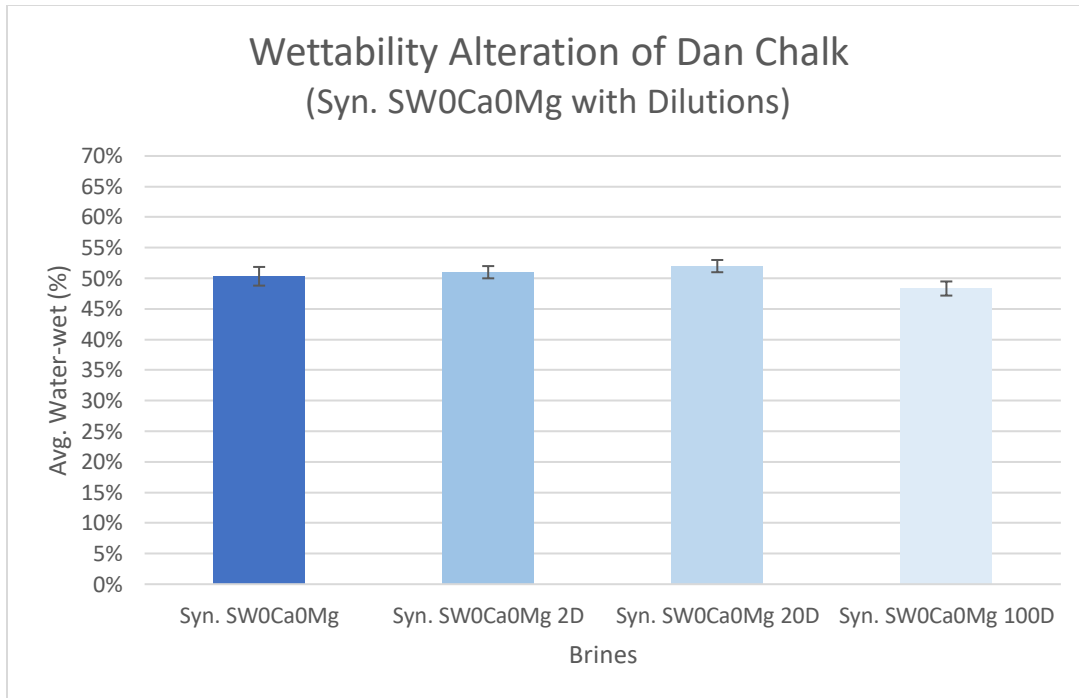


Figure 5.1-4- Effect of different dilutions of syn. SW0Ca0Mg on wettability at 100 °C. Error bars represent the standard deviation (in percent) of the data.

In addition to performing the MFT experiment using the brines previously mentioned, a set of experiments were done using the following three brines:

- Ekofisk Formation Water
- Synthetic Seawater without Sulphate (zero sulphate)
- Synthetic Seawater without Sulphate, Calcium and Magnesium

In order to have a general view and compare the results of the experiments using flotation technique with different compositions of synthetic seawater, a comparative diagram was prepared as shown in figure 5.1-5. From the figure, it can be seen that the highest percentage of wettability of chalk was achieved by synthetic seawater (approximately 59%) which includes all the divalent ions and the lowest percentage of water-wet grains was achieved by synthetic seawater, zero sulphate, calcium and magnesium (approximately 39.67%). Looking at the figure, it turns out that the percentage of

wettability of chalk using Ekofisk Formation water is very low as well (approximately 41.33%). This result reveals the fact that the increasing in salinity of the brine will lead to decrease in water-wet fraction and will make the system more oil-wet. According to the composition of formation water, even though there is sulfate (the most active ion regarding wetting properties in carbonate reservoir), the high concentration of calcium especially in combination with high temperature causes decreasing the wettability of rock due to formation of precipitation of anhydrate,  $\text{CaSO}_4$  in the presence of the low amount of sulphate [1], [39].

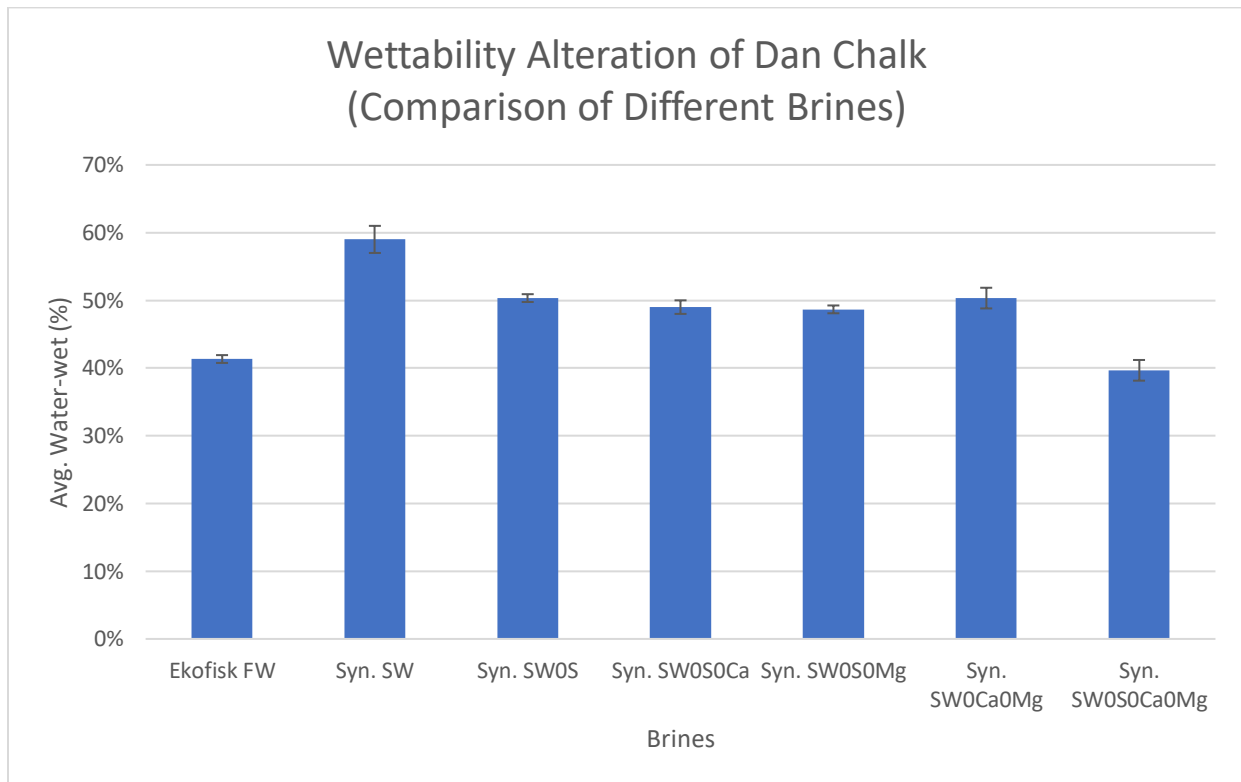


Figure 5.1-5- Comparison of wettability alteration using different brine at 100 °C. Error bars represent the standard deviation (in percent) of the data.

According to the results of experiments showing in the figures and with consideration of previous studies as well, it can be concluded that the divalent ions, calcium, magnesium and sulphate in the seawater play a decisive role in the wettability of the rock in reservoir.

These ions act as potential determining ions in oil recovery since they can change the surface charge of CaCO<sub>3</sub> lead to release oil from the rock surface [39]. From figure 5.1-5 can be seen, the wettability of chalk effectively changed by just removing or adding of these three ions in the seawater composition.

### 5.1.4. Effect of Divalent Ions Concentrations on Wettability

According the previous researches and investigations, [39], [1], the presence of divalent ions (sulphate, calcium and magnesium) and their concentrations as determining ions in seawater have the greatest impact on the wettability of rock system and, consequently, the recovery of oil. In order to investigate and analyze the relation between divalent ion concentration and wettability of rock, a graph was prepared as shown in figure 5.1-6.

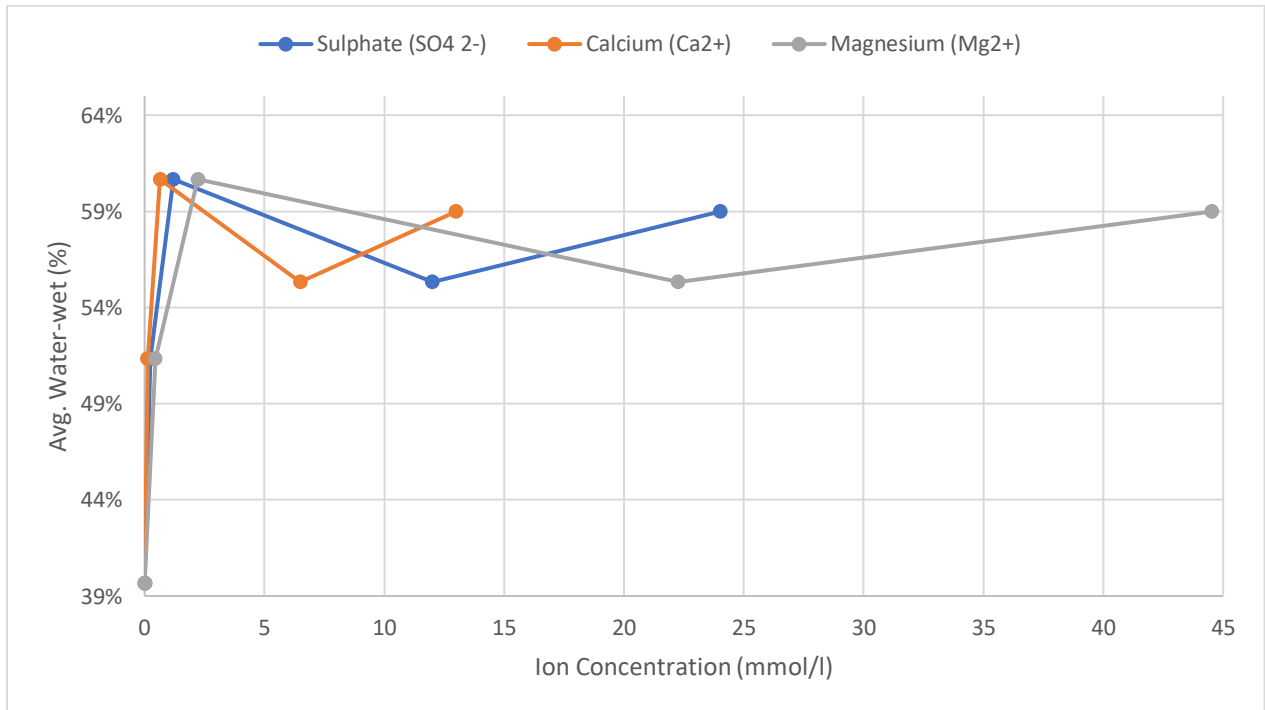


Figure 5.1-6- Wettability alteration of Dan Chalk and variation of divalent ions concentration for non-diluted synthetic seawater and its dilutions at 100 °C

As it can be seen from the graph and considering the wettability alteration with synthetic seawater and its dilutions, calcium with a concentration less than 1 mmol/l achieved the wettability of 60.67% in presence of sulphate and magnesium followed by the concentrations of 1.2 and 2.2 mmol/l, respectively.

### **5.1.5. Correlation Between pH and TDS with Wettability Alteration**

Having used data (pH, TDS and avg. water-wet) from flotation experiments and plotted them in graphs (figures 5.1-7 and 5.1-8), it was possible to observed that the pH of the synthetic seawater is increased as the dilution of seawater takes place. Following the pH curve from point Syn. SW to Syn. SW 2D, there is no specific changes neither in the value of pH nor TDS while a significant reduction occurs in the wettability. From point Syn. SW 2D to Syn. SW 20D, the pH increases from 7.8 to 8.32 since the ionic charge equilibrium is changed and leads to interact on the rock surface. The chalk can get the maximum wettability in this range of graph while the amount of TDS is reduced by about 90%. With respect to the trend of the TDS curve from point Syn. SW 20D to Syn. SW 100D, the wettability is extremely reduced although the TDS does not change significantly. The value of ionic strength in this range of the graph is almost close to zero.

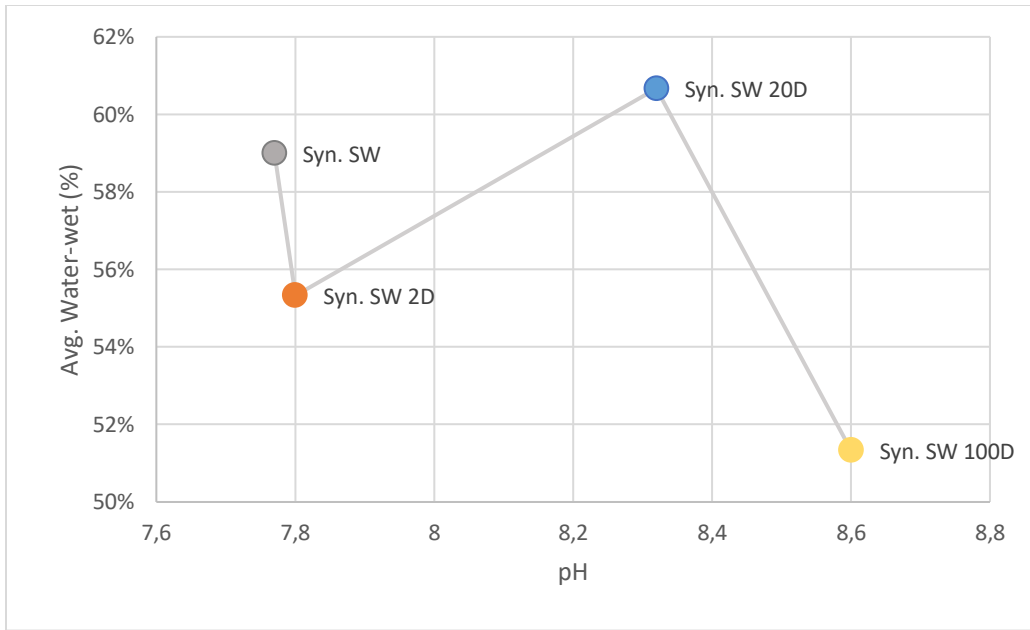


Figure 5.1-7- Dependency of rock wettability on pH for non-diluted seawater and its dilutions at 100 °C

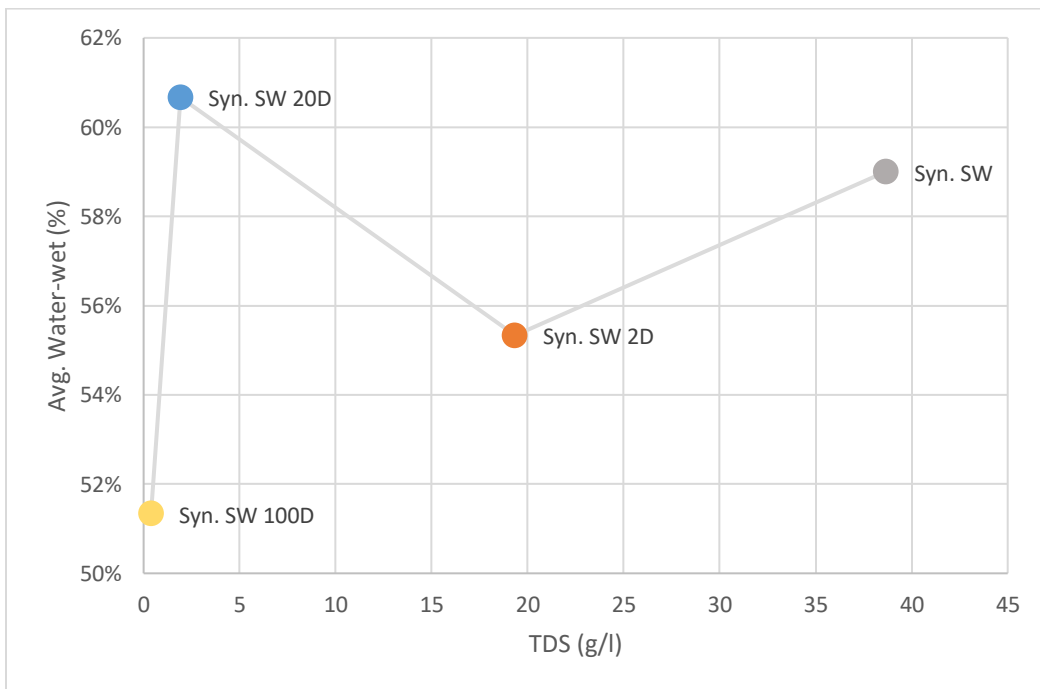


Figure 5.1-8- Dependency of rock wettability on TDS for non-diluted seawater and its dilutions at 100 °C

## 5.1.6. Oil Coating and Wettability Index

### Oil Coating

The modified flotation technique, as an effective method for investigating the waterflooding process in reservoir, determines not only the best composition of the injectable advanced water into the reservoir, but also provides information about the amount of oil which is attached on the surface of water-wet grains after wettability alteration and it is very hard to measure with other methods. During the MFT experiments, it was observed that a thin layer of oil coted some of the water-wet grains exhibiting a brownish color. According to a study, the fact was observed that the organic compounds of crude oil such as organic acids adsorbed on carbonate surfaces strongly whereas other compounds of the crude oil such as amines and alcohols adsorbed weakly [85]. The compounds which weakly adsorbed on the rock surface could be removed or replaced easily (by most solvent) but strongly adsorbed compounds could not [19]. Figures 5.1-9, 5.1-10, 5.1-11, 5.1-12 and 5.1-13 show the average mass of attached oil on the chalk versus the average mass of water-wet grains for different brines and their dilutions:

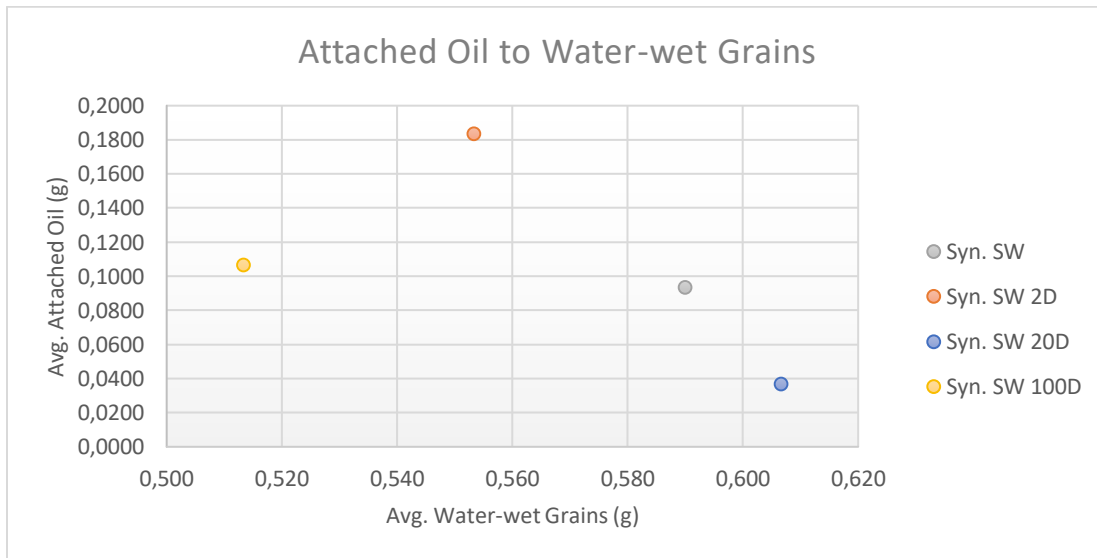


Figure 5.1-9- Attached oil to water-wet grains for synthetic seawater and its dilutions at 100 °C

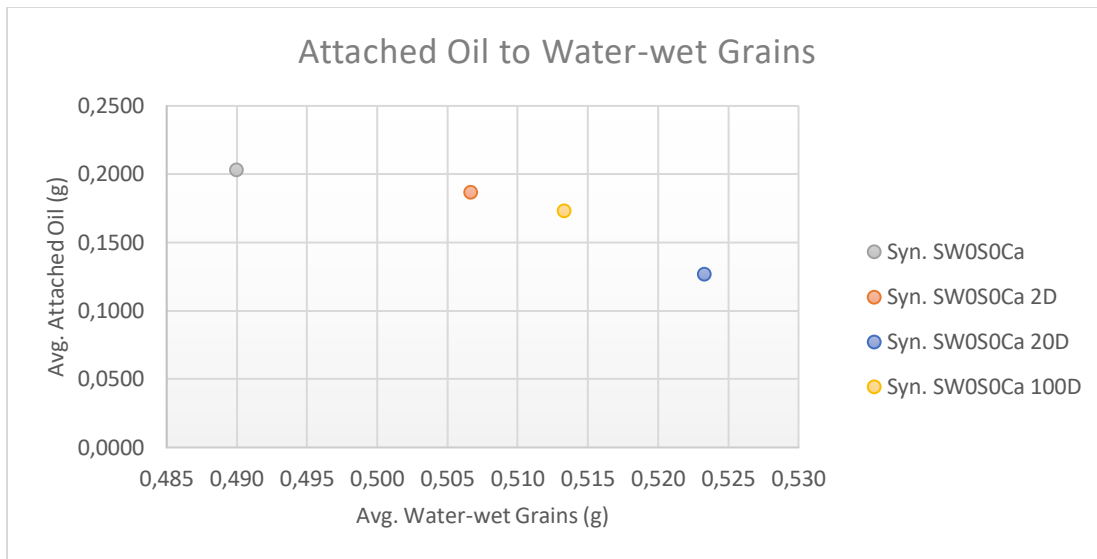


Figure 5.1-10- Attached oil to water-wet grains for syn. SW0S0Ca and its dilutions at 100°C

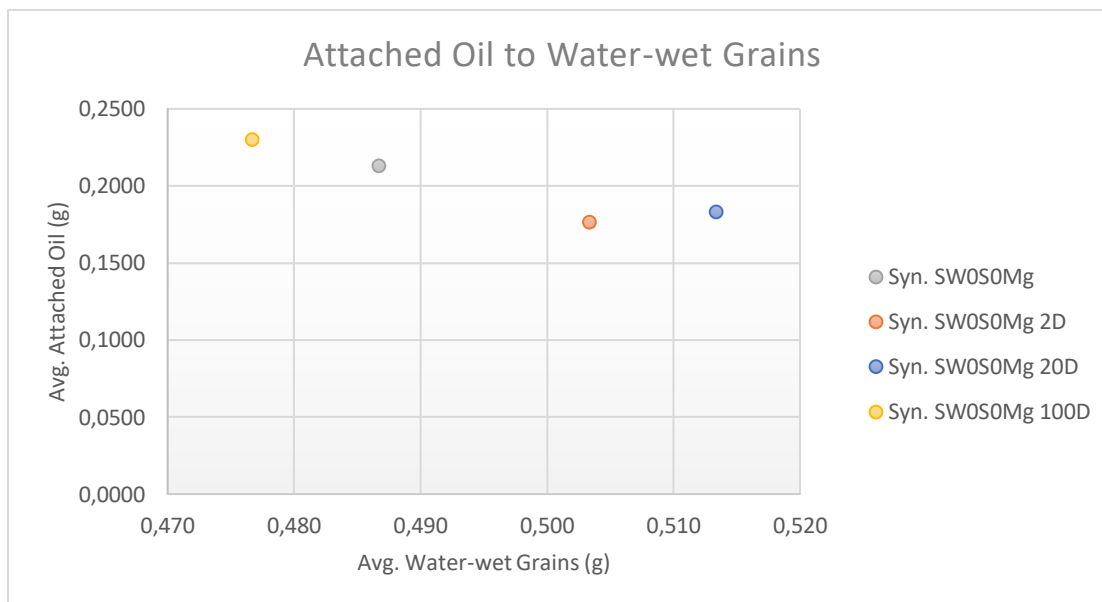


Figure 5.1-11- Attached oil to water-wet grains for syn. SW0S0Mg and its dilutions at 100°C

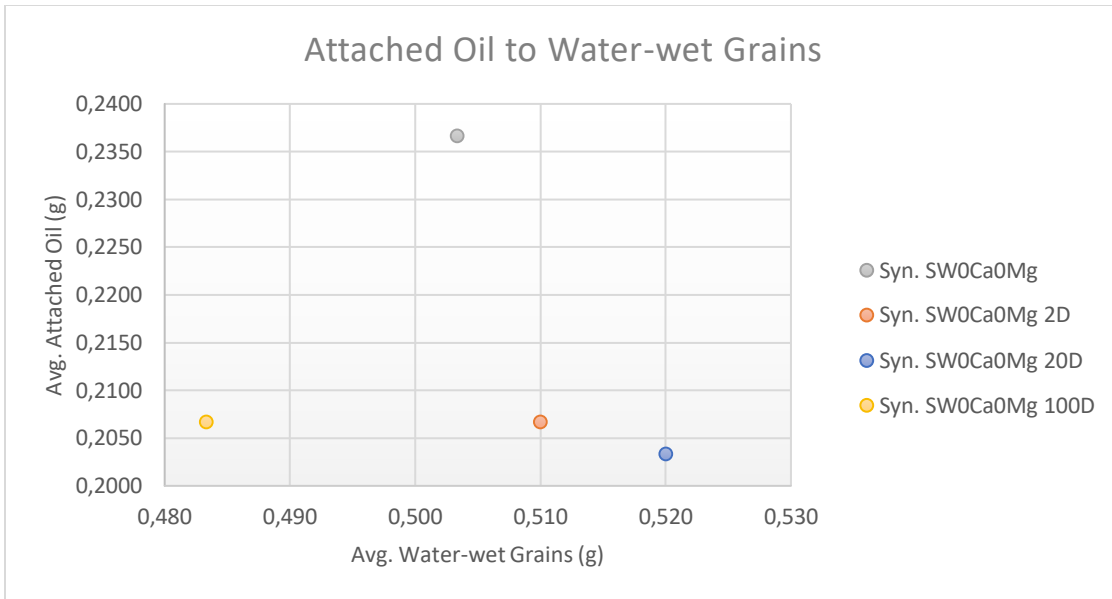


Figure 5.1-12- Attached oil to water-wet grains for syn. SW0Ca0Mg and its dilutions at 100°C

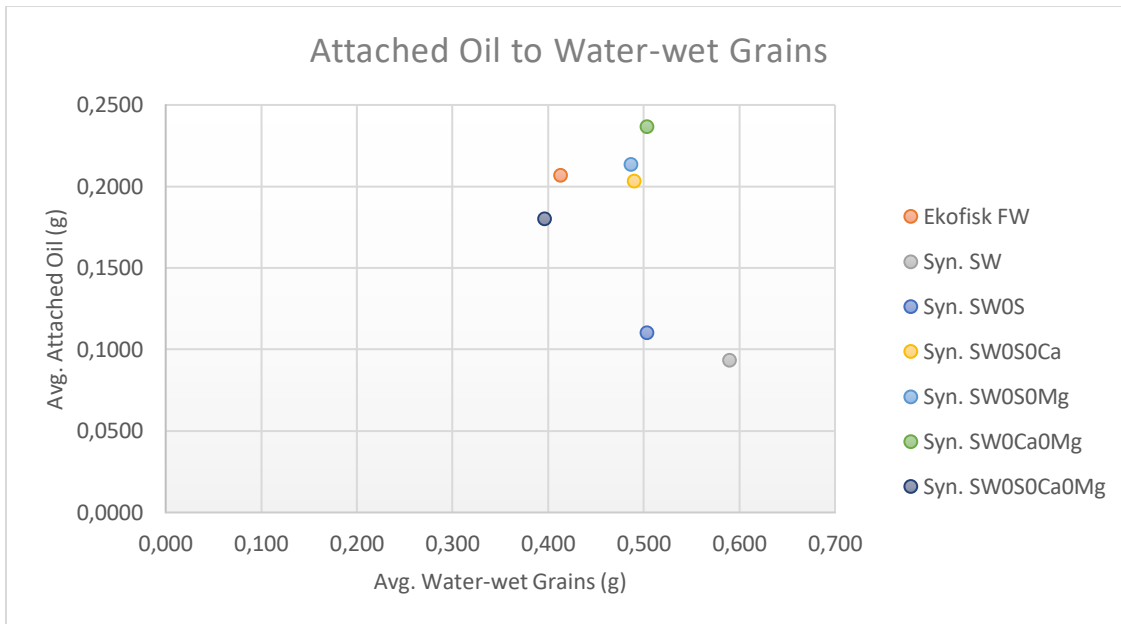


Figure 5.1-13- Comparison of attached oil to water-wet grains for different brines at 100°C

The biggest amount of attached oil on the chalk in the case of synthetic seawater and its dilutions was for 2x dilution and in the case of synthetic seawater, zero sulphate and zero

calcium and its dilutions, the greatest amount of attached oil was for non-diluted syn. seawater, zero sulphate and zero calcium. In the cases of synthetic seawater (zero sulphate, zero magnesium) and synthetic seawater (zero calcium, zero magnesium) and their dilutions, the biggest amount of attached oil were 100x dilution and non-diluted syn. seawater (zero calcium, zero magnesium), respectively. Considering the figures, it can be seen that there is no direct correlation between the amount of retained oil and water-wet grains in the CBR system. These results can be confirmed from Zohal [19].

### **Flotation Wettability Index**

Flotation wettability index (FWI) is a newly developed wetting index that determines the optimum wetting condition and it is used to express the degree of wettability detained by the chalk samples in the flotation technique [19]. The flotation wettability index is calculated using the following equation and it is based on the results of flotation technique:

$$FWI = \frac{(mass\ of\ water - wet\ grains) - (mass\ of\ oil - wet\ grains)}{total\ mass}$$

*Equation 5.1-1*

The value of the flotation wettability index varies between -1 (completely oil-wet condition) and +1 (completely water-wet condition) and zero indicates the neutral-wet condition. The FWI was calculated based on the data obtained from the flotation experiments with different brines and it is illustrated in figures 5.1-14, 5.1-15, 5.1-16, 5.1-17 and 5.1-18:

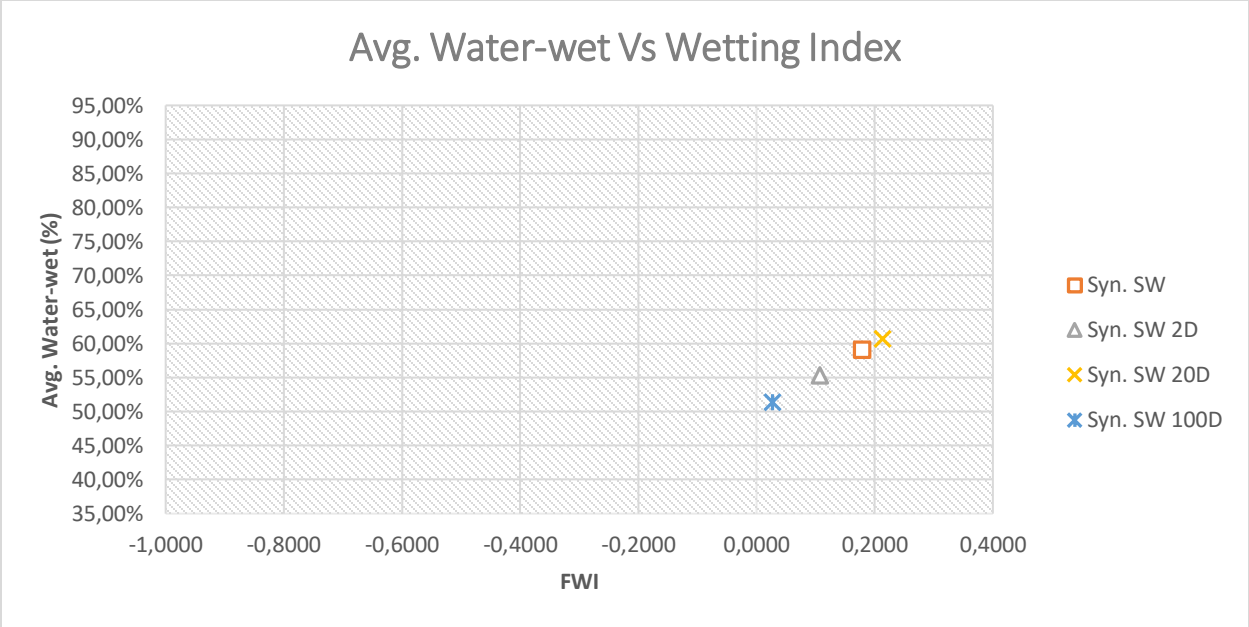


Figure 5.1-14- Flotation wetting index for Dan Chalk using synthetic seawater and its dilutions at 100°C

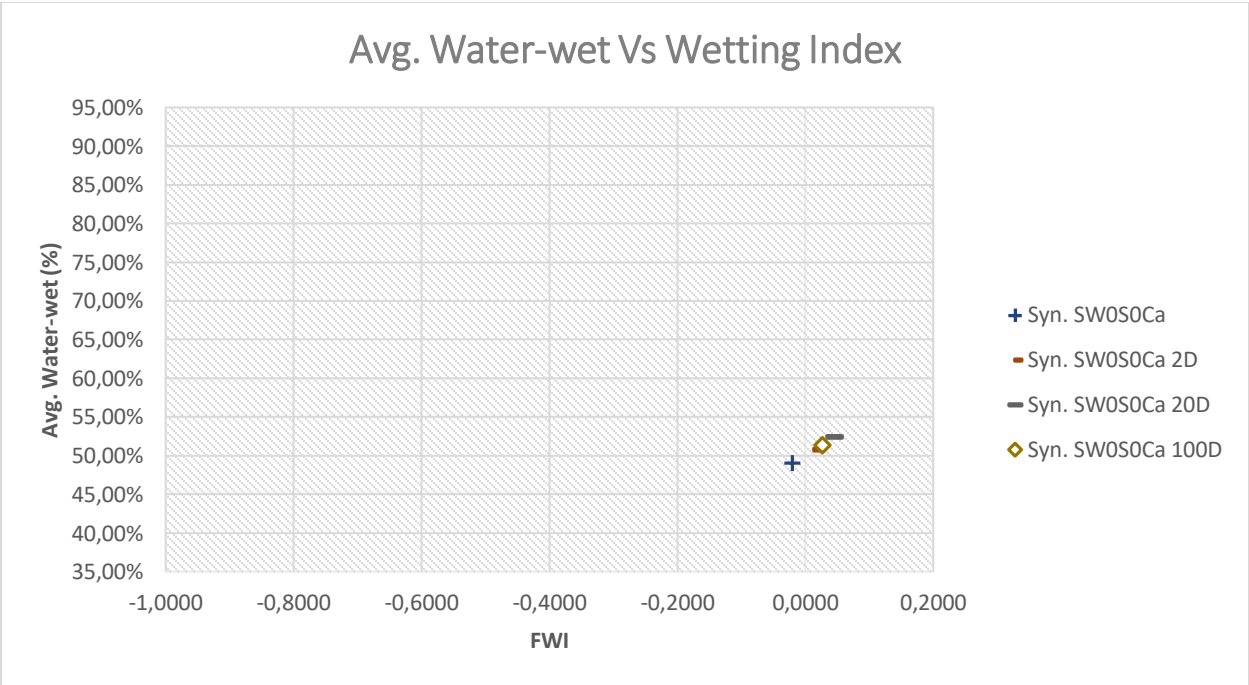


Figure 5.1-15- Flotation wetting index for Dan Chalk using syn. SW0S0Ca and its dilutions at 100°C

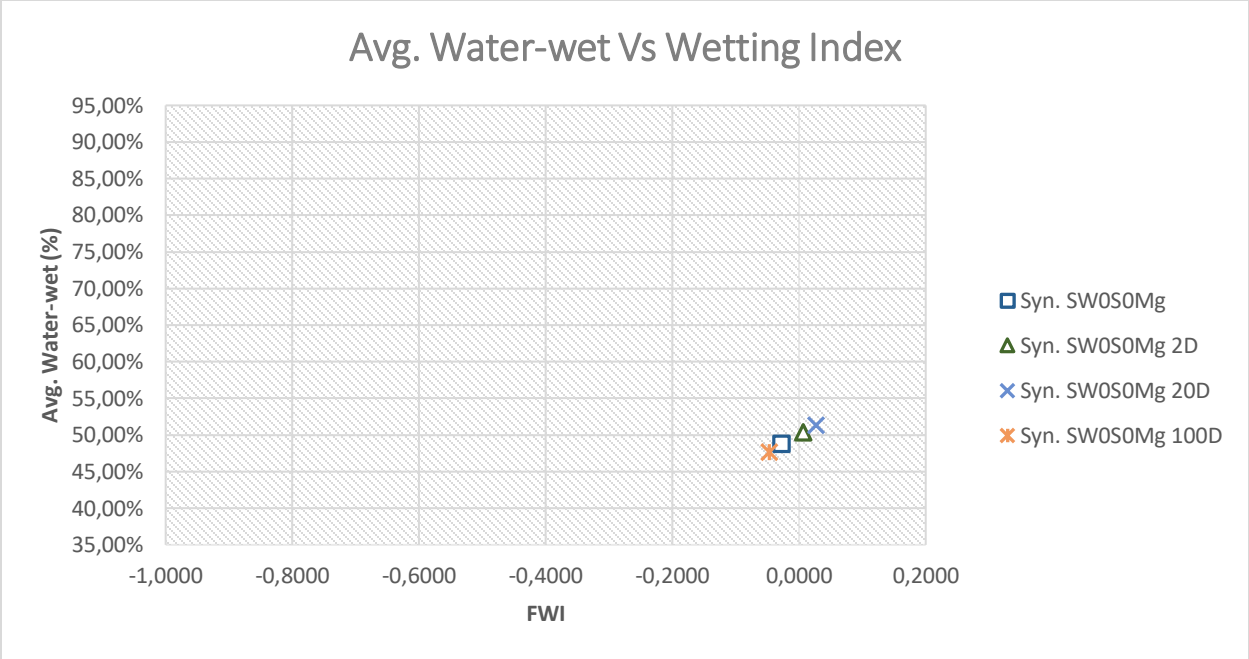


Figure 5.1-16- Flotation wetting index for Dan Chalk using syn. SW0S0Mg and its dilutions at 100°C

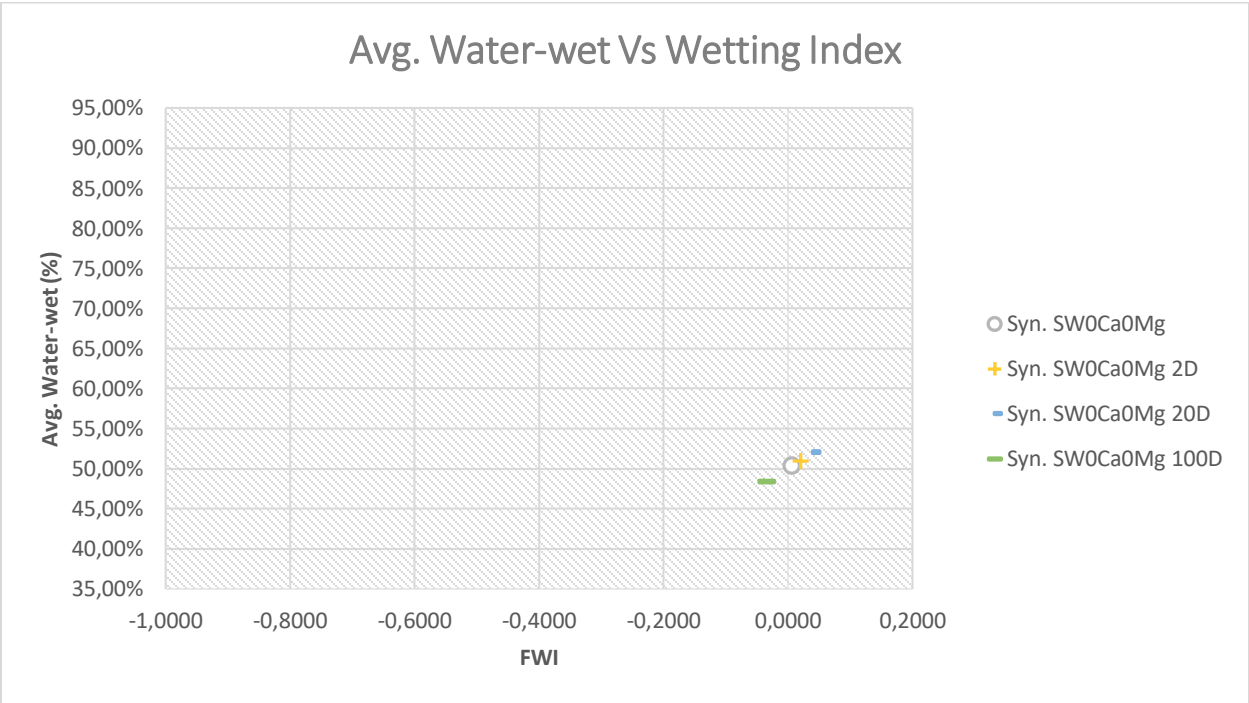


Figure 5.1-17- Flotation wetting index for Dan Chalk using syn. SW0Ca0Mg and its dilutions at 100°C

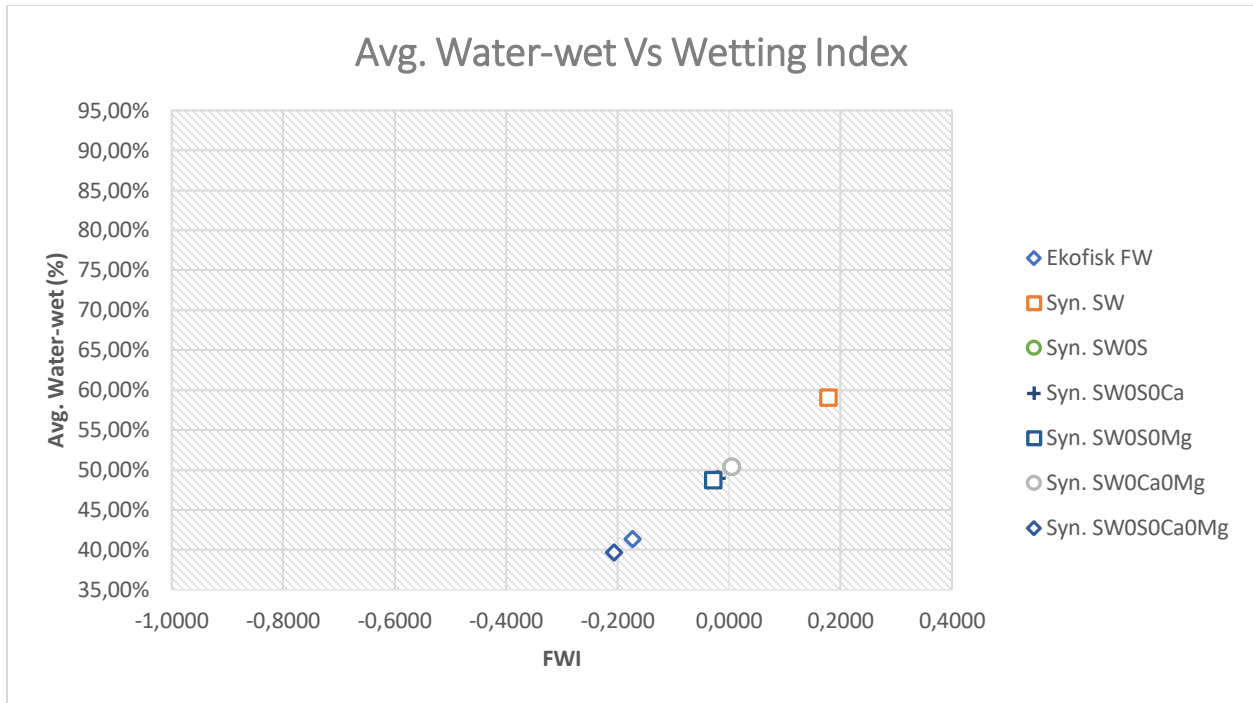


Figure 5.1-18- Comparison of flotation wetting index for Dan Chalk using different brines at 100°C

According to a conclusion from the literature, Sohal [19], the maximum amount of oil recovery occurs for a wetting index ranging between 0 and 0.25 and further increase in water wetness would not improve oil recovery. Looking at the figures it turns out that the optimum wetting condition was reached by 20x dilution of synthetic seawater with FWI value of 0.214 and non-diluted and 2x diluted syn. seawater followed by the values of 0.18 and 0.11 after 20x diluted syn. seawater, have the highest values of wetting conditions, respectively.

## **5.2. Sea Water Filtration and Smart Water Production**

### **5.2.1. General Principles**

The characteristics of the fluid injected into reservoir play an important role in the wettability of the rock and ultimately in the amount of oil recovery. According to the thesis objectives, production of water with desired composition (Smart Water) and suitable for injection into the reservoir to improve the oil recovery is the main focus of this section. Regarding the results from the MFT experiments, the desirable composition of seawater is low salinity (low concentration of NaCl) while retaining divalent ions (sulphate, calcium and magnesium) that known as the determining ions to improve the wettability of rock. In order to achieve this purpose, membrane technology including nanotechnology (NF) and reverse osmosis (RO) membrane systems was performed.

A set of filtration experiments using nanofiltration membrane (NF) was carried out at different pressures. The retentate flow from nanofiltration membrane was taken as the main constituent part of advanced water since it retains the divalent ions in its retentate flow. Another set of filtration experiments using reverse osmosis membranes (RO) was done in different pressures as well. The permeate flow from reverse osmosis membrane process with low TDS level was taken and mixed with the retentate flow from NF in order to reduce the salinity. Normal filtered seawater was used as feed for experiments in whole the process.

### **5.2.2. Experiments Using Nanofiltration Membrane (NF)**

As previously mentioned, filtration experiments with nanofiltration process (NF) were done using Filmtec Flat Sheet membrane, NF270, PA-TFC through the dead-end process under varying the pressure (4, 6, 8, 10 and 12 bar). The nominal area of the membrane in all steps was 14.6 cm<sup>2</sup>. The detail of the results and calculated performance parameters are present as follow:

### 5.2.2.1. Rejection of Ions

The rejection of individual ion was calculated using data from IC and ICP for each sample. Figure 5.2-1 shows the rejection of ions in different pressure using NF membrane:

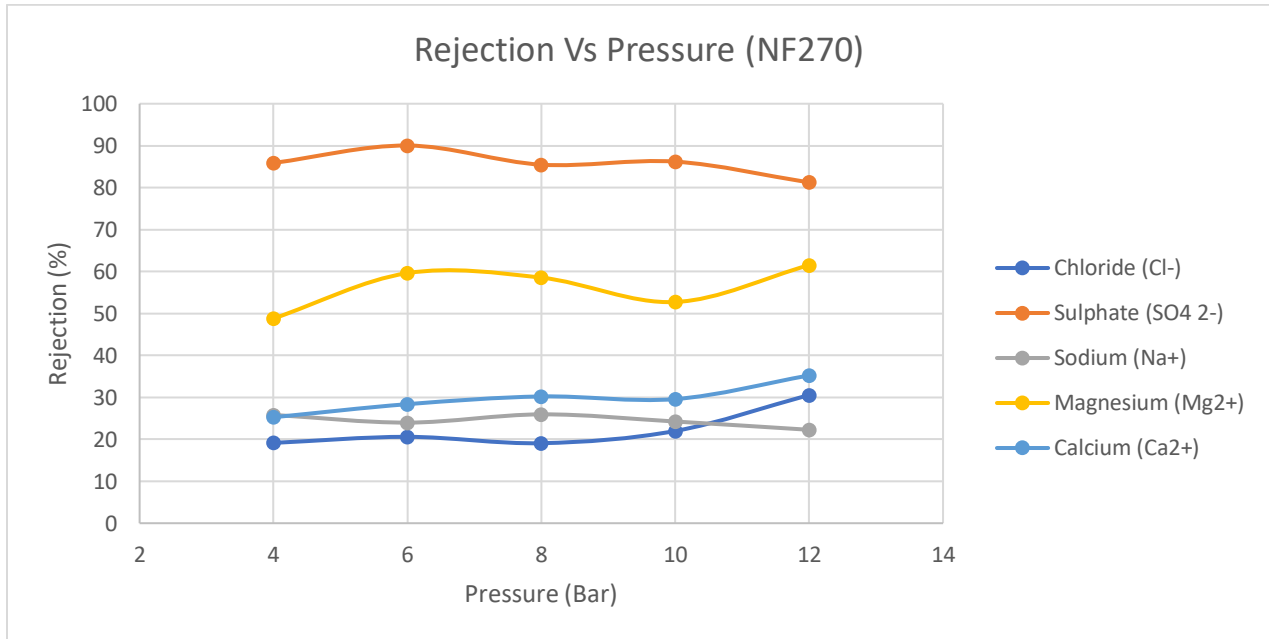


Figure 5.2-1- Rejection of ions using Nanofiltration membrane (NF270) in different pressures

Looking at the graph, it can be seen that sulphate is at highest level of rejection and chloride is at the lowest level which means that almost 90% of the sulphate was retained behind the membrane and conversely, almost 80% of chloride passed through the membrane. This is the typical characteristics of nanofiltration membrane. Due to the separation principles and mechanism of nanofiltration, the rejection of ions depends on the size of ions, molecular dimensions of hydrated ion in the water and salt coefficient diffusion. The small size and low hydration energy of Na<sup>+</sup> and Cl<sup>-</sup> cause to pass sodium and chloride easily through the NF membrane. The big size of the sulphate and the repulsive force of the negatively charged NF membrane causes sulphate has the highest retention in the NF process. With respect to magnesium and calcium, they were retained due to their big size and also to satisfy the charge balance with rejected sulphate. By

comparing the rejection of magnesium and calcium on the graph, it is seen that the rejection of the calcium is less than magnesium even molecular size of the calcium is bigger than magnesium. This can be explained due to lower hydration energy of calcium compared to magnesium and higher affinity of calcium toward the negatively charged NF membrane.

### 5.2.2.2. Flux

The values of the flux were calculated based on the data obtained from experiments in each step under varying the operating pressure. The results are present in the figure 5.2-2:

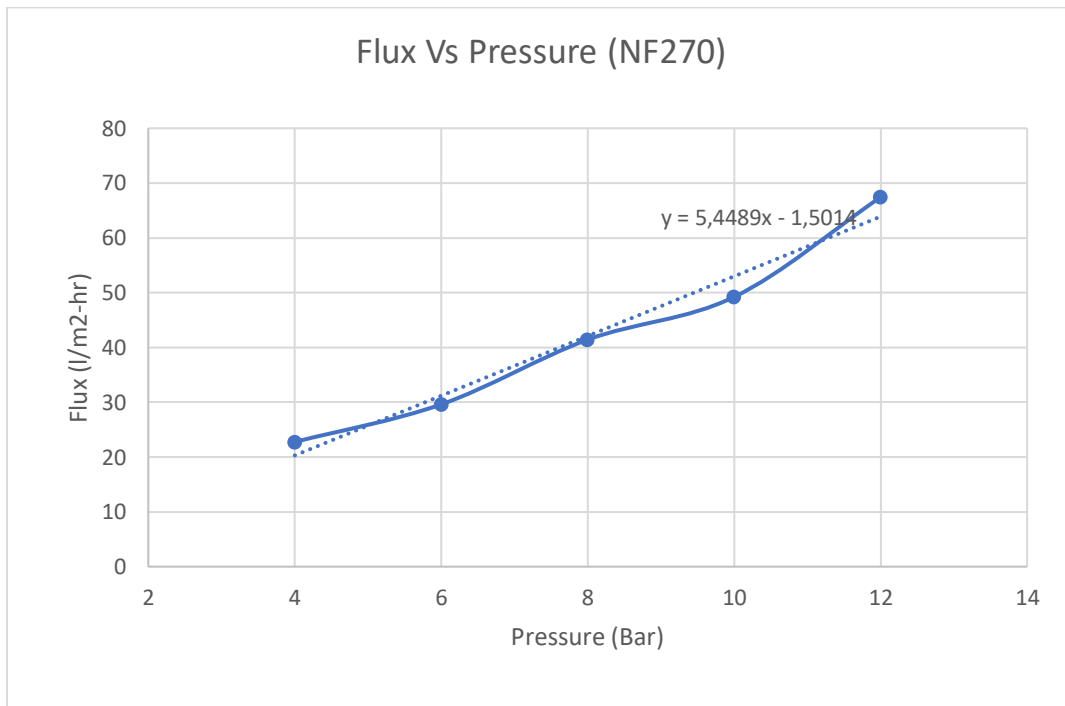


Figure 5.2-2- Flux of nanofiltration process in different pressures

From the graph, can be observed that flux is almost linearly proportional to pressure and it is due to the typical characteristics of nanofiltration membrane. Any increase in pressure of the process increases the flux and the sensitivity of NF membrane to flux changes with pressure can be seen from the slope of the flux curve.

### 5.2.2.3. Total Dissolved Solids (TDS)

The total dissolved solids (TDS) of permeate and retentate flow in different pressures obtained from samples are shown in the figure 5.2-3:

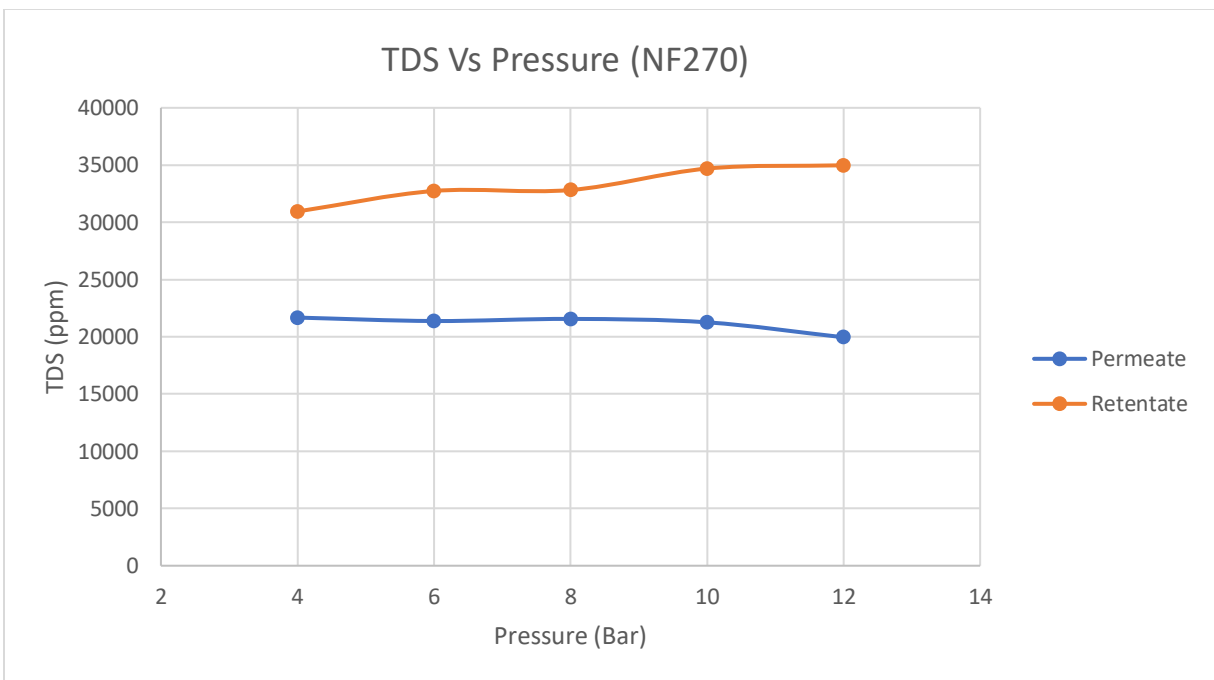


Figure 5.2-3- Total Dissolved Solids vs. pressure for nanofiltration process

According to the tendency of the permeate curve in the graph, the TDS of the permeate flow slightly decreases when the pressure increases. Regarding the salt transport through the membrane because of diffusion and convection, increasing the operating pressure leads to increasing in salt rejection gently. Vice versa, in the retentate curve, the TDS increases when the operating pressure increases and it is due to the typical characteristics of membrane process.

### 5.2.3. Experiments Using Reverse Osmosis Membrane (RO)

As previously mentioned, filtration experiments with reverse osmosis process (RO) were done using Filmtec Flat Sheet membrane, RO, XLE, PA-TFC through the dead-end process under varying the pressure (10, 15, 20, 25 and 30 bar). The nominal area of the membrane in all steps was 14.6 cm<sup>2</sup>. The results from filtration of seawater with reverse osmosis membrane were used to evaluate and analyze the options of smart water production. The detail of the results and calculated performance parameters are present as follow:

#### 5.2.3.1. Rejection of Ions

The rejection of individual ion was calculated using data from IC and ICP for each sample. The rejection of ions in different pressure using RO membrane are shown in figure 5.2-4:

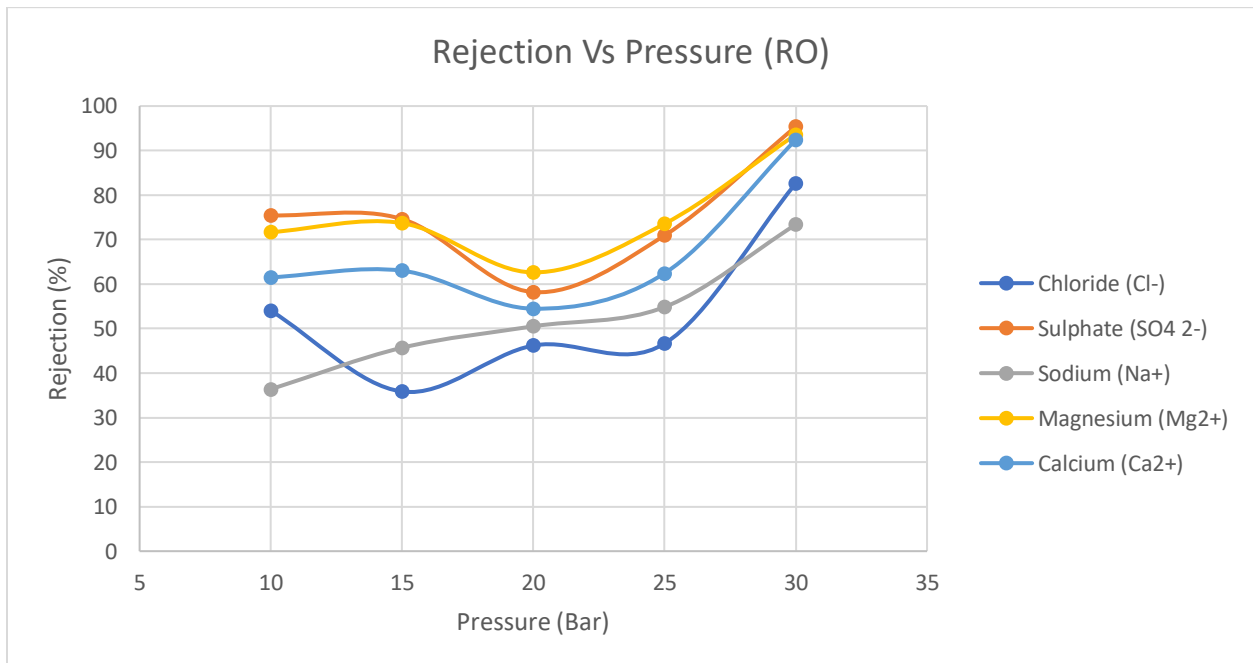


Figure 5.2-4- Rejection of ions using Reverse Osmosis membrane (RO) in different pressures

From the results can be observed that the rejection of all ions (monovalent and divalent ions) is almost high and this trend increases with increasing the operating pressure. The highest rejection of ions occurred at maximum pressure (30 bar) which means that the reverse osmosis membrane gives desired results at high pressures due to the typical characteristics of RO membrane.

### 5.2.3.2. Flux

The values of the flux were calculated based on the data obtained from filtration experiments with the reverse osmosis membrane in each step under varying the operating pressure. The results are shown in the figure 5.2-5:

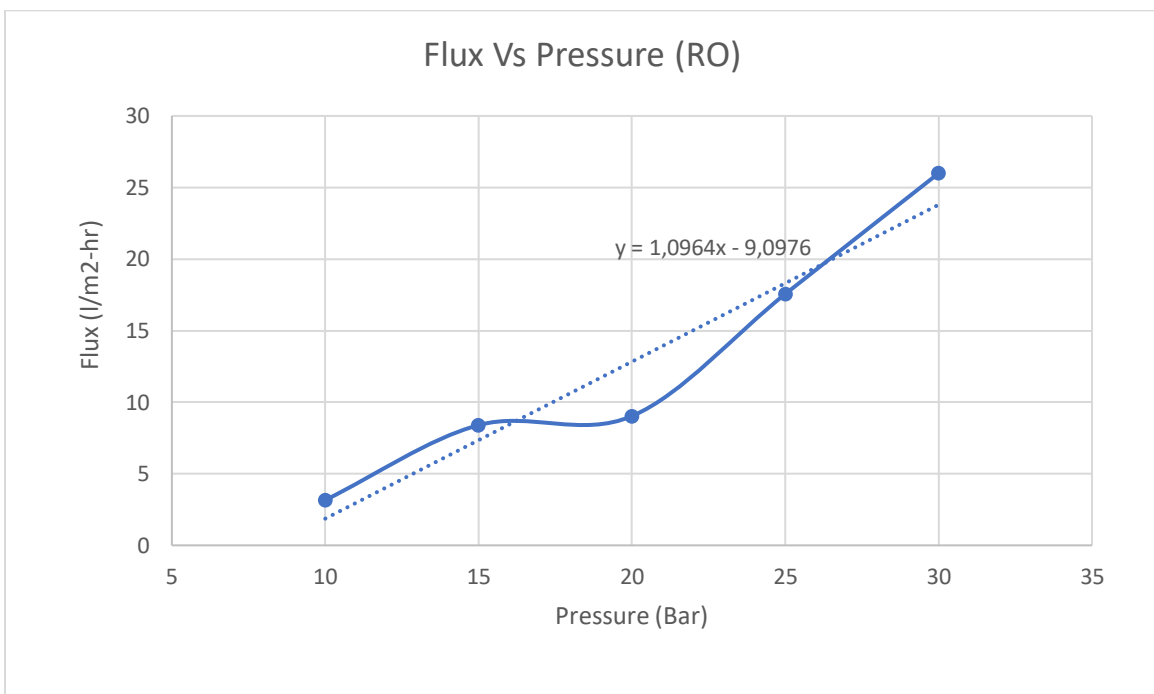


Figure 5.2-5- Flux of reverse osmosis process in different pressures

A mentioned before, the applied pressure on RO membrane must be greater than osmotic pressure of feed otherwise resulting in no permeate. From the graph, it can be seen that

the values of flux are extremely low and it is not possible to measure it at low pressure. This is the typical characteristics of reverse osmosis membrane.

### 5.2.3.3. Total Dissolved Solids (TDS)

The total dissolved Solids (TDS) of permeate and retentate flow in different pressures obtained from samples of RO membrane experiments are shown in the figure 5.2-6:

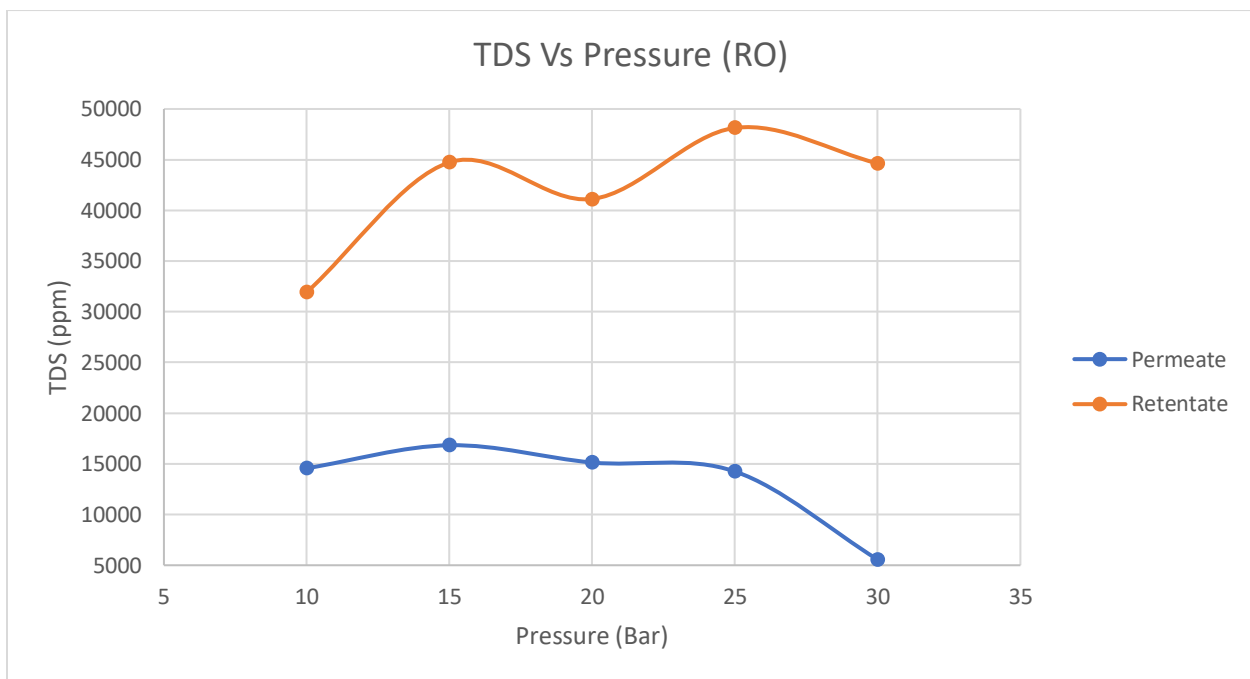


Figure 5.2-6- Total Dissolved Solids vs. pressure for reverse osmosis process

According to the results from RO membrane experiment, it is observed that the values of TDS were very low compared to the NF membrane. The minimum amount of TDS occurred when 30 bar pressure was applied. As previously discussed, the RO membrane gives favorable results at high pressures where can reject almost 90% of monovalent ions.

Considering previous studies, [75], [13], that used cross-flow mode and spiral-wound module (for both NF and RO), almost same tendency of ions rejection, total dissolved

solid and flux with increasing pressure were obtained. Highest value of rejection was for sulphate followed by magnesium, calcium, sodium and chloride, respectively. However, the slope of flux is lesser compared to the literature which indicates that with increasing in the pressure of the process, flux increases lesser and it is because of the difference in the type of processes (dead-end and cross-flow).

## 5.2.4. Nanofiltration Membrane vs. Reverse Osmosis Membrane

The filtration experiments using nanofiltration (NF) and reverse osmosis (RO) membranes were done and the results for each membrane were separately analyzed. In this section, a comparative analysis of the results between the two membranes is explained in order to have a general overview of the two methods of filtration and a deeper understanding of their mechanism for combining them as an option for smart water production.

### 5.2.4.1. Ion Rejection in NF vs. RO

Figure 5.2-7 shows the comparison of ion rejection of nanofiltration and reverse osmosis membranes:

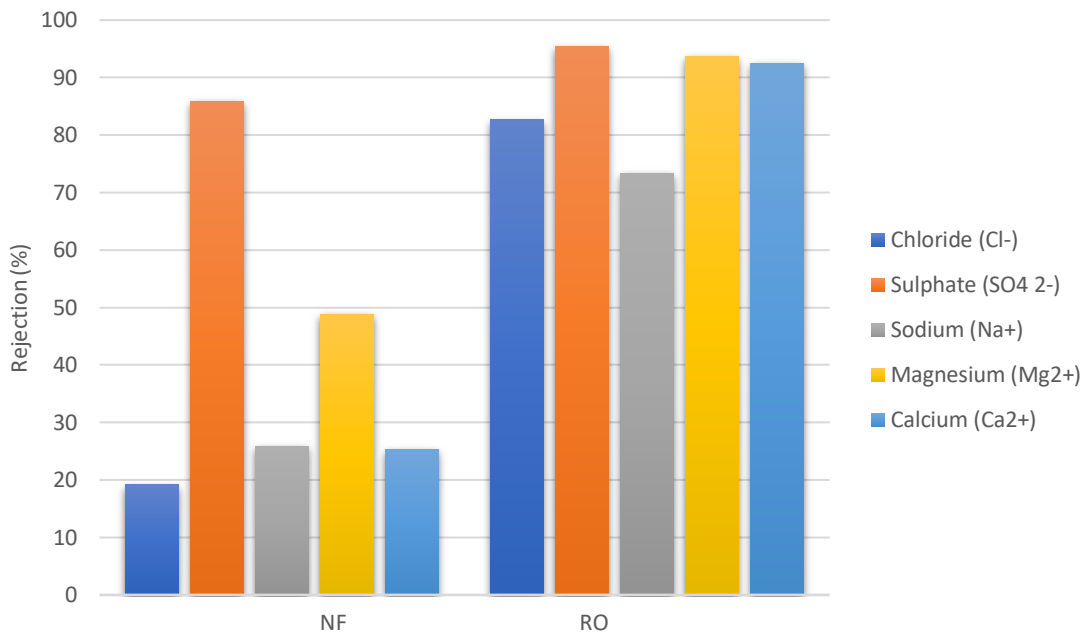


Figure 5.2-7- Comparison of ion rejection between nanofiltration (NF) and reverse osmosis (RO) membranes

With respect to the graph, it can be seen that the ions rejection of RO membrane is much higher than NF membrane (mainly monovalent ions), so that almost all the solutes are rejected and only solvent (water) and some of the solutes permeate through the membrane. This feature of RO membrane causes the low TDS level in the permeate and suitable for combination with retentate of NF as an option for smart water production. However, the NF membrane rejects only the divalent ions in high level.

### 5.2.4.2. Flux of NF vs. RO

A comparative graph of NF and RO flux at different pressures is shown in figure 5.2-8:

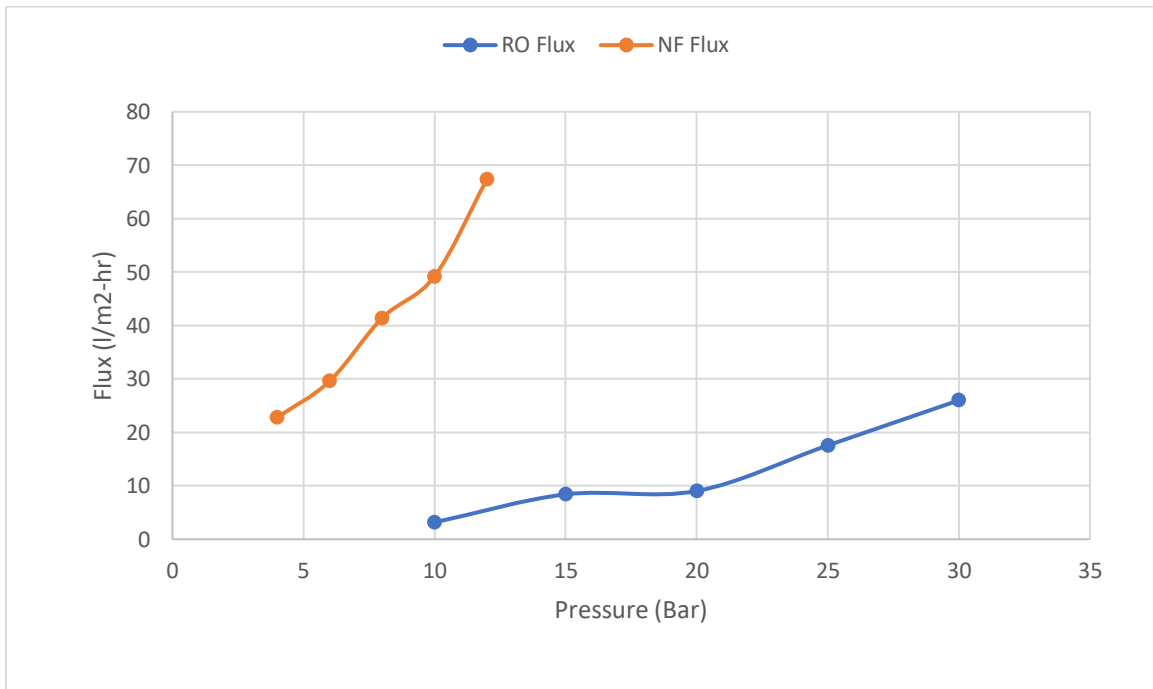


Figure 5.2-8- Comparison of flux between nanofiltration (NF) and reverse osmosis (RO) membranes

By comparing the NF and RO flux curve can be observed that high flux at low operating pressure can be achieved by NF membrane while it is possible for RO membrane at much

higher pressure. This feature makes RO membrane less economical. The steep slope of NF membrane indicates the with a slight increase in the pressure (2 bar), the flux can be greatly increased whereas due to the RO flux curve, the slope of the curve is much less than the slope of the NF flux curve. It means that with a large increase in pressure, the flux doesn't change significantly.

### 5.2.4.3. Total Dissolved Solids (TDS) in NF vs. RO

Figure 5.2-9 shows a comparative graph of TDS in permeate flow of NF and RO membranes as a function of pressure:

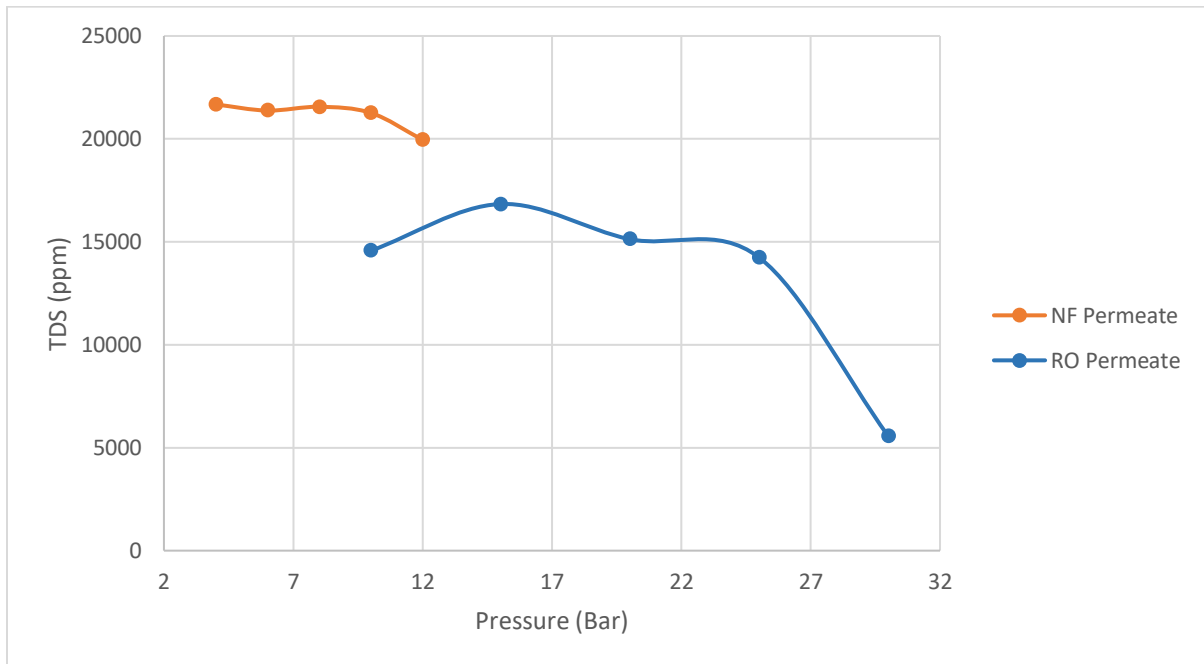


Figure 5.2-9- Comparison of TDS between nanofiltration (NF) and reverse osmosis (RO) membranes

The TDS level of permeate from RO membrane is lower than TDS level of permeate from NF membrane. However, the TDS level of permeate in the NF process is very close to the TDS of the feed.

### 5.2.5. Smart Water Production

As previously discussed, the favorable characteristics of water injecting into the carbonate reservoir are low salinity (low concentration of monovalent ions) and high concentration of divalent ions which leads to improvement of the wettability of rock system resulting to more oil recovery. As an option to produce smart water using nanofiltration and reverse osmosis membranes, the retentate flow from NF membrane containing the main constituents of smart water (sulphate, calcium and magnesium) was combined with the permeate flow from RO membrane (at a ratio of one to six) in order to reduce the TDS of the retentate to a target of 10000 ppm or less while retaining the divalent ions in the smart water [13]. The process of the smart water production using membrane technology is schematically shown in figure 5.2-10:

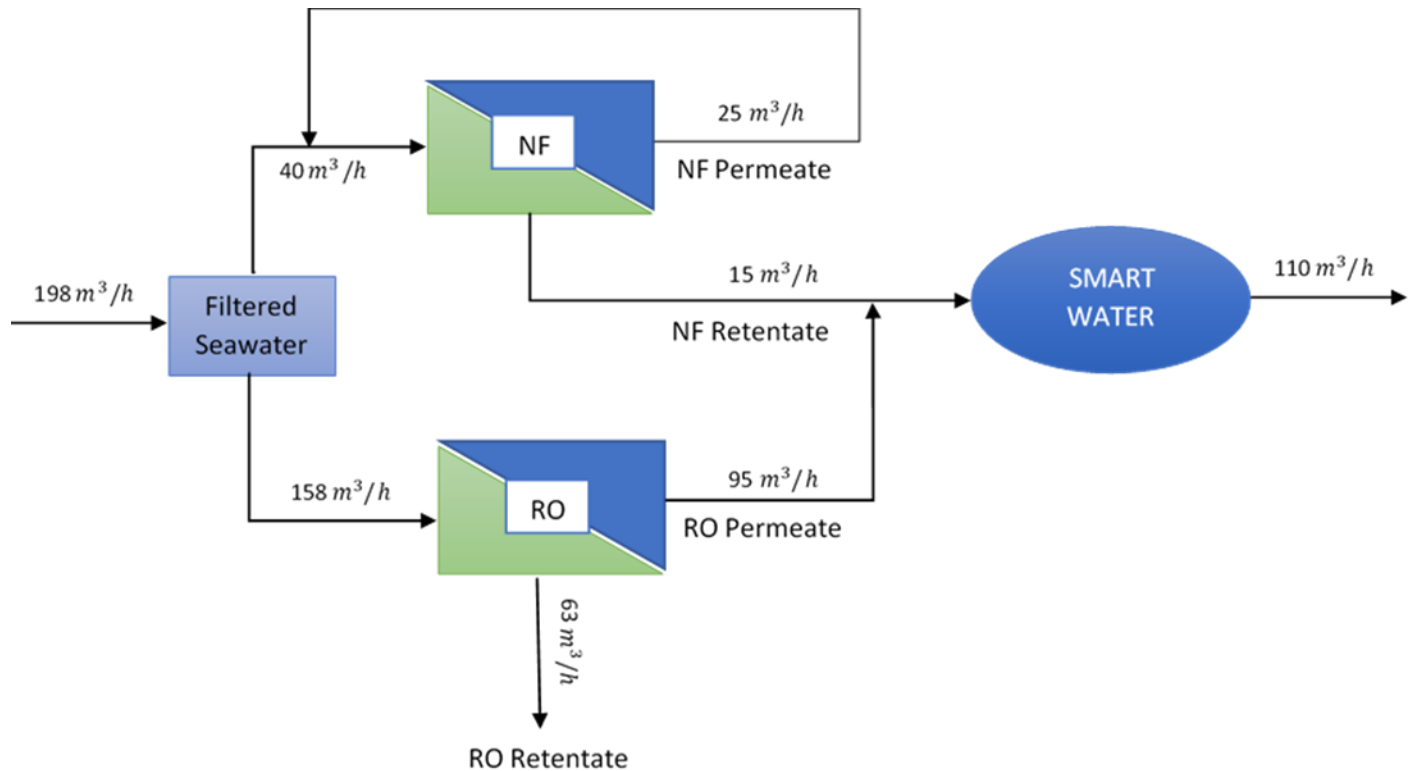


Figure 5.2-10- A schematic of smart water production using nanofiltration (NF) and reverse osmosis (RO) membranes (at one to six ratio)

The ionic composition (major ions) and other important characteristic of the smart water are shown in the following table:

Table 5.2-1- Characteristics of smart water produced from membrane technology

<b>Characteristics of Smart Water</b>	
Ions	Concentration (mg/l)
Chloride ( $Cl^-$ )	3210,643
Sulphate ( $SO_4^{2-}$ )	544,557
Sodium ( $Na^+$ )	3076,643
Magnesium ( $Mg^{2+}$ )	289,286
Calcium ( $Ca^{2+}$ )	122,440
<b>Other Characteristics of Filtered Seawater</b>	
pH	7.50
TDS (mg/l)	7243
Conductivity (mS/cm)	11.40

### 5.3. Flotation Technique Using Smart Water

A set of MFT experiments were carried out using smart water (produced by nanofiltration and reverse osmosis technique) and real seawater as the brine (s.l.)s in order to investigate how these brines alter the wettability of the chalk. The results of the chalk wettability alteration upon interaction with smart water and seawater at 100 °C are shown in figure 5.3-1:

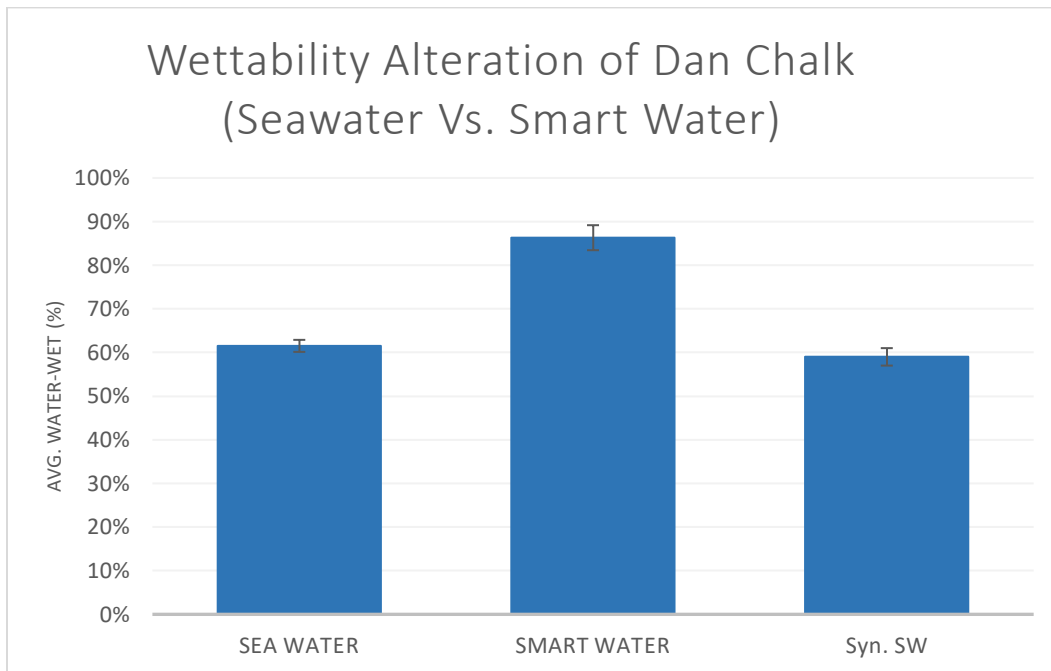


Figure 5.3-1- Wettability alteration of Dan Chalk using seawater and smart water at 100 °C

Due to the results from flotation experiments shown in the figure 5.1-28, the smart water wetted the chalk ca. 86.30% while the normal seawater wetted the chalk ca. 61.52%. This result was expected due to last studies and the results from the first series of flotation experiments in this project as well. According to the main mechanism of wettability alteration of rock, the wettability condition can be altered by adjusting the ion composition of the water (fluid) injected into the reservoir resulting to displace oil more easily from the porous network and eventually more oil recovery.

# **6. CHAPTER 6**

## ***(Scenarios and Recommendation)***

## **6.1. Suggested Scenarios for Smart Water Production and Economic Analysis**

Considering the waterflooding method as a cost-effective method for enhanced oil recovery (EOR), huge quantities of water with desired composition and quality is required in order to increase the amount of oil production. As previously explained, membrane technology can be considered as a suitable method for producing smart water with the desired composition and quality. However, it is necessary to investigate the proposed method economically and technically. For this purpose, the following two scenarios were studied for choosing the optimal method of smart water production. The scenarios were simulated using IMSDesign (Hydranautics, Integrated Membrane Solutions Design) designed by Nitto Group Company [84] at six ratio of NF/RO combinations (1:3, 1:4, 1:5, 1:6, 1:7 and 1:8) to evaluate and estimate energy consumption of the membranes process trains. 110 m<sup>3</sup>/h was assumed as the amount of the smart water used for injection into reservoir produced by each scenario [86].

### 6.1.1. Scenario 1

In this scenario, the retentate flow (contains divalent ions and high salinity) from the nanofiltration process is combined with the permeate flow coming out from the reverse osmosis process in order to lower the salinity. The process of the suggested scenario is schematically shown in figure 6.1-1:

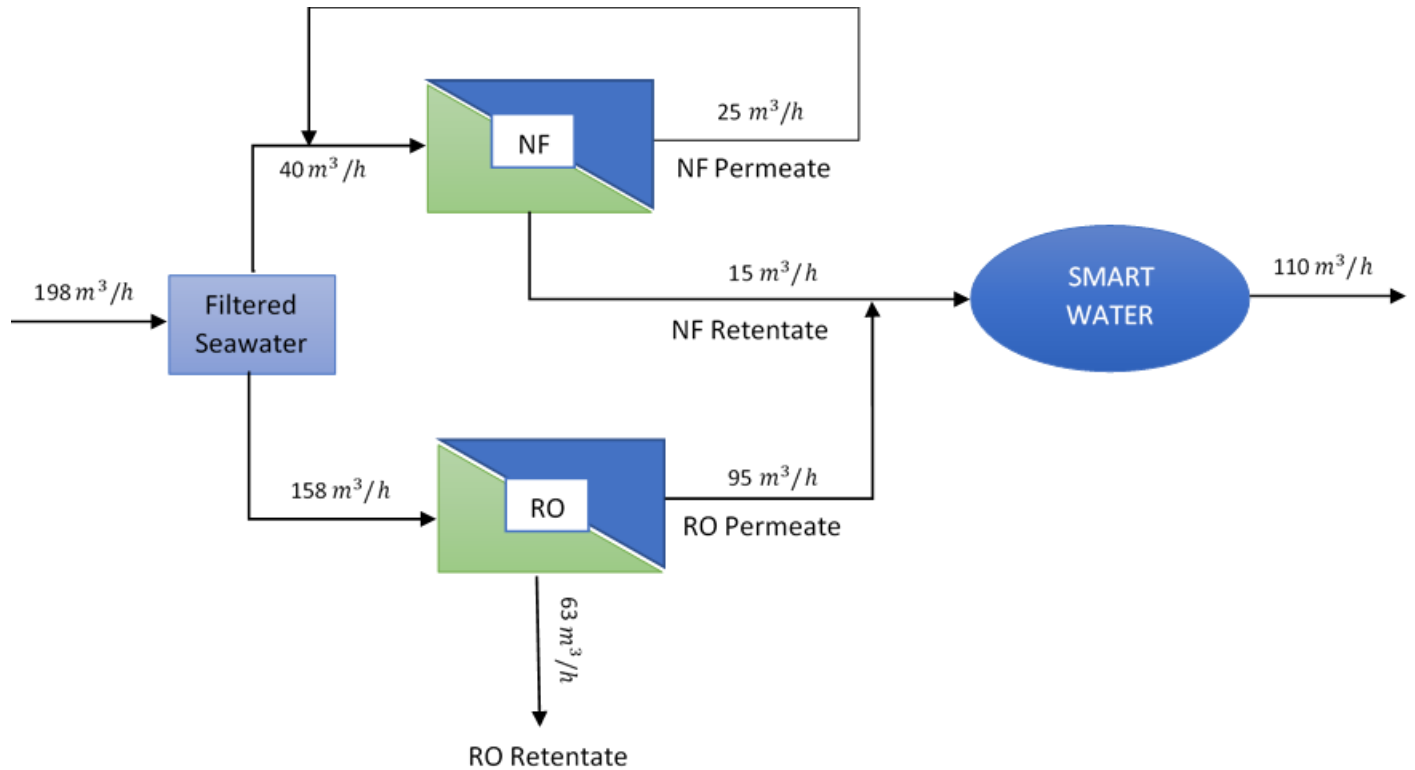


Figure 6.1-1- Combination of nanofiltration and reverse osmosis process to produce smart water at one to six ratio (Scenario 1)

## 6.1.2. Scenario 2

In this scenario, the permeate flow from nanofiltration passes through reverse osmosis membrane and the permeate flow exiting from RO membrane is then combined with a portion of the retentate flow from NF process. The schematic of the whole process is shown below:

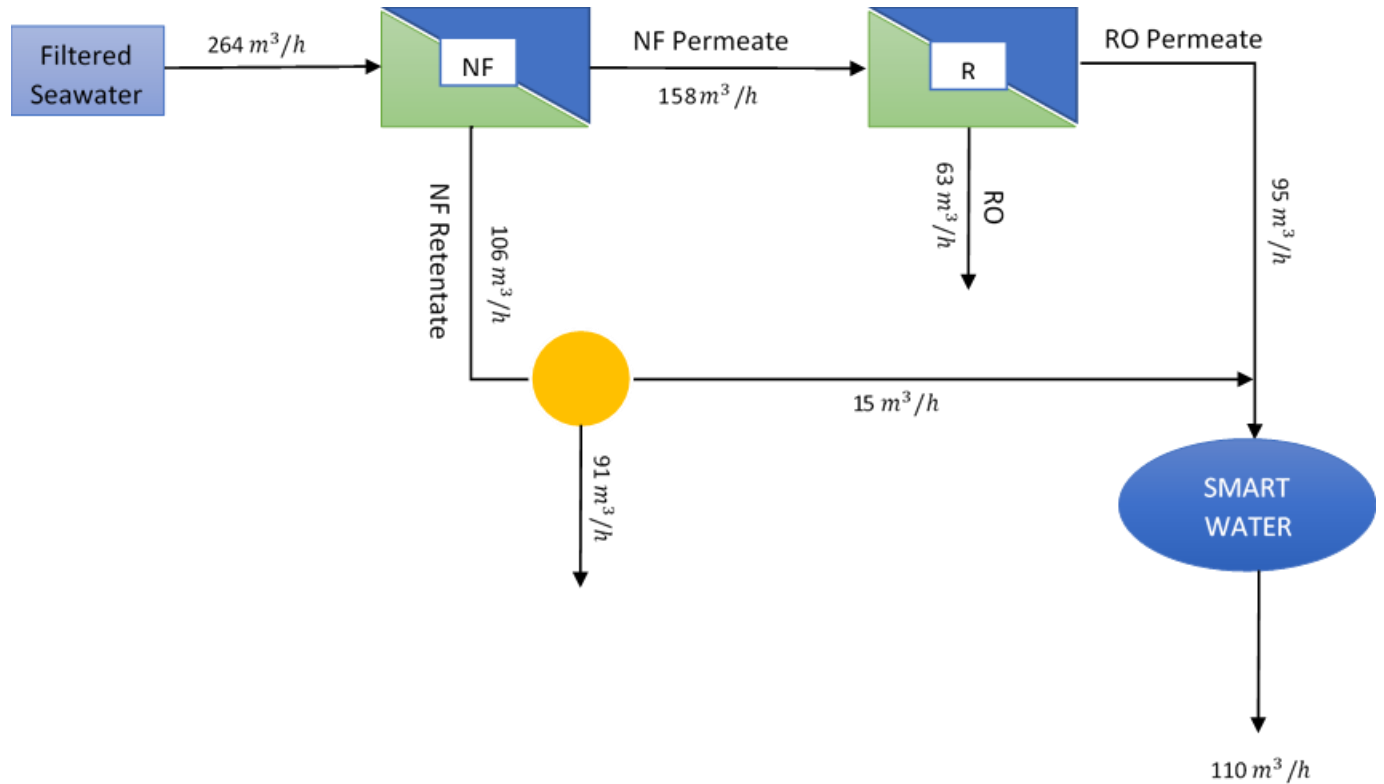


Figure 6.1-2- Proposed train for smart water production using NF and RO at one to six ratio (Scenario 2)

Having run the simulation, the optimal scenario was chosen based on the evaluation of energy consumption of each train. The results are present in figure 6.1-3:

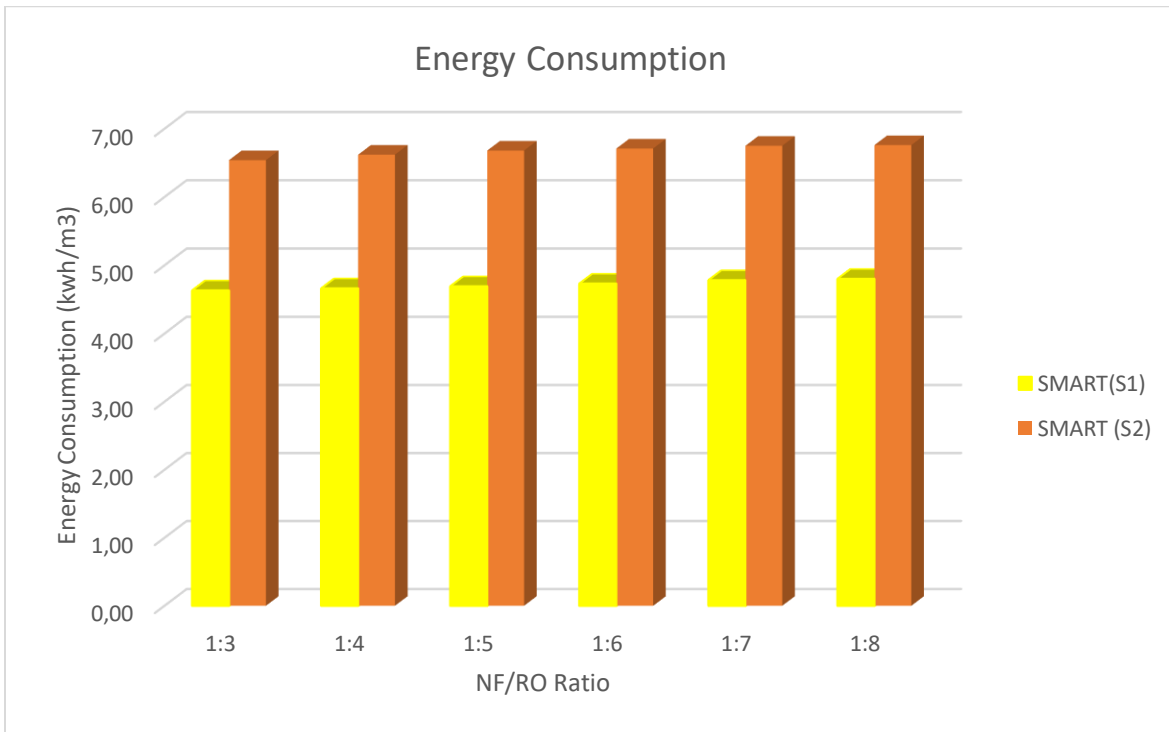


Figure 6.1-3- Energy Consumption by different processes of smart water production in different ratio

Due to the values of energy consumption for both scenarios, the energy required to produce one m<sup>3</sup>/h smart water using scenario 1 ranges between 4,63 and 4,80 (kwh) and using scenario 2 ranges between 6,54 and 6,76 (kwh) for different ratio of NF/RO combinations. On the other hand, considering 1:6 ratio of NF/RO combination, in order to have 110 m<sup>3</sup>/h of smart water output from the first scenario, 198 m<sup>3</sup>/h feed (filtered seawater) is required while for the second scenario 264 m<sup>3</sup>/h feed required. Considering this parameter and analysis, it can be concluded that production of smart water with desirable composition using scenario 1 is the economical option compared to the scenario 2.

According to previous studies, [13], [75], there are other dilution options for smart water production in order to overcome high salinity of retentate flow from NF membrane such as combination of NF retentate with fresh water or with Multi-flash distillation (MSFD). The space and weight constraints on offshore, which are considered as major parameters in facility design and evaluation of processes, as well as the special conditions on offshore and staying away from land, make the above-mentioned options non-economic options. Technical and economic evaluation of smart water production using NF and RO membrane proved that the membrane technology can be considered as an effective and economic technique in enhanced oil recovery compared to other advanced desalination methods. In addition, the performing this technology doesn't require the use of chemicals and therefore it virtually makes the process as and acceptable process for the environment.

# ***7. CHAPTER 7*** ***(Conclusions)***

As the first objective of the thesis, the wettability alteration of rock in the carbonate reservoir after waterflooding process was investigated. Several sets of laboratory experiments were carried out using modified flotation technique (MFT) in order to study how changes in various parameters in CBR system can affect the wetting condition of the rock in the reservoir and ultimately affect the amount of oil recovery during EOR process. The two main components of the system, including oil and rock (Dan Chalk) samples, taken from the same field in the North Sea, were kept constant and the ionic composition of the injected fluid (brine) was varied at a temperature of 100 °C. Different composition of seawater and their dilutions were synthetically prepared by varying the presence of divalent ions in the chemical composition of the seawater. The ionic strength, TDS, ionic composition and pH were measured and calculated in each step in order to perform a detailed analysis of the effect of the parameters on the wettability alteration of the chalk.

As the next objective of the thesis, production of smart water with desired composition (low salinity and high concentration of divalent ions) suitable for injection into reservoir, using membrane technology, was aimed. For this purpose, two sets of laboratory experiments using nanofiltration (NF) and reverse osmosis (RO) membranes under varying the operating pressure were carried out. Using this method, it was possible to separate the ions present in seawater and produce smart water with desired composition by combination of retentate flow from NF membrane with permeate flow from RO membrane. The performance of the membranes was separately measured and calculated in order to analyze and compare the efficiency of the membranes for ion separation.

As the last objective of the thesis, the produced smart water from membrane process was tested by carrying out a set of flotation experiment. This part of the experiments was aimed to investigate the ability of the produced smart water with low salinity while retaining the divalent ions to affect the wettability condition of the chalk.

After summarizing the results and observations of all experiments, the conclusions of the current study can be stated as follow:

- Highest average water-wet percentage of chalk was achieved by 20 times diluted synthetic sea water among all the synthetic brines at 100 °C (approximately 60.67%);

- Removing any of divalent ions ( $Ca^{2+}$ ,  $Mg^{2+}$ ,  $SO_4^{2-}$ ) from synthetic seawater recipe decreases the average water-wet percentage of chalk significantly (approximately 10%);
- A slight increase in the wettability of chalk by using the dilutions of brines was observed that is due to the reduction in the salinity of the brine;
- pH plays a significant role in the wettability alteration of the chalk whereas the variation in the TDS values plays lesser role in the wetting condition of the chalk;
- The highest water wetness occurred using a brine with an ionic strength of 0.033 mol/l and a salinity of 1.93 g/l;
- Considering amount of oil attached to the water-wet grains, it was not observed any correlation between the amount of attached oil and water-wet grains in the CBR system. However, the oil fraction (oil coating) was considered as the direct adsorption of the oil on the chalk particles;
- The calculated values of flotation wetting index (FWI) provides an easy and general overview of wettability alteration potential using different brines;
- In order to get trustworthy and consistent results during the modified flotation technique, it is essential that the experiments be performed with high precision and reliability of results can be shown by calculation of data standard deviation;
- The use of membrane technology can be considered as an optimal option to produce smart water with favorable composition from seawater;
- High retention of divalent ions ( $Ca^{2+}$  : 25-35%,  $Mg^{2+}$  : 55-65%,  $SO_4^{2-}$  : 85-90%) by nanofiltration (NF) membrane makes its retentate flow as main constituent of smart water;
- High rejection of salts by reverse osmosis (RO) membrane makes its permeate flow as a desirable option to reduce the salinity of the seawater;
- Production of smart water by NF and RO membranes does not need to use chemical that makes the process environmentally friendly. On the other hand, it requires lower investment, lower operating and maintenance cost compared to the other techniques;

- Having done MFT experiment using produced smart water from NF and RO membranes, the average water-wet percentage of chalk increased approximately 25% compared to seawater;

In order to analyze the process of smart water production using NF and RO membrane economically, two scenarios were simulated and evaluated in terms of energy consumption. For a given output of 110 m<sup>3</sup> smart water, the first scenario with energy consumption of 4,67 (kwh/m<sup>3</sup>) was considered as the optimal process for production of smart water.

## 7.1. Future Work

Due to the time limitation of project, as well as since the MFT experiment is a time-consuming process, study and analysis other parameters that affect wettability of rock requires time and they were not covered in this study. For example, effect of temperature on the wettability or effect of oil with different characteristics would be interesting to investigate by doing flotation experiment.

It could be interesting to consider and introduce new ions such as zinc cation and phosphate anion (careful attention to avoid precipitation) in the smart water composition and investigate that in what extent it can influence the wettability of rock in the reservoir.

Considering the production of smart water using membrane technology, future research can consider the potential of nanofiltration membrane in produced water treatment train. As it can be seen from figure 7.1-1, nanofiltration process can be located after tertiary stage in the train where the flow is almost oil-free and it needs to be softened.

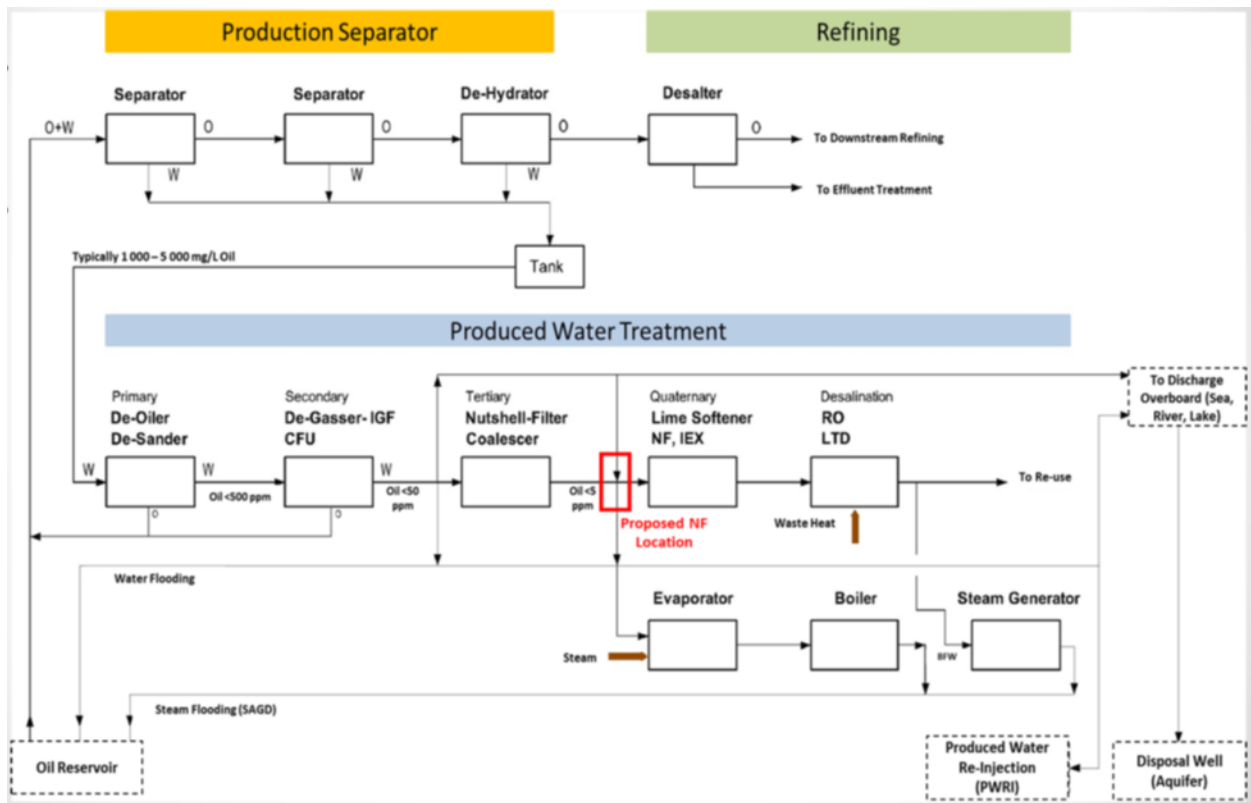


Figure 7.1-1- A schematic of topside processes [87]

## 8. Bibliography

- [1] T. Austad, "Water Based EOR in Carbonates and Sandstones: New Chemical Understanding of the EOR-Potential Using "Smart Water", in *"Enhanced Oil Recovery Field Cases."*, Elsevier, 2012.
- [2] E. d. S. Godinho and K. Jefimov, "Effectiveness of produced water in advanced waterflooding: estimation of the wettability alteration by modified flotation technique," Aalborg University, Esbjerg, 2017.
- [3] D. w. green and G. p. willhite, *Enhanced oil recovery*, vol. 6, Texas: Society of Petroleum Engineers, 1996.
- [4] H. Slider, *Worldwide Practical Petroleum Reservoir Engineering Methods*, Tulsa: Penn Well, 1983.
- [5] E. C. Donaldson, *Enhanced Oil Recovery, II processes and operations*, Tokyo: Elsevier Science Publisher B.V., 1989.
- [6] E. Donaldson, G. Chilingarian and T. Yen, *Enhanced Oil Recovery*, vol. 2, Elsevier Science, 1989.
- [7] Petropedia, "Petropedia," 2019. [Online]. Available: <https://www.petropedia.com/definition/6773/hot-water-flooding>.
- [8] S. Thomas, "Enhanced Oil Recovery – An Overview," *Oil & Gas Science and Technology*, vol. 63, no. 1, pp. 09-19, 2008.
- [9] R. R. NAIR, "SMART WATER FOR EOR BY MEMBRANES," Stavanger University, Stavanger, 2014.
- [10] E. C. Donaldson, T. F. Yen and G. V. Chilingarian, *Enhanced Oil Recovery, Fundamental and Analyses*, vol. 1, Tokyo: Society of Petroleum Engineers, 1985.
- [11] I. D. P. Torrijos, "Enhanced oil recovery from Sandstones and Carbonates with "Smart Water" (pHD Thesis)," Stavanger University, Stavanger, 2017.
- [12] "Waterstandard," Waterstandard, 2019. [Online]. Available: <http://waterstandard.com/wp/wp-content/uploads/Screen-Shot-2013-02-08-at-1.46.34-PM.png>.
- [13] T. Bilstad, R. R. Nair and E. Protasova, "NF MEMBRANES FOR PRODUCTION OF SMART WATER FROM SEAWATER," p. 3, 2014.
- [14] A. Lager, K. J. Webb, C. J. J. Black, M. Singleton and K. S. Sorbie, "LOW SALINITY OIL RECOVERY - AN EXPERIMENTAL INVESTIGATION," September 2006.
- [15] D. Keszthelyi, D. K. Dysthe and B. Jamtveit, "Compaction of North-Sea Chalk by Pore-Failure and Pressure Solution in a Producing Reservoir," *Physics of Geological Processes*, p. 2, 16 February 2016.

- [16] T. Ahmed, Reservoir Engineering Handbook, Fourth ed., ELSEVIER, 2010.
- [17] E. D. S. Godinho, "Effectiveness of Produced Water in Advanced Waterflooding: estimation of the wettability alteration by modified flotation technique," Aalborg University, Esbjerg, 2017.
- [18] "Kitchen Decor," 2019. [Online]. Available: <https://kitchendecor.club/files/types-mineral-groups.html>. [Accessed 2019].
- [19] M. A. Sohal, "Wettability modification in chalk: systematic evaluation of salinity, brine composition and temperature effects," Aalborg University, Esbjerg, 2016.
- [20] J. M. HANCOCK, The petrology of the Chalk, London: Proc. Geol. Ass, 1975.
- [21] R. Clews, "Fundamentals of the Petroleum Industry," *Project Finance for the International Petroleum Industry*, 2016.
- [22] ChemEngineering, "Petroleum Crude Oil Composition," 2017.
- [23] A. Groysman, "Corrosion Problems and Solutions in Oil Refining and Petrochemical Industry," *Israeli Society of Chemical Engineers & Chemists*, 2017.
- [24] E. J. Burcik, PROPERTIES OF PETROLEUM RESERVOIR FLUIDS, Boston: International Human Resources Development Corporation, 1979.
- [25] J. Speight, High Acid Crudes, Gulf Professional Publishing, 2014.
- [26] J. Sheng, Enhanced Oil Recovery Field Case Studies, Gulf Professional Publishing, 2013.
- [27] F. F. Craig, The Reservoir Engineering Aspects of Waterflooding, New Yourk: Society of Petroleum Engineers of AIME, 1971.
- [28] J. T. Smith and W. M. Cobb, Waterflooding, Cody: Journal of petroleum technology, 1997.
- [29] A. M. E. Shafey, "Effect of nanoparticles and polymer nanoparticles implementation on chemical flooding, wettability and interfacial tension for the enhanced oil recovery processes," *African Journal of Engineering Research*, vol. 5 (3), pp. 35-53, 2017.
- [30] J. Dickhout, J. Moreno, P. Biesheuvel, R. L. L. Boels b and W. d. Vos, "Produced water treatment by membranes: A review from a colloidal perspective," *Colloid and Interface Science*, pp. 524-534, 2017.
- [31] P. V. Brady and G. Thyne, "Functional Wettability in Carbonate Reservoirs," 30 July 2016.
- [32] N. R. Morrow, "Wettability and Its Effect on Oil Recovery," *Society of Petroleum Engineers*, p. 1476, 1990.
- [33] W. G. Anderson, "Wettability Literature Survey-Part 2: Wettability Measurement," *Journal of Petroleum Technology*, p. 1246, 1986.

- [34] T. Puntervold, "Waterflooding of carbonate reservoirs (Doctorial Thesis)," Stavanger University, Stavanger, 2008.
- [35] M. A. Sohal, G. Thyne and E. G. Sjøgaard, "Review of Recovery Mechanisms of Ionically Modified Waterflood in Carbonate Reservoirs," *Energy Fuels*, vol. 30, pp. 1904-1914, 2016.
- [36] M. A. Sohal, S. Kucheryavskiy, G. Thyne and E. G. Sjøgaard, "Study of Ionically Modified Water Performance in the Carbonate Reservoir System by Multivariate Data Analysis," *Energy Fuels*, vol. 31, pp. 2414-2429, 2017.
- [37] J. Pawliszyn, Handbook of Solid Phase Microextraction, Chemical Industry Press, 2009.
- [38] Q. Xie, Y. Liu, J. Wu and Q. Liu, "Ions tuning water flooding experiments and interpretation by thermodynamic of wettability," *Petroleum Science and Engineering*, pp. 350-358, 2014.
- [39] P. Zhang, M. T. Tweheyo and T. Austad, "Wettability alteration and improved oil recovery by spontaneous imbibition of seawater into chalk: Impact of the potential determining ions  $Ca^{2+}$ ,  $Mg^{2+}$ , and  $SO_4^{2-}$ ," *Colloids and Surfaces*, no. 2006, pp. 199-208, 2006.
- [40] S. J. Fathi, T. Austad and S. Strand, "Water-Based Enhanced Oil Recovery (EOR) by "Smart Water": Optimal Ionic Composition for EOR in Carbonates," *Energy Fuel*, vol. 25, pp. 5173-5179, 2011.
- [41] K. B. Steffensen, "Optimization of Injection Fluids with Scope of Reservoir Wettability," Aalborg University Esbjerg (AAUE), Esbjerg, 2018.
- [42] O. A. KEHINDE, "THE EFFECT OF pH ON INTERFACIAL PROPERTIES OF HEAVY OIL/BRINE AND SURFACTANT ADSORPTION DURING SURFACTANT ENHANCED ALKALINE FLOODING," Dalhousie University, Halifax, Nova Scotia, 2012.
- [43] W. G. Anderson, "Wettability literature survey-Part 1: Rock/Oil/Brine interactions and the effects of core handling on wettability," *Journal of petroleum Technology*, pp. 1125- 1144, 1986.
- [44] D. Rao, "Wettability effects in thermal recovery operations," *SPE/DOE Improved Oil Recovery Symposium*, 21-24 April 1996.
- [45] T. Uragami, Science and Technology of Separation Membranes, John Wiley & Sons, Incorporated, 2017.
- [46] K.-V. Peinemann and S. P. Nunes, Membranes for Water Treatment, vol. 4, Weinheim: WILEY-VCH Verlag GmbH & Co. KGaA, 2010.
- [47] T. C. Zhang, R. Y. Surampalli, S. Vigneswaran and R. D. Tyagi, Membrane Technology and Environmental Applications, Virginia: American Society of Civil Engineers, 2012.
- [48] V. Pileggi, "Investigation of the Performance of an Anaerobic Membrane Bioreactor in the Treatment of Mixed Municipal Sludge Under Ambient, Mesophilic and Thermophilic Operating Conditions," University of Waterloo, Ontario, 2016.

- [49] A. M. S. San, "Akafor," Akafor , 2019. [Online]. Available: <https://www.akafor.com/bilgimerkezi/membran-teknolojileri>.
- [50] R. W. BAKER, Membrane Technology and Applications, Third ed., Newark: John Wiley and Sons Ltd, 2012.
- [51] What-When-How, "What-When-How," 2019. [Online]. Available: <http://what-when-how.com/nanoscience-and-nanotechnology/nanofiltration-separations-part-1-nanotechnology/>.
- [52] s. Filtration, 23 January 2019. [Online]. Available: <http://synderfiltration.com/learning-center/articles/introduction-to-membranes/membrane-materials-organic-inorganic/>.
- [53] V. P.M. and O. Nazarenko, Nanostructured Polymer Membranes, vol. 2, John Wiley & Sons, 2016.
- [54] Ladewig, Bradley, Al-Shaeli and M. N. Zemam, Fundamentals of Membrane Bioreactors, Springer Transactions in Civil and Environmental Engineering, 2017.
- [55] M. Cheryan, "Ultrafiltration and Microfiltration Handbook," in *Ultrafiltration and Microfiltration Handbook*, USA, Environmental Science and Technology, 1998, pp. 3710-3716.
- [56] C. Guizard, A. B. M. Barboiu and N. Hovnanian, "Hybrid organic-inorganic membranes with specific transport properties: Applications in separation and sensors technologies," *Separation and Purification Technology*, pp. 167-180, 2001.
- [57] N. N.Li, A. G.Fane, W. S. Winston.Ho and T. Matsuura, ADVANCED MEMBRANE TECHNOLOGY AND APPLICATIONS, Hoboken: WILEY, 2008.
- [58] S. FILTRATION, "SYNDER FILTRATION," SYNDER FILTRATION, 2018. [Online]. Available: <http://synderfiltration.com/learning-center/articles/module-configurations-process/tubular-membranes/>.
- [59] S. FILTRATION, "SYNDER FILTRATION," SYNDER FILTRATION, 2018. [Online]. Available: <http://synderfiltration.com/learning-center/articles/module-configurations-process/capillary-filtration/>.
- [60] S. FILTRATION, "SYNDER FILTRATION," SYNDER FILTRATION, [Online]. Available: <http://synderfiltration.com/learning-center/articles/module-configurations-process/hollow-fiber-membranes/>.
- [61] K. Nath, Membrane Separation Processes, Dehli: PHI learning private limited, 2017.
- [62] S. Assadi, H. Mosavian and A. Ahmadpour, "Effect of the membrane operating parameters on the separation of oxygen an hydrogen disulphide," *Indian Journal of Chemical Technology*, vol. 23, pp. 77-80, 2016.

- [63] G. Vaseghia, A. Ghassemib and J. Loya, "Characterization of reverse osmosis and nanofiltration membranes: effects of operating conditions and specific ion rejection," *Desalination and Water Treatment*, vol. 23, pp. 461-472, 2015.
- [64] H. C. Vogel and C. L. Todaro, *Fermentation and Biochemical Engineering Handbook*, Noyes Publications, 1997.
- [65] L. B. Group, "Lenntech B.V.," Lenntech B.V., 2019. [Online]. Available: <https://www.lenntech.com/membrane-systems-management.htm>.
- [66] P. F. Group, "Porex Filtration," Porex Filtration Group, 2019. [Online]. Available: <http://www.porexfiltration.com/learning-center/technology/what-is-cross-flow-filtration/>.
- [67] M. A. Sohal, G. Thyne and E. G. Søggaard, "Novel Application of the Flotation Technique To Measure the Wettability Changes by Ionically Modified Water for Improved Oil Recovery in Carbonates," *Energy and Fuels*, 2016.
- [68] C. Housecroft and A. G. Sharpe, *Inorganic Chemistry*, 5th ed., Basel: Pearson • Paper, 2018.
- [69] LibreTexts, "Chemistr," 2018. [Online]. Available: [https://chem.libretexts.org/Bookshelves/Physical\\_and\\_Theoretical\\_Chemistry\\_Textbook\\_Maps/Supplemental\\_Modules\\_\(Physical\\_and\\_Theoretical\\_Chemistry\)/Physical\\_Properties\\_of\\_Matter/States\\_of\\_Matter/Properties\\_of\\_Solids/Ionic\\_Solids](https://chem.libretexts.org/Bookshelves/Physical_and_Theoretical_Chemistry_Textbook_Maps/Supplemental_Modules_(Physical_and_Theoretical_Chemistry)/Physical_Properties_of_Matter/States_of_Matter/Properties_of_Solids/Ionic_Solids).
- [70] T. Wenzel, "Libretexts," 04 06 2017. [Online]. Available: [https://chem.libretexts.org/Bookshelves/Analytical\\_Chemistry/Supplemental\\_Modules\\_\(Analytical\\_Chemistry\)/Analytical\\_Sciences\\_Digital\\_Library/JASDL/Courseware/Separation\\_Science/07\\_Specialty\\_Topics/Ion-exchange\\_Chromatography/03\\_Basic\\_Principles\\_of\\_Ion\\_Chromatography](https://chem.libretexts.org/Bookshelves/Analytical_Chemistry/Supplemental_Modules_(Analytical_Chemistry)/Analytical_Sciences_Digital_Library/JASDL/Courseware/Separation_Science/07_Specialty_Topics/Ion-exchange_Chromatography/03_Basic_Principles_of_Ion_Chromatography).
- [71] T. Scientific, "ThermoFisher Scientific," 2019. [Online]. Available: <https://www.thermoFisher.com/se/en/home/industrial/spectroscopy-elemental-isotope-analysis/spectroscopy-elemental-isotope-analysis-learning-center/trace-elemental-analysis-tea-information/inductively-coupled-plasma-mass-spectrometry-icp-ms-information.htm>.
- [72] R. University, "Radboud University," 2019. [Online]. Available: <https://www.ru.nl/science/gi/facilities-activities/elemental-analysis/icp-ms/>.
- [73] R. M. Abhang, K. Wani, V. Patil, B. Pangarkar and S. Parjane, "Nanofiltration for Recovery of Heavy Metal Ions from Waste Water," *International Journal of Research in Environmental Science and Technology*, pp. 29-34, 2013.
- [74] W. R. Bowen and J. S. Welfoot, "Modelling the performance of membrane nanofiltration—critical assessment and model development," *Elsevier Science*, p. 57, 2002.
- [75] R. Nair, K. Saltveit and T. Bilstad, "Improved oil production by membranes," *AGI, Drilling, Oil, Gas*, vol. 32, 2015.

- [76] College of Engineering (Michigan University), 2019. [Online]. Available: <http://encyclopedia.che.engin.umich.edu/Pages/SeparationsChemical/Membranes/Membranes.html>.
- [77] "SterliTech," DOW, 2019. [Online]. Available: <https://www.sterlitech.com/nanofiltration-nf-membrane-ymnf2703001.html#>.
- [78] M. N. Finia, H. T. Madsenb and J. Muffa, "The effect of water matrix, feed concentration and recovery on the rejection of pesticides using NF/RO membranes in water treatment," *Separation and Purification Technology*, pp. 521-527, 2019.
- [79] I. Wenten, "Reverse osmosis applications: Prospect and challenges," *Desalination*, pp. 112-125, 2016.
- [80] A. Mnuhal, *Reverse Osmosis and Nanofiltration*, American Water Works Assoc., 2007.
- [81] X. Lewabrane, "Priciple o Reverse Osmosis Membrane Separation (Theory)," LANXESS, *Energising Chemistry*, 2018.
- [82] N. Hilal, A. F. Ismail, T. Matsuura and D. Oatley-Radcliffe, *Membrane Characterization*, Elsevier, 2017.
- [83] "SterliTech," DOW, 2019. [Online]. Available: <https://www.sterlitech.com/dow-filmtec-flat-sheet-membrane-xle-pa-tfc-ro-cf016-5-pk.html>.
- [84] IMSDesign, "Nitro Group Company," 2019. [Online]. Available: <http://membranes.com/solutions/software/>.
- [85] M. M. Thomas, J. A. Clouse and J. M. Longo, "Adsorption of organic compounds on carbonate minerals: 1. model compounds and their influence on mineral wettability," *Chemical Geology*, no. Elsevier, pp. 201-213, 1993.
- [86] M. Heatherly, M. Howell and J. McElhiney, "Sulfate Removal Technology For Seawater Waterflood Injection," 1994.
- [87] R. R. Nair, "SMART WATER BY MEMBRANES," Stavanger University, Stavanger, 2016.

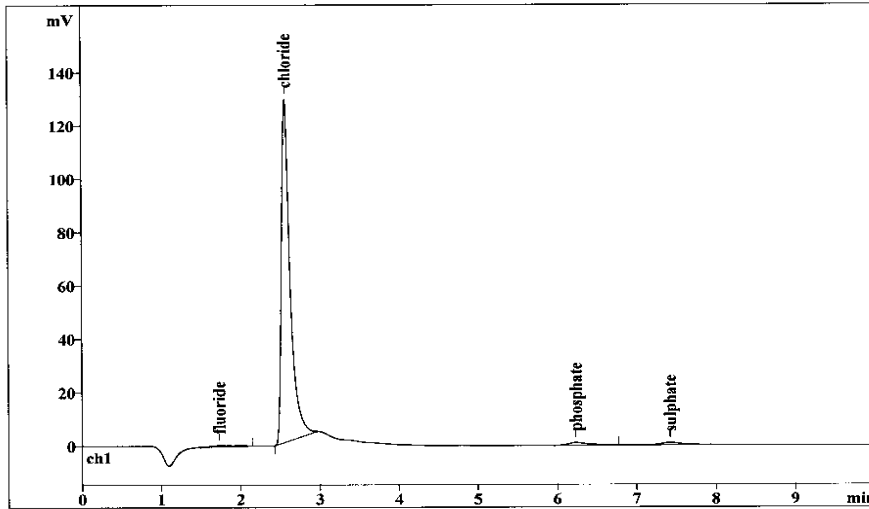
## 9. Appendix

### 9.1. Data Entry Table for Flotation Experiment

Test Tube (--)		
Parameters	Amount	Unite
Empty Test Tube Weight		g
Sample Name		
Sample Mass		g
Brine Used		
Grain Size		μm
Brine Volume		ml
Oil Volume		ml
Test Temperature		°C
pH of Decanted Brine		
Start Brine Aging		
End Brine Aging		
Total Brine Aging Time		hrs
Start Oil Aging		
End Oil Aging		
Total Oil Aging Time		hrs
Start Oil/Brine/Grain Aging		
End OilBrine/Grain Aging		
Total Mixture Aging Time		hrs
Test Tube Weight with dry grains		g
Weight of Oil-wet Grains		g
Weight of Water-wet Grains		g
Percentage of Oil-wet Grains		%
Percentage of Water-wet Grains		%

## 9.2. Ions Analysis Results (IC and ICP Machines)

Report date: 29-01-2019 11:32:06  
 Printed by: Dorte Spangsmark  
 Ident: P-NF-12 bar- x1000  
 Analysis from: 29-01-2019 11:22:06  
 File: \_2019-01-29\_ Last save: 29-01-2019 11:32:06  
 Method: Anioner KEMI CPR.mtw Last save: 28-01-2019 1  
 Run operator: Dorte Spangsmark  
 Analysis number: 1760  
 ELUENT: 3.2 mM Na<sub>2</sub>CO<sub>3</sub> / 1.0 mM NaHCO<sub>3</sub>  
 Flow: 1.00 mL/min  
 Temperature: 20.0°C  
 Pressure: 71.0 bar



Quantitation method: Custom

No	Retention min	Height mV	Area mV*sec	Conc. mg/L	Name	File
1	1.73	0.54	10.105	0.087	fluoride	_2019-01-29_
2	2.57	128.59	972.525	13.818	chloride	_2019-01-29_
3	6.24	1.05	18.622	1.170	phosphate	_2019-01-29_
4	7.42	0.90	16.818	0.394	sulphate	_2019-01-29_
4	10.00	131.09	1018.070	15.469		

This report has been created by IC Net  
 METROHM LTD

Figure 9.2-1- Anions present in permeate flow of nanofiltration under pressure of 12 bar

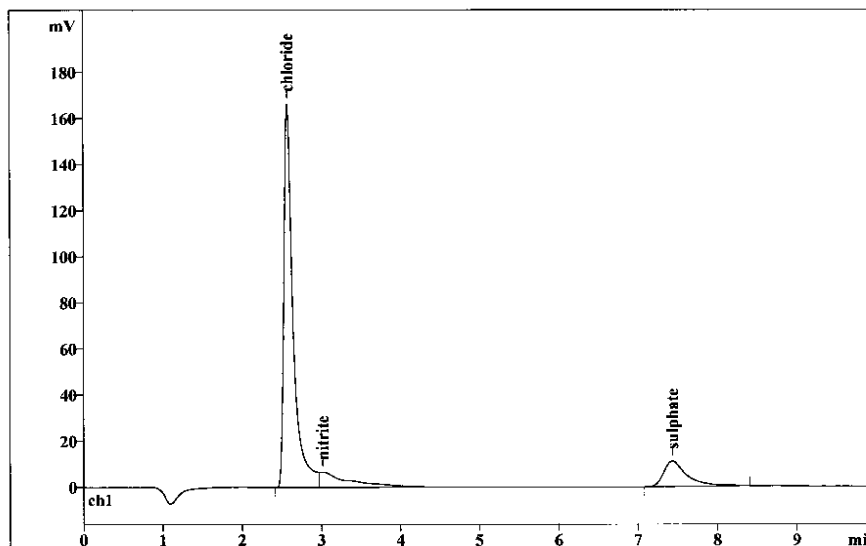
Report date: 29-01-2019 10:53:45  
 Printed by: Dorte Spangsmark

Ident: R-NF-12 bar- x1000  
 Analysis from: 29-01-2019 10:43:45  
 File: \_2019-01-29\_ Last save: 29-01-2019 10:53:45

Method: Anioner KEMI CPR.mtw Last save: 28-01-2019 1  
 Run operator: Dorte Spangsmark  
 Analysis number: 1757

ELUENT: 3.2 mM Na2CO3 / 1.0 mM NaHCO3

Flow: 1.00 mL/min  
 Temperature: 20.0°C  
 Pressure: 71.0 bar



Quantitation method: Custom

No	Retention min	Height mV	Area mV*sec	Conc. mg/L	Name	File
1	2.58	166.35	1344.861	19.108	chloride	_2019-01-29_
2	3.01	6.59	175.938	3.189	nitrite	_2019-01-29_
3	7.43	11.05	225.564	5.278	sulphate	_2019-01-29_
3	10.00	183.98	1746.364	27.575		

This report has been created by IC Net  
 METROHM LTD

Figure 9.2-2- Anions present in retentate flow of nanofiltration under pressure of 12 bar

=====  
Analysis BegunStart Time: 29-01-2019 09:03:55  
Logged In Analyst: Administrator  
Spectrometer: Optima 8000Plasma On Time: 29-01-2019 08:43:04  
Technique: ICP Continuous  
Autosampler: S10Sample Information File: C:\Users\Public\PerkinElmer\ICP\Data\Sample Information\Untitled.SIF  
Batch ID:  
Results Data Set: Akam, Ca, Mg, Na  
Results Library: C:\Users\Public\PerkinElmer\ICP\Data\Results\Results.mdb=====  
Sequence No.: 1  
Sample ID: R-NF-10 bar-x100  
Analyst:  
Initial Sample Wt:  
Dilution:  
Wash Time:  
Autosampler Location: 9  
Date Collected: 29-01-2019 09:03:55  
Data Type: Original  
Initial Sample Vol:  
Sample Prep Vol:

Replicate Data: R-NF-10 bar-x100							
Repl#	Analyte	Net Intensity	Corrected Intensity	Calib. Conc. Units	Sample Conc. Units	Analysis Time	
1	Ca 422.673	9734809.4	9734756.6	5.607 mg/L	5.607 mg/L	09:05:26	
1	Na 589.592	Saturated3	Saturated3			09:05:39	
	Saturated in preshot (code 3)						
1	Mg 279.553	Saturated3	Saturated3			09:06:05	
	Saturated in preshot (code 3)						
2	Ca 422.673	10080904.9	10080852.2	5.786 mg/L	5.786 mg/L	09:05:29	
2	Na 589.592	164169713	164065402	78.30 mg/L	78.30 mg/L	09:05:47	
	Saturated within auto integration window (code 4)						
2	Mg 279.553	130540155	130538668	14.92 mg/L	14.92 mg/L	09:06:12	
	Saturated within auto integration window (code 4)						
3	Ca 422.673	10186154.1	10186101.4	5.840 mg/L	5.840 mg/L	09:05:32	
3	Na 589.592	163597176	163492864	78.03 mg/L	78.03 mg/L	09:05:54	
	Saturated within auto integration window (code 4)						
3	Mg 279.553	129389232	129387745	14.79 mg/L	14.79 mg/L	09:06:19	
	Saturated within auto integration window (code 4)						

Mean Data: R-NF-10 bar-x100							
Analyte	Mean Intensity	Corrected Intensity	Calib. Conc. Units	Std.Dev.	Sample Conc. Units	Std.Dev.	RSD
Ca 422.673	10060570.0		5.744 mg/L	0.1220	5.744 mg/L ✓	0.1220	2.12%
Na 589.592	Saturated4		78.17 mg/L	0.192	78.17 mg/L ✓	0.192	0.25%
Mg 279.553	Saturated4		14.85 mg/L	0.093	14.85 mg/L ✓	0.093	0.63%

=====  
Sequence No.: 2  
Sample ID: R-NF-10 bar-x1000  
Analyst:  
Initial Sample Wt:  
Dilution:  
Wash Time: 40  
Autosampler Location: 10  
Date Collected: 29-01-2019 09:07:17  
Data Type: Original  
Initial Sample Vol:  
Sample Prep Vol:  
Auto Dilution Factor: 1

Replicate Data: R-NF-10 bar-x1000							
Repl#	Analyte	Net Intensity	Corrected Intensity	Calib. Conc. Units	Sample Conc. Units	Analysis Time	
1	Ca 422.673	865995.4	865942.7	1.025 mg/L	1.025 mg/L	09:08:47	
1	Na 589.592	17002795.6	16898484.0	8.573 mg/L	8.573 mg/L	09:08:59	
1	Mg 279.553	15135358.5	15133871.7	1.680 mg/L	1.680 mg/L	09:09:13	
2	Ca 422.673	872062.7	872010.0	1.028 mg/L	1.028 mg/L	09:09:50	
2	Na 589.592	16832928.4	16728616.8	8.493 mg/L	8.493 mg/L	09:09:03	
2	Mg 279.553	15426315.3	15424828.6	1.713 mg/L	1.713 mg/L	09:09:17	
3	Ca 422.673	857048.2	856995.5	1.020 mg/L	1.020 mg/L	09:08:52	
3	Na 589.592	17186204.4	17081892.8	8.660 mg/L	8.660 mg/L	09:09:06	
3	Mg 279.553	15064487.0	15063000.2	1.672 mg/L	1.672 mg/L	09:09:20	

Mean Data: R-NF-10 bar-x1000							
Analyte	Mean Intensity	Corrected Intensity	Calib. Conc. Units	Std.Dev.	Sample Conc. Units	Std.Dev.	RSD
Ca 422.673	864982.7		1.024 mg/L	0.0039	1.024 mg/L	0.0039	0.38%
Na 589.592	16902997.9		8.575 mg/L	0.0837	8.575 mg/L ✓	0.0837	0.98%

Figure 9.2-3- Cations present in retentate flow of nanofiltration under pressure of 10 bar

## Replicate Data: P-NF-10 bar-x100

Repl#	Analyte	Net Intensity	Corrected Intensity	Calib. Conc. Units	Sample Conc. Units	Analysis Time
1	Ca 422.673	9115224.6	9115171.9	5.287 mg/L	5.287 mg/L	09:18:07
1	Na 589.592	Saturated3	Saturated3			09:18:20
	Saturated in preshot (code 3)					
1	Mg 279.553	67301530.5	67300043.7	7.665 mg/L	7.665 mg/L	09:18:46
2	Ca 422.673	9114690.4	9114637.6	5.286 mg/L	5.286 mg/L	09:18:10
2	Na 589.592	197968240	197863928	94.32 mg/L	94.32 mg/L	09:18:28
	Saturated within auto integration window (code 4)					
2	Mg 279.553	68272885.1	68271398.4	7.777 mg/L	7.777 mg/L	09:18:53
3	Ca 422.673	9362656.0	9362603.2	5.414 mg/L	5.414 mg/L	09:18:13
3	Na 589.592	198819388	198715076	94.72 mg/L	94.72 mg/L	09:18:35
	Saturated within auto integration window (code 4)					
3	Mg 279.553	68765889.2	68764402.5	7.833 mg/L	7.833 mg/L	09:19:00

## Mean Data: P-NF-10 bar-x100

Analyte	Mean Corrected Intensity	Calib. Conc. Units	Std.Dev.	Sample Conc. Units	Std.Dev.	RSD
Ca 422.673	9197470.9	5.329 mg/L	0.0739	5.329 mg/L ✓	0.0739	1.39%
Na 589.592	Saturated4	94.52 mg/L	0.285	94.52 mg/L ✓	0.285	0.30%
Mg 279.553	68111948.2	7.758 mg/L	0.0855	7.758 mg/L ✓	0.0855	1.10%

Sequence No.: 6

Sample ID: P-NF-10 bar-x1000

Analyst:

Initial Sample Wt:

Dilution:

Wash Time: 40

Autosampler Location: 22

Date Collected: 29-01-2019 09:19:57

Data Type: Original

Initial Sample Vol:

Sample Prep Vol:

Auto Dilution Factor: 1

## Replicate Data: P-NF-10 bar-x1000

Repl#	Analyte	Net Intensity	Corrected Intensity	Calib. Conc. Units	Sample Conc. Units	Analysis Time
1	Ca 422.673	786064.9	786012.1	0.983 mg/L	0.983 mg/L	09:21:28
1	Na 589.592	28167659.0	28063347.3	13.86 mg/L	13.86 mg/L	09:21:39
1	Mg 279.553	7175760.6	7174273.9	0.767 mg/L	0.767 mg/L	09:21:58
2	Ca 422.673	770026.5	769973.7	0.975 mg/L	0.975 mg/L	09:21:30
2	Na 589.592	28484432.2	28380120.6	14.01 mg/L	14.01 mg/L	09:21:45
2	Mg 279.553	7183183.5	7181696.7	0.768 mg/L	0.768 mg/L	09:22:01
3	Ca 422.673	774124.0	774071.2	0.977 mg/L	0.977 mg/L	09:21:32
3	Na 589.592	28010630.0	27906318.4	13.79 mg/L	13.79 mg/L	09:21:49
3	Mg 279.553	7162791.1	7161304.4	0.765 mg/L	0.765 mg/L	09:22:03

## Mean Data: P-NF-10 bar-x1000

Analyte	Mean Corrected Intensity	Calib. Conc. Units	Std.Dev.	Sample Conc. Units	Std.Dev.	RSD
Ca 422.673	776685.7	0.978 mg/L	0.0043	0.978 mg/L	0.0043	0.44%
Na 589.592	28116595.4	13.89 mg/L	0.114	13.89 mg/L	0.114	0.82%
Mg 279.553	7172425.0	0.767 mg/L	0.0012	0.767 mg/L	0.0012	0.15%

Sequence No.: 7

Sample ID: P-NF-12 bar-x100

Analyst:

Initial Sample Wt:

Dilution:

Wash Time: 40

Autosampler Location: 23

Date Collected: 29-01-2019 09:22:57

Data Type: Original

Initial Sample Vol:

Sample Prep Vol:

Auto Dilution Factor: 1

## Replicate Data: P-NF-12 bar-x100

Repl#	Analyte	Net Intensity	Corrected Intensity	Calib. Conc. Units	Sample Conc. Units	Analysis Time
1	Ca 422.673	4180391.1	4180338.3	2.737 mg/L	2.737 mg/L	09:24:28
1	Na 589.592	Saturated3	Saturated3			09:24:40
	Saturated in preshot (code 3)					
1	Mg 279.553	36088482.1	36086995.4	4.084 mg/L	4.084 mg/L	09:25:07
2	Ca 422.673	4126089.0	4126036.2	2.709 mg/L	2.709 mg/L	09:24:31
2	Na 589.592	145801562	145697250	69.60 mg/L	69.60 mg/L	09:24:48
	Saturated within auto integration window (code 4)					
2	Mg 279.553	36185082.3	36183595.5	4.095 mg/L	4.095 mg/L	09:25:13
3	Ca 422.673	4417833.9	4417781.1	2.860 mg/L	2.860 mg/L	09:24:33
3	Na 589.592	146089044	145984732	69.74 mg/L	69.74 mg/L	09:24:55
	Saturated within auto integration window (code 4)					

Figure 9.2-4- Cations present in permeate flow of nanofiltration under pressure of 10 bar